Archives of Computational Methods in Engineering (2026) 33:81–138
https://doi.org/10.1007/s11831-025-10304-w

REVIEW

A Comprehensive Survey of Henry Gas Solubility Optimization Algorithm with its Theory, Variants, and Applications

Amylia Ait Saadi[1,2] · Sylia Mekhmoukh Taleb[3] · Selma Yahia[3] · Musa Dogan[4] · Elham Tahsin Yasin[5] · Yassine Meraihi[3] · Murat Koklu[4] · Seyedali Mirjalili[6,7,8] · Amar Ramdane-Cherif[1]

Received: 6 April 2025 / Accepted: 6 June 2025 / Published online: 10 July 2025

Abstract

Henry Gas Solubility Optimization (HGSO) algorithm is a well-known physics-based nature-inspired optimization algorithm inspired by the behavior of Henry's law. The HGSO algorithm, developed by Hashim et al. in 2019, has attracted significant interest from scientists and researchers. It has been widely applied to solve various optimization problems in different fields due to its unique structure, simplicity, easiness of implementation, and reasonable execution time. This paper explores and examines over 200 previous existing research on the HGSO algorithm covering its advancements, enhanced variants (multi-objective, hybridized, and modified), and a wide range of real-world applications such as intrusion detection, wireless sensor networks, optimal parameters control, photovoltaic systems, image processing, and feature selection. Additionally, The performance of the HGSO algorithm is assessed using 23 IEEE CEC benchmark functions in comparison with 14 well-regarded optimization meta-heuristics published in the literature. Furthermore, the results of the HGSO algorithm are compared with some of its key variants. The survey also provides a critical evaluation of HGSO's convergence behavior, highlighting its strengths and limitations. Finally, the paper concludes with some potential directions for future work. The insights gained from this survey offer valuable guidance for researchers aiming to apply or enhance the HGSO algorithm in a wide range of optimization problems.

1 Introduction

Meta-heuristics constitute a new generation of powerful approached optimization techniques, adaptable and applicable to a wide range of real-world problems. They are iterative stochastic methods, which escape local minima and progress towards a global optimum of a function. They enable the generation of good quality feasible solutions within a reasonable time. Meta-heuristics can be categorized into

✉ Yassine Meraihi
y.meraihi@univ-boumerdes.dz

Amylia Ait Saadi
Amylia.belhabib@esme.fr

Sylia Mekhmoukh Taleb
s.mekhmoukh@univ-boumerdes.dz

Selma Yahia
selmayh4@gmail.com

Musa Dogan
musa.dogan@selcuk.edu.tr

Elham Tahsin Yasin
ilham.tahsen@gmail.com

Murat Koklu
mkoklu@selcuk.edu.tr

Seyedali Mirjalili
ali.mirjalili@gmail.com

1 LISV Laboratory, University of Paris-Saclay, 10-12 Avenue of Europe, Velizy, France

2 ESME Engineering School, Ivry-sur-Seine, France

3 LIST Laboratory, University of M'Hamed Bougara Boumerdes, Avenue of Independence, 35000 Boumerdes, Algeria

4 Technology Faculty, Department of Computer Engineering, Selcuk University, Konya, Türkiye

5 Graduate School of Natural and Applied Sciences, Selcuk University, Konya, Türkiye

6 Centre for Artificial Intelligence Research and Optimisation, Torrens University Australia, Fortitude Valley, Brisbane, QLD 4006, Australia

7 University Research and Innovation Center, Obuda University, Budapest, Hungary

8 Faculty of Electrical Engineering and Computer Science, VSB-Technical University of Ostrava, Ostrava, Czech Republic

two main classes [1]: those based on a single solution and those based on a population of solutions as shown in Fig. 1.

Single-based meta-heuristics, also known as trajectory methods, begin with a single initial solution and iteratively modify it, forming a search trajectory within the solution space. The neighborhood mechanism is used to enhance this solution. Some of the well-known and popular single-based meta-heuristics are: Simulated Annealing (SA) [2], Tabu Search (TS) [3], Greedy Randomized Adaptive Search Procedure (GRASP) [4], Variable Neighborhood Search (VNS)

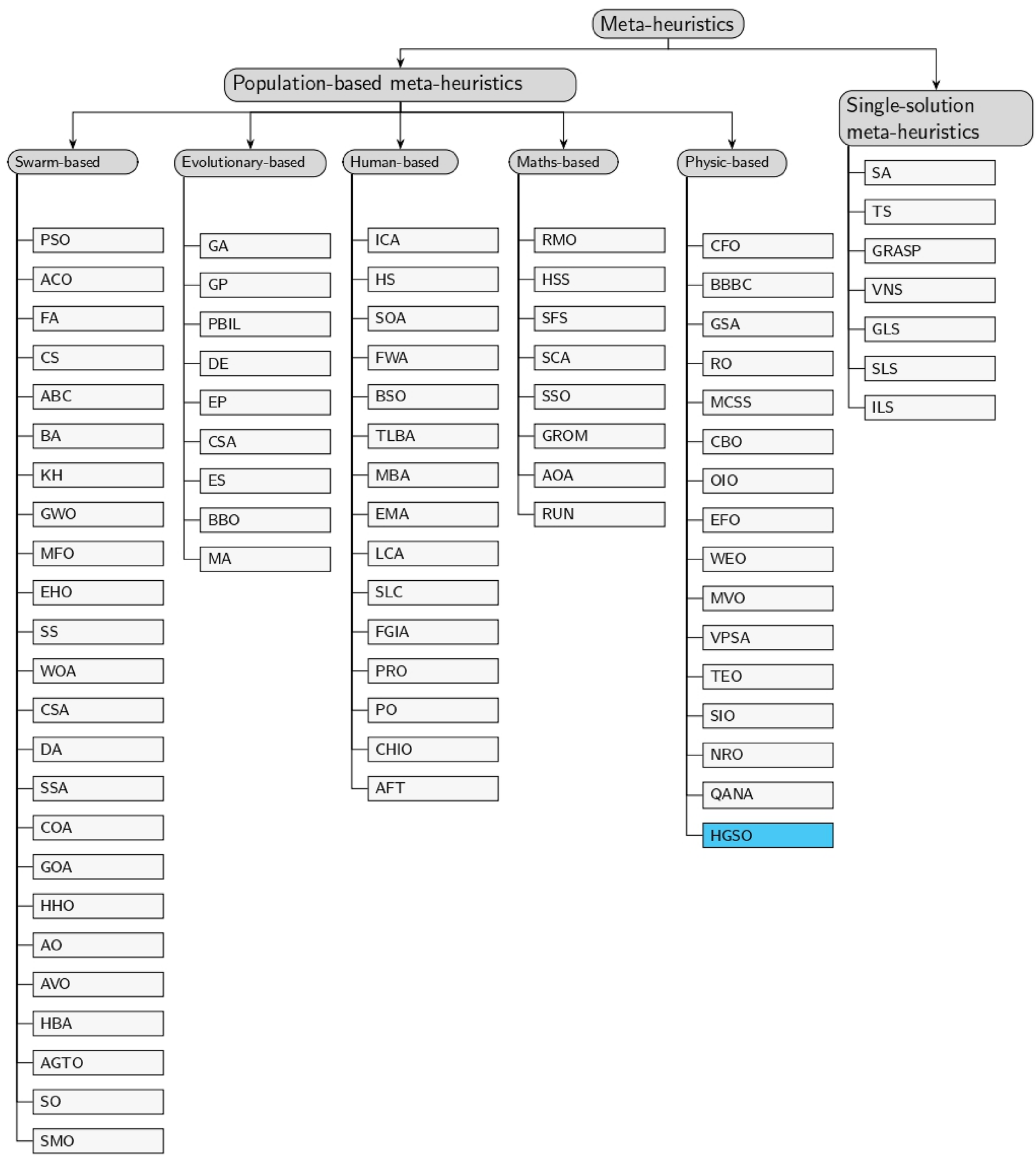

Fig. 1 Classification of meta-heuristic algorithms

[5], Guided Local Search (GLS) [6], Stochastic Local Search (SLS) [7], Iterated Local Search (ILS) [8], and their variants.

Unlike single-based meta-heuristics, population-based meta-heuristics iteratively refine a set of solutions rather than a single one. They begin with an initial population of solutions and generate new candidates at each iteration. These newly created solutions are then integrated into the current population through selection mechanisms. The process continues until a predefined stopping criterion is met. Population-based meta-heuristics can be categorized into five main classes:

The Evolutionary Algorithms (EAs) category includes population-based meta-heuristics which are inspired by natural evolutionary processes that make use of three main operators i.e., mutation, selection, and recombination. Some well-known EAs are: Genetic Algorithm (GA) [9], Genetic Programming (GP) [10], Probability-Based Incremental Learning (PBIL) [11], Differential Evolution (DE) [12, 13], Evolutionary Programming (EP) [14], Clonal Selection Algorithm (CSA) [15], Evolutionary Strategies (ES) [16], Biogeography-Based Optimizer (BBO) [17], and Memetic Algorithm (MA) [18].

The class of swarm-based algorithms mimics the behavior of swarms of animals that exist in nature such as swarms of fish, insects, or birds. particle swarm optimization (PSO) [19, 20], and Ant Colony Optimization (ACO) [21] are the first swarm intelligence algorithms. Other optimization algorithms that come from analogies with natural biological phenomena have been proposed. Among the most significant we cite the Firefly Algorithm (FA) [22], Cuckoo Search (CS) [23], Ant Bee Colony (ABC) [24], Bat Algorithm (BA) [25], Krill Herd Algorithm (KH) [26, 27], Grey Wolf Optimization (GWO) [28, 29], Moth Flame Optimization (MFO) [30], Elephant Herding Optimization (EHO) [31], Social Spider Algorithm (SS) [32], Ant Lion Optimizer (ALO) [33], Whale Optimization Algorithm (WOA) [34], Crow Search Algorithm (CSA) [35, 36], Dragonfly Algorithm (DA) [37], Salp Swarm Algorithm (SSA) [38], Coyote Optimization Algorithm (COA) [39], Grasshopper Optimization Algorithm (GOA) [40, 41], Harris Hawks Optimization (HHO) [42], Aquila Optimizer (AO) [43, 44], Black Widow Optimization (BWO) [45, 46], African Vultures Optimization (AVO) [47], Honey Badger Algorithm (HBA) [48], Reptile Search Algorithm (RSA) [49, 50], White Shark Optimization (WSO) [51], Artificial Gorilla Troops Optimizer (AGTO) [52], Snake Optimizer (SO) [53], Starling Murmuration Optimizer (SMO) [54], Shrimp and Goby association search algorithm (ShGA) [55], Termite life cycle optimizer (TLCO) algorithm [56], Dynamic Hunting Leadership (DHL) algorithm [57], Artificial Meerkat Algorithm (AMA) [58], Rhinopithecus Swarm Optimization (RSO) algorithm [59], Eurasian Lynx Optimizer (ELO) [60], and Draco Lizard Optimizer (DLO) [61].

Human-based algorithms (HM) are inspired by the human-made events. Some of the most well-regarded human-based algorithms are: Imperialist Competitive Algorithm (ICA) [62], Harmony Search (HS) [63], Seeker Optimization Algorithm (SOA) [64], Fire Work Algorithm (FWA) [65], Brain Storm Optimization (BSO) [66], Teaching Learning-Based Algorithm (TLBA) [67], Mine Blast Algorithm (MBA) [68], Exchange Market Algorithm (EMA) [69], League Championship Algorithm (LCA) [70], Soccer League Competition (SLC) algorithm [71], Football Game Inspired Algorithm (FGIA) [72], Poor and Rich Optimization (PRO) Algorithm [73], Political Optimizer (PO) [74], Coronavirus Herd Immunity Optimizer (CHIO) [75], and Ali Baba and the Forty Thieves (AFT) [76].

Maths-based Algorithms (MA) imitate mathematical rules. Some of the most well-known maths-based algorithms are: Radial Movement Optimization (RMO) [77], Hyper-Spherical Search (HSS) Algorithm [78], Stochastic Fractal Search (SFS) [79], Sine Cosine Algorithm (SCA) [80, 81], Spherical Search Optimizer (SSO) [82], Golden Ratio Optimization Method (GROM) [83], Arithmetic Optimization Algorithm (AOA) [84], and RUNge Kutta Optimizer (RUN) [85].

Physics-based algorithms mimic the physical rules of the universe. Some of the most popular algorithms are: Central Force Optimization (CFO) [86], Big-Bang Big-Crunch (BBBC) [87], and Gravitational Search Algorithm (GSA) [88]. Other recently developed physics-based algorithms are: Ray Optimization (RO) algorithm [89], Magnetic Charged System Search (MCSS) [90], Colliding Bodies Optimization(CBO) [91], Optics Inspired Optimization (OIO) [92], Electromagnetic Field Optimization (EFO) [93], Water Evaporation Optimization (WEO) [94], Multi-Verse Optimizer (MVO) [95], Vibrating Particles System Algorithm (VPSA) [96], Thermal Exchange Optimization (TEO) [97], Sonar Inspired Optimization (SIO) [98], Nuclear Reaction Optimization (NRO) [99], Gradient-based optimizer (GBO) [100, 101], Quantum-based Avian Navigation Optimizer Algorithm (QANA) [102], Tornado optimizer with Coriolis force (TOC) [103], and Henry Gas Solubility Optimization (HGSO) [104].

The Henry Gas Solubility Optimization (HGSO) algorithm is a novel physical-based meta-heuristic, proposed by Hashim et al. [104] in July 2019. The HGSO algorithm mimics the behavior of Henry's law, which is a fundamental gas law that establishes the relationship between the quantity of a specific gas dissolved in a particular type and volume of liquid at a constant temperature. In comparison with other well-known optimization algorithms, the HGSO algorithm demonstrates its efficiency in solving challenging real-world optimization problems. As a result, it was used to solve a variety of problems, including feature selection,

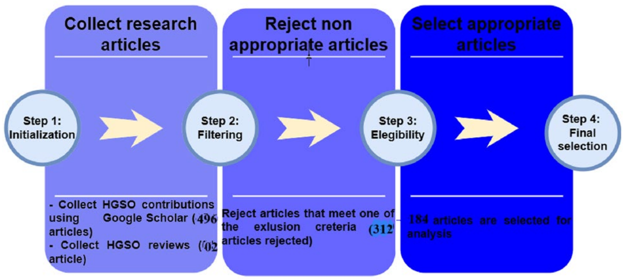

Fig. 2 Diagram illustrating the paper collection process

classification, image processing, intrusion detection, power systems, and many others.

This paper provides a survey of the HGSO algorithm, exploring its variations (including modified, multi-objective, and hybridized versions) and examining its diverse applications across various domains. In order to collect published HGSO articles, we consider various well-regarded publishers (i.e. Elsevier, Springer, IEEE, Wiley, and others). Additionally, we utilize Google Scholar and use specific search strings to construct a database of articles related to the HGSO algorithm:

– Henry Gas Solubility Optimization algorithm
– Improved Henry Gas Solubility Optimization algorithm
– Modified Henry Gas Solubility Optimization algorithm
– Enhanced Henry Gas Solubility Optimization algorithm
– Binary Henry Gas Solubility Optimization algorithm
– Adaptive Henry Gas Solubility Optimization algorithm
– Multi-Objective Henry Gas Solubility Optimization algorithm
– Hybridized Henry Gas Solubility Optimization algorithm
– Applications of Henry Gas Solubility Optimization algorithm
– Henry Gas Solubility Optimization algorithm survey
– Henry Gas Solubility Optimization algorithm review
– Henry Gas Solubility Optimization algorithm overview
– HGSO algorithm

The collected papers were screened, as illustrated in Fig. 2, to retain only credible and original studies published in well-known journals (WoS Q1, WoS Q2, WoS Q3, and WoS Q4 publishers), applying a combination of inclusion and exclusion criteria as shown in Table 1. These criteria ensure an objective and systematic selection process, effectively minimizing the inclusion of irrelevant or low-quality publications.

The statistical results of our investigation are presented in the figures below. Figure 3 illustrates the count of relevant HGSO publications categorized by both publisher and publication type. As we can see, a total of 55 papers were published by Elsevier, 52 by Springer, 24 by IEEE, 17 by Wiley, and 36 by various other publishers. Figure 4 displays the annual count of HGSO publications. A significant interest has been observed over the past five years, with a peak recorded in 2023. Since the introduction of the HGSO algorithm in July 2019, more than 180 studies have been published on this algorithm.

The Top 10 Journals ranked by the number of HGSO publications are listed in Table 2. The 10 HGSO co-cited articles are given in Table 3. Additionally, Fig. 5 provides the top 10 countries based on the number of HGSO publications. India and China stand out as the most active contributors, followed by Egypt, Turkey, Algeria, Iran, Saudi Arabia, Malaysia, Pakistan, and Indonesia. Lastly, in Fig. 6, the tag cloud visually represents the top ten HGSO-related keywords.

As far as we are aware, there are only two HGSO surveys developed by El-Shorbagy et al. (2024) [114] and Abualigah et al. (2024) [115]. The survey of El-Shorbagy et al. analyzed 110 research articles on HGSO and the performance of HGSO was assessed using only 12 IEEE CEC benchmark functions in comparison with seven meta-heuristics. The survey of Abualigah et al. analyzed only 36 HGSO articles without performance comparison. Our recent HGSO survey, on the other hand, provides a more comprehensive review covering over 180 articles published between 2019 and the end of May 2025. The performance of HGSO is assessed using 23 IEEE CEC benchmark functions (categorized into three groups: unimodal, multimodal, and fixed-dimension numerical optimization problems). The performance of the HGSO algorithm is also compared with some of its key variants. This makes our survey different from the aforementioned survey, offering a broader and more up-to-date look into HGSO research.

The primary contributions of our survey are as follows.

1. **Comprehensive survey**: The paper consolidates research on the HGSO algorithm and its improved variants, including modified, multi-objective, and hybridized versions.
2. **Wide range of applications**: We present and analyze applications of the HGSO algorithm in various fields such as intrusion detection, wireless sensor networks, optimal parameters control, photovoltaic systems, image processing, and feature selection.
3. **Performance comparison**: The performance of the HGSO algorithm was validated using 23 IEEE CEC benchmark functions in comparison with fourteen meta-heuristics, showcasing its competitive performance.
4. **Benefits and drawbacks evaluation**: A critical evaluation of the HGSO algorithm is provided, highlighting its strengths and limitations.
5. **Future research directions**: We provide insights into potential areas for further research and development of the HGSO algorithm, encouraging its continued evolution.

Table 1 Inclusion and exclusion criteria

Inclusion criteria	Exclusion criteria
Works published in credible and well-known journals	Published in predatory journals
Papers presenting reviews on different HGSO based approaches	Published in less than four pages
Works representing a complete version when several versions exist	Papers Which are incomplete, i.e. in the case where several versions of an article exist
Papers presenting new propositions involving HGSO algorithm	Papers that do not provide details on the areas of interest of HGSO algorithm
Papers written in English language	Works published in the form of tutorials, abstracts, posters, keynotes, or conference summaries
All available HGSO papers from 2019 to 2025	Papers for which the full text is not available for download
	Not peer-reviewed scientific papers

Table 2 Top 10 Journals ranked by the number of HGSO publications

Journals	Rank	Number of HGSO publications
IEEE ACCESS	1	8
Neural Computing and Applications	2	6
Expert Systems With Applications	3	5
Concurrency and Computation	3	5
Engineering Applications of Artificial Intelligence	3	5
Artificial Intelligence Review	3	5
Applied Intelligence	4	3
Advances in Engineering Software	4	3
Cybernetics and Systems	4	3
Scientific Reports	4	3

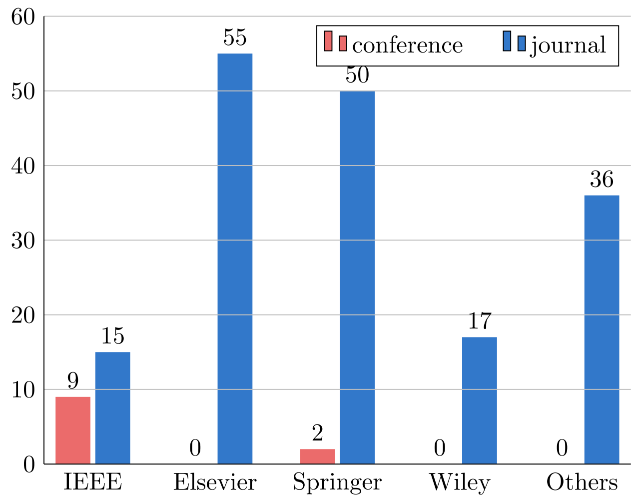

Fig. 3 Number of HGSO related publications per Database

Table 3 Top 10 HGSO co-cited articles

Studies	Rank	Number of citations
Hashim et al. [104]	1	951
Neggaz et al. [105]	2	196
Nandhini et al. [106]	3	118
Yıldız et al. [107]	4	115
Abd Elaziz and Attiya [108]	5	108
Ekinci et al. [109]	6	108
Ghadimi et al. [110]	7	106
Hashim et al. [111]	8	86
Yıldız et al. [112]	9	83
Mirza et al. [113]	10	69

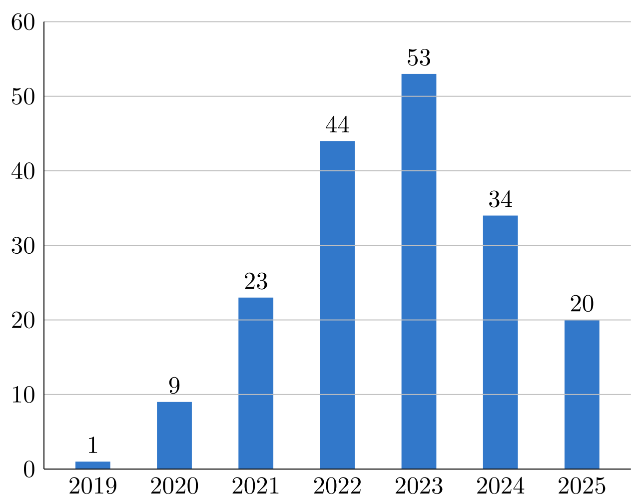

Fig. 4 Number of HGSO related publications per year

This paper is outlined as follows. Section 2 details the foundational structure of the HGSO algorithm. Following this, Sect. 3 offers a comprehensive exploration of the modified,

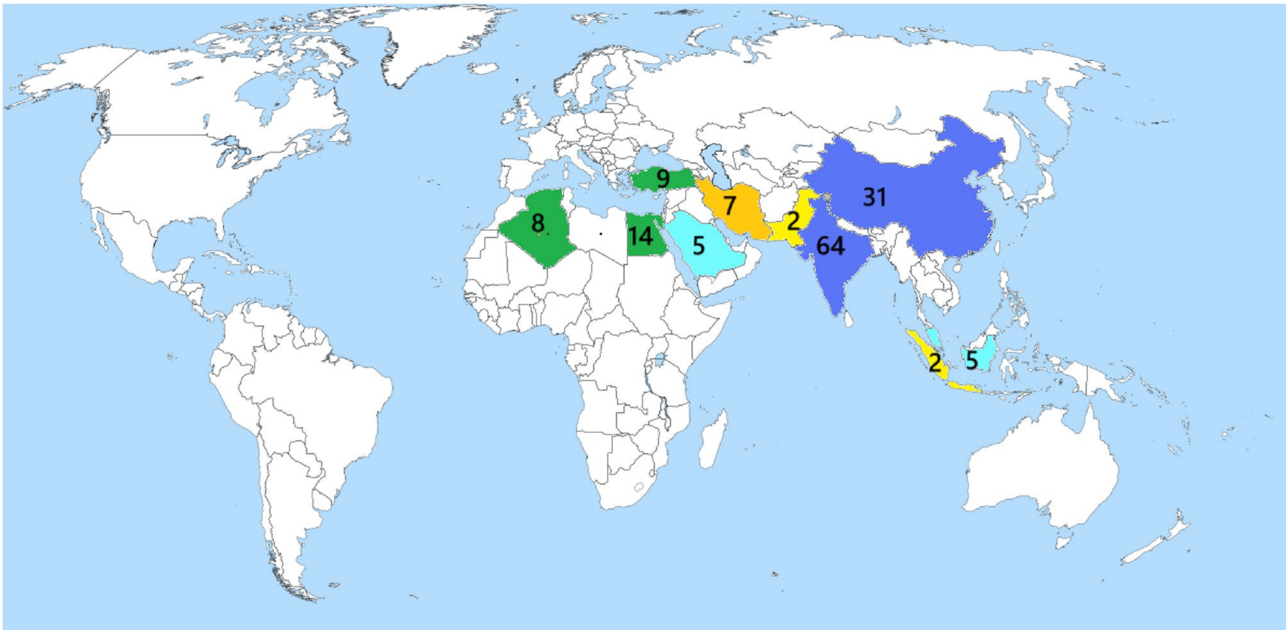

Fig. 5 Top 10 countries ranked by the number of publications on the HGSO algorithm

Fig. 6 HGSO-related keywords

multi-objective, and hybridized variants of the HGSO algorithm, shedding light on the specific adaptations and enhancements introduced. The practical applications of the HGSO algorithm across diverse domains are given in Sect. 4. Section 5 gives Comparisons and results of the HGSO algorithm with some well-regarded optimization meta-heuristics. Section 6 engages in a detailed discussion, offering insights and recommendations for further research directions. Finally, Sect. 7 concludes the paper.

2 Henry Gas Solubility Optimization Algorithm

The Henry Gas Solubility Optimization (HGSO) algorithm, as proposed by Hashim et al. (2019), is a meta-heuristic optimization method inspired by the principles of Henry's law in chemistry. This law, pivotal in understanding the solubility of gases in liquids, states that the solubility S_g of a gas is directly proportional to its partial pressure P_g, expressed as given in Eq. (1)

$$S_g = H \times P_g, \tag{1}$$

where H is the temperature-dependent Henry's constant. The HGSO algorithm applies this concept to optimization problems, where solutions represent gas molecules, and their quality or 'solubility' is evaluated through an objective function.

Additionally, it is important to consider the temperature dependence of Henry's law constants. These constants change with variation in the system's temperature, which can be represented by the Van't Hoff model given by Eq. (2):

$$\frac{d(\ln H)}{d(\frac{1}{T})} = -\frac{\Delta_{sol}E}{R} \tag{2}$$

where $\Delta_{sol}E$ represents the enthalpy of dissolution, R denotes the gas constant, and T is the current temperature.

Lets A and B are two parameters for T dependence of H, Consequently, Eq. (1) can be integrated as follows:

$$H(T) = A \times \exp\left(\frac{B}{T}\right) \tag{3}$$

Henry's constant H varies with temperature, so we can create an expression based on H at the reference temperature T_θ= 298.15 K using Eq. (4):

$$H(T) = H_\theta \times \exp\left(-\frac{\Delta_{sol}E}{R}\left(\frac{1}{T} - \frac{1}{T_\theta}\right)\right), \tag{4}$$

where H_θ denotes the reference Henry's constant.

The Van't Hoff model is valid when $\Delta_{sol}E$ is a constant, Thus, Eq. (7) can be rewritten as follows:

$$H(T) = H_\theta \times \exp\left(-C\left(\frac{1}{T} - \frac{1}{T_\theta}\right)\right), \tag{5}$$

The HGSO algorithm iteratively adapts and updates solutions, akin to the changing solubility of gases, guided by the modified forms of Henry's law, thereby seeking the most soluble or optimal solution in a given optimization scenario. The visual representation of the physical phenomenon of the HGSO algorithm is shown in Fig. 7.

2.1 Mathematical Formulation of the HGSO Algorithm

The HGSO algorithm, which is inspired by the principles of Henry's law, incorporates a unique mathematical framework. This framework aligns with common methodologies found in meta-heuristic algorithms, including the initiation of potential solutions, updating mechanisms for these solutions, and the evaluation and selection of the most suitable solution. As a method relying on a population-based approach, the HGSO algorithm creates a set of potential solutions represented as gas particles, each with distinctive attributes that are dynamically adjusted throughout the search process, aiding in the identification of optimal solutions in the search domain. The mathematical modeling of this optimization technique can be represented as follows:

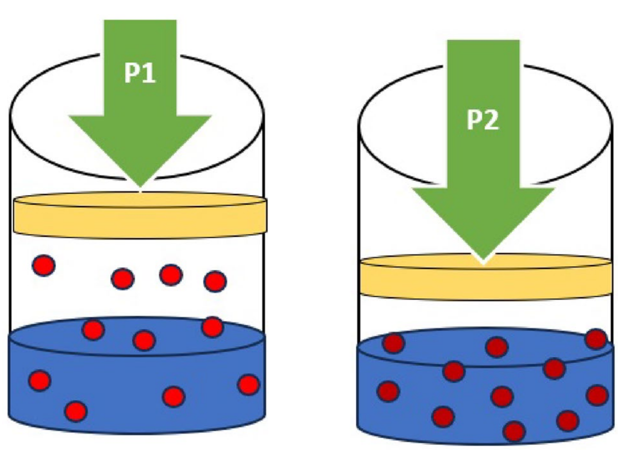

Fig. 7 Visual representation of the physical phenomenon of the HGSO algorithm

Step 1: Initialization The algorithm starts by setting initial parameters. The number of gases in the system (N) and their initial positions are determined via Eq. (6):

$$X_i^{(t+1)} = X_{\min} + r \cdot (X_{\max} - X_{\min}) \tag{6}$$

where $X_i^{(t+1)}$ signifies the position of the ith gas at iteration $t + 1$, r is a uniformly distributed random variable in [0, 1], and $X_{\min}$, $X_{\max}$ are the defined lower and upper problem space bounds, respectively.

Moreover, initialization of Henry's constant for each gas type j ($H_j^{(t)}$), the partial pressure $P_{i,j}$ of gas i in cluster j, and a specific constant value C_j for each type are conducted as given in Eq. (7):

$$H_j^{(t)} = l_1 \cdot \text{rand}(0,1), \quad P_{i,j} = l_2 \cdot \text{rand}(0,1), \quad C_j = l_3 \cdot \text{rand}(0,1) \tag{7}$$

with constants l_1, l_2, l_3 preset to $5 \times 10^{-2}, 100, 1 \times 10^{-2}$ respectively.

Step 2: Cluster Formation In this phase, the algorithm partitions the entire population of gas agents into distinct groups, corresponding to the diversity of gas types encountered. These groups are referred to as 'clusters,' each comprising gases with similar properties. The critical factor for clustering is the uniformity in the value of Henry's constant (H_j) for gases within the same cluster. This uniformity ensures that each cluster represents gases that exhibit consistent behavior in terms of their solubility characteristics.

Step 3: Clusters Evaluation During this stage, the algorithm conducts a thorough assessment of each cluster, labeled as cluster j. The primary objective of this evaluation is to pinpoint the gas within each cluster that reaches the most favorable equilibrium state compared to its counterparts. Following this identification, a ranking process is implemented among the gases across all clusters. This ranking is instrumental in determining which gas exhibits the most optimal equilibrium characteristics within the entire collection of gases. **Step 4: Update of Henry's Coefficient** This step involves the recalibration of Henry's coefficient for each cluster. The update is executed using Eq. (8):

$$H_j^{(t+1)} = H_j^{(t)} \cdot \exp\left(-C_j \cdot \left(\frac{1}{T^{(t)}} - \frac{1}{T_\theta}\right)\right) \tag{8}$$

In this formula, $H_j^{(t+1)}$ represents the updated Henry's coefficient for cluster j at the next iteration, $H_j^{(t)}$ is the current coefficient, and C_j is a predetermined constant for the cluster. The temperature at iteration t, denoted as $T^{(t)}$, is calculated as $T^{(t)} = \exp(-\frac{t}{\text{iter}})$, where iter stands for the total number of iterations. T_θ is a constant temperature, typically set to 298.15 K.

Step 5: Update of Solubility In this phase, the algorithm recalibrates the solubility of each gas within the clusters. The solubility update is governed by Eq. (9):

$$S_{i,j}^{(t)} = K \cdot H_j^{(t+1)} \cdot P_{i,j}^{(t)} \tag{9}$$

Here, $S_{i,j}^{(t)}$ denotes the solubility of gas i in cluster j at iteration t, $H_j^{(t+1)}$ is the updated Henry's coefficient for cluster j, and $P_{i,j}^{(t)}$ represents the partial pressure of gas i in the same cluster. The constant K is a predefined parameter that influences the solubility calculation.

Step 6: Position Update The position of each gas is adjusted according to Eq. (10):

$$\begin{aligned} X_{i,j}^{(t+1)} =& X_{i,j}^{(t)} + F \cdot r \cdot \gamma \cdot (X_{i,\text{best}}^{(t)} - X_{i,j}^{(t)}) \\ &+ F \cdot r \cdot \alpha \cdot (S_{i,j}^{(t)} \cdot X_{\text{best}}^{(t)} - X_{i,j}^{(t)}) \end{aligned} \tag{10}$$

where $\gamma = \beta \cdot \exp\left(\frac{-(F_{\text{best}}^{(t)}+\epsilon)}{(F_{i,j}^{(t)}+\epsilon)}\right)$ and $\epsilon = 0.05$. Constants α and β, fitness $F_{i,j}^{(t)}$ of gas i in cluster j, $F_{\text{best}}^{(t)}$ being the fitness of the best gas, and F is a flag for directional change and diversity introduction.

Step 7: Escaping Local Optima To circumvent local optima, selection and positional update of the underperforming gases are achieved through Eq. (11):

$$N_w = N \cdot (\text{rand}(c_2 - c_1) + c_1) \tag{11}$$

where $c_1 = 0.1$ and $c_2 = 0.2$.

Step 8: Position Update for Worst Agents Positional revision for these gases is as given in Eq. (12):

$$G_{i,j} = G_{\min}(i,j) + r \cdot (G_{\max}(i,j) - G_{\min}(i,j)) \tag{12}$$

where $G_{i,j}$ represents the updated position of the least effective gas i within cluster j. The variable r is a randomly generated number, serving as a stochastic element in the position update process. The terms $G_{\min}(i,j)$ and $G_{\max}(i,j)$ denote the lower and upper bounds of the position range for the respective gas and cluster. This step ensures that the agents with suboptimal performance undergo a strategic repositioning within the defined problem space, potentially enhancing their efficacy in subsequent iterations.

The algorithm iterates through these steps, methodically updating and optimizing the gas properties and positions until the designated iteration limit is attained or an optimal solution is established. The pseudo-code of the proposed algorithm is presented in Algorithm 1, and its flowchart is illustrated in Fig. 8

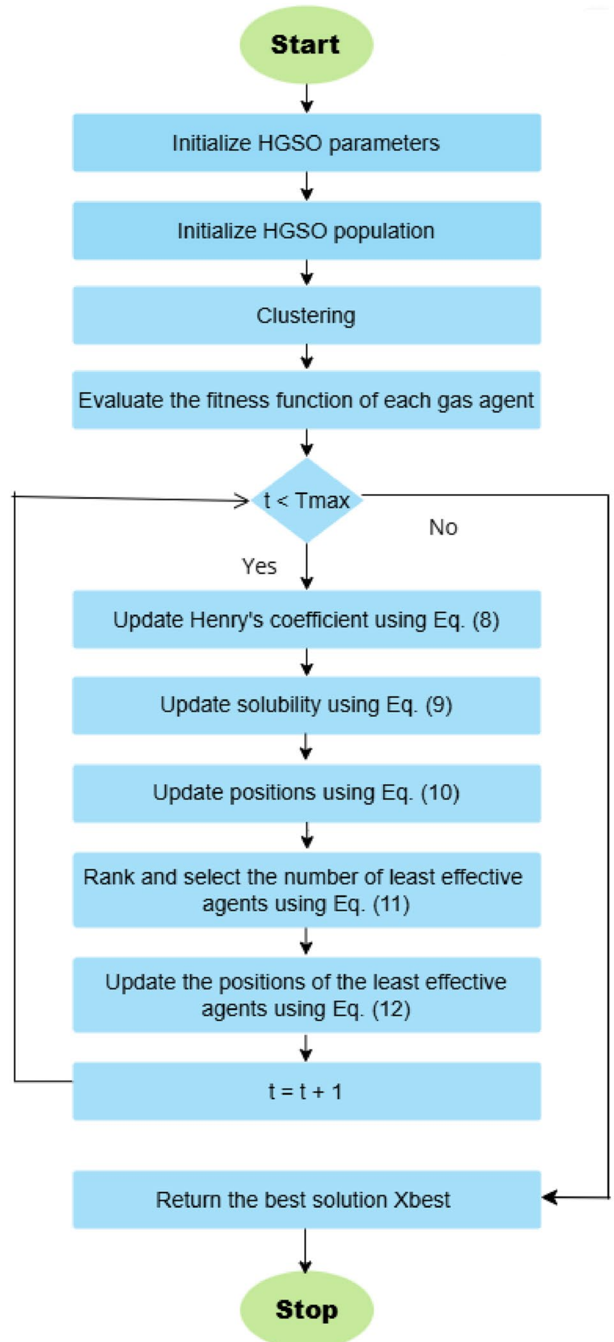

Fig. 8 Flowchart of the HGSO algorithm

Algorithm 1 Pseudo-code for the HGSO Algorithm

1: **Initialization**: Establish initial positions X_i for $i = 1, 2, \ldots, N$, designate gas types, set Henry's constant H_j, partial pressures $P_{i,j}$, and constants C_j, l_1, l_2, and l_3.
2: **Cluster Formation**: Group the gas agents into clusters based on the types, ensuring each cluster has a consistent Henry's constant H_j.
3: **Cluster Evaluation**: Perform an assessment of each cluster j to identify the gas reaching the optimal equilibrium state.
4: **Optimal Gas and Agent Identification**: Determine the highest performing gas $X_{i,\text{best}}$ within each cluster and the leading agent X_{best} across the swarm.
5: **while** $t <$ maximum iteration count Tmax **do**
6:     **for** each agent in the swarm **do**
7:         Apply positional updates for all agents using Eq. (10).
8:     **end for**
9:     Refine Henry's coefficient for each gas type as per Eq. (8).
10:     Adjust the solubility values for all gases according to Eq. (9).
11:     Assess and enumerate the least effective agents via Eq. (11).
12:     Update the positions of the least effective agents following Eq. (12).
13:     Ascertain and update the leading gas $X_{i,\text{best}}$ and agent X_{best}.
14: **end while**
15: Increment the iteration variable t.
16: **return** the agent with the superior performance X_{best}.

3 Recent Variants of the Henry Gas Solubility Optimization Algorithm

In this section, a variant of the HGSO algorithm found in the literature, classified into modified, multi-objective, and hybridized versions are given as illustrated in Fig. 9.

3.1 Modified Versions of Henry Gas Solubility Optimization Algorithm

Different modified versions of the HGSO algorithm (Fig. 10) are highlighted in the following section and their summary is given in Table 4.

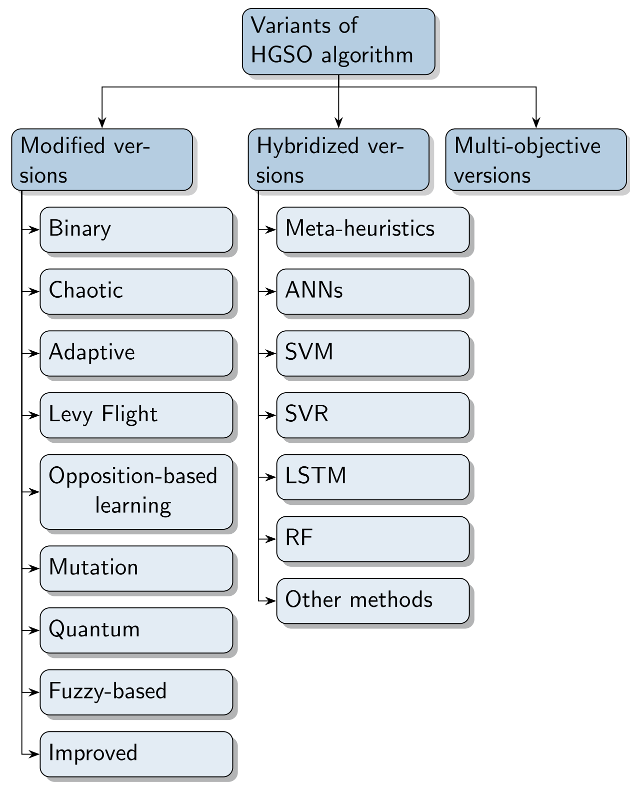

Fig. 9 Variants of MRFO algorithm

3.1.1 Binary Henry Gas Solubility Optimization Algorithm

Yadav and Saraswat [139] developed a binary version of the HGSO algorithm (EHGSO) for solving the feature selection problem. The effectiveness of the proposed EHGSO algorithm was validated using 26 benchmark datasets and compared with five metaheuristic approaches, including GSA, GWO, HGSO, SSA, and BCS. Results showed better performance of the proposed method in terms of accuracy and computational complexity.

Kahloul and Zouache [138] introduced a binary version of the HGSO algorithm (B-HGSO) for feature selection in classification tasks. The performance of the proposed B-HGSO algorithm was evaluated using twelve UCI datasets, including Dermatology, Lung-Cancer, and Breast-cancer considering the average number of features, accuracy, and computational metrics. Simulation results revealed the significant performance of the proposed B-HGSO algorithm over other binary meta-heuristics such as B-PSO, B-GWO, B-WOA, and B-MRFO.

3.1.2 Chaotic Henry Gas Solubility Optimization Algorithm

Yildiz et al. [107] introduced a novel chaotic HGSO algorithm (CHGSO) for solving four real-world engineering problems. The concept of chaos was integrated into the

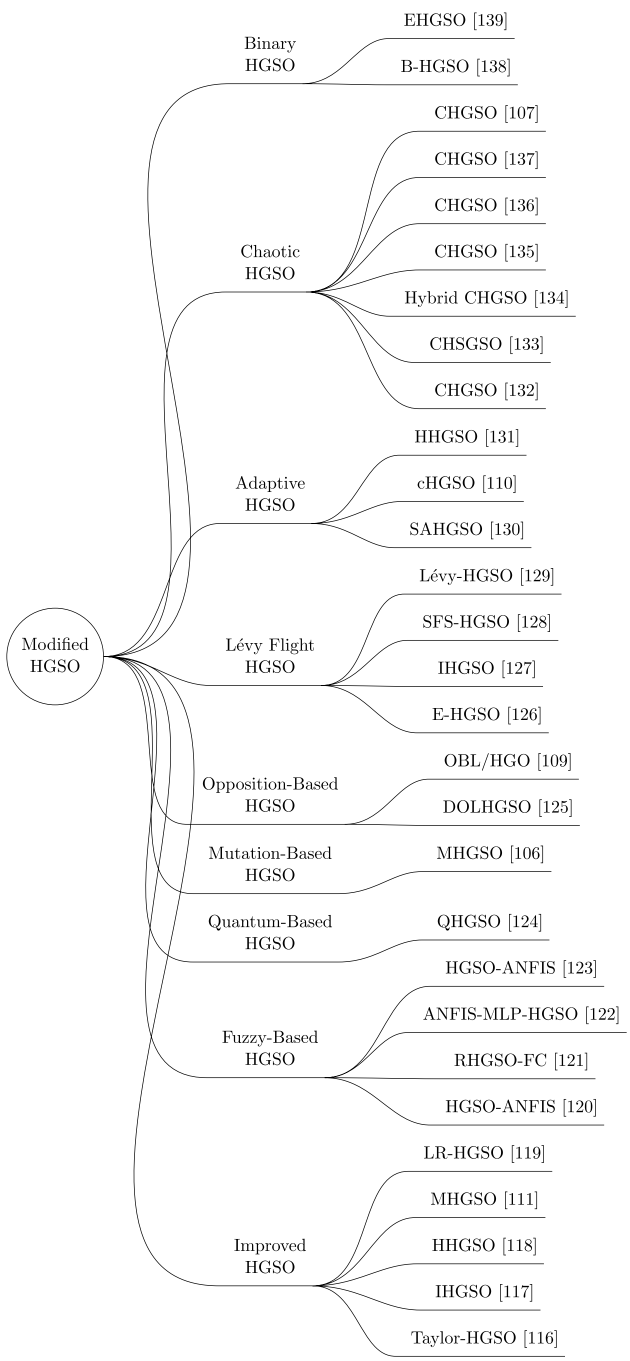

Fig. 10 Taxonomy of modified HGSO variant

basic HGSO algorithm to improve its performance. Results showed the robustness and the efficiency of the CHGSO algorithm compared to some well-regarded meta-heuristics such as ABC, ACO, CS, SSA, GOA, MBA, HHO, MVO, ALO, GSA, and the standard HGSO algorithm by obtaining optimal solutions in manufacturing and mechanical design problems.

Authors in [137], suggested a new variant of the HGSO algorithm, named Chaotic HGSO algorithm (CHGSO), for solving the soil images classification problem. The efficiency of the CHGSO algorithm was evaluated using 23 standard benchmark functions and soil images datasets. Simulation results showed that using the logistic chaotic map, the CHGSO outperforms the state-of-the-art approaches in terms of fitness value and classification metrics.

Yadav and Saraswat [136] introduced a new chaotic HGSO algorithm (CHGSO) for solving global optimization problems. The proposed CHGSO algorithm was assessed on 47 benchmark test functions including unimodal, multimodal, and fixed-dimension multimodal scenarios. Experiments demonstrated the efficiency of the proposed CHGSO algorithm over existing optimization algorithms in terms of standard deviation and mean fitness value.

Karasu and Altan [135] proposed a novel chaotic HGSO (CHGSO) algorithm for solving the feature selection problem. In the proposed CHGSO, the logistic map was introduced to avoid local optima and provide a good balance between exploitation and exploration. Simulation results proved the superiority of the proposed algorithm CHGSO over other optimization techniques.

In the work of Loganathan et al. [134], a novel hybrid ensemble model was introduced for early Autism Spectrum Disorder (ASD) diagnosis. The proposed hybrid model is based on the combination of ResNet101, Weighted Average Ensemble (WAE), and Bidirectional Gated recurrent unit (Bi-GRU), optimized by Chaotic HGSO (CHGSO) algorithm. Experimental results showed the superiority of the hybrid model compared to other well-known models in terms of accuracy, precision, sensitivity, specificity, F1-score, and MCC.

Hussien et al. [133] proposed a modified chaotic HGSO (CHSGSO) algorithm for resource allocation and joint mining decision in wireless blockchain networks. The chaotic map was incorporated into the HGSO algorithm to accelerate the convergence rate and improve resource allocation. Extensive experiments validated the superiority and efficiency of the proposed CHSGSO algorithm compared to four well-regarded meta-heuristics such as ACO, DE, DEMiDRA, and BOToP algorithms.

Sarikaya et al. [132] proposed an improved version of the HGSO algorithm (CHGSO) by integrating the Chaos concept to enhance the performance of the HGSO algorithm. The proposed CHGSO method was applied to both 47 benchmark functions and the optimization of Proportional Integral Derivative (PID) controller parameters. Experimental results revealed that the proposed CHGSO method achieves the best performance when compared to several widely recognized meta-heuristics in the literature, including PSO, WOA, GWO, EA, SA, and the original HGSO algorithm.

Table 4 Modified versions of the HGSO algorithm

	Name	Pros	Cons	Application	Study	Year
Binary HGSO	EHGSO	Efficient fitness cost; good accuracy; lower computational time	Global optimal non guarantee	Feature selection problem	[139]	2024
	B-HGSO	Good accuracy; optimal feature in reduced dimension	Additional process cost	Feature selection problem	[138]	2025
Chaotic HGSO	CHGSO	Good convergence and diversity; simple structure	Computation takes relatively more time	Real-world engineering problems	[107]	2021
	CHGSO	Good statistical results; good accuracy	Using only one map; structure relatively complex	Soil image classification	[137]	2021
	CHGSO	Good statistical results	Using only one map	Global optimization problems	[136]	2021
	CHGSO	Optimal number of features; good error rates	Using only one map; structure complex; no comparison with new methods	Feature selection problem	[135]	2022
	CHGSO	Good classification results	Complex structure; lack in evaluated datasets	Early Autism Spectrum Disorder diagnosis	[134]	2023
	CHGSO	Good performance results	Using only one map; no comparison with new meta-heuristics	Resource allocation in wireless networks	[133]	2023
	CHGSO	Good population diversity; convergence efficiency	No comparison with recent meta-heuristics	PID controller	[132]	2024
Adaptive HGSO	HHGSO	Good results	Additional process cost and complexity; absence of convergence analysis	Team formation problem	[131]	2021
	cHGSO	Optimal costs; good statistical results	Few compared approaches; absence of convergence analysis	Optimal design of solar/battery/diesel systems	[110]	2023
	SAHGSO	Good accuracy; optimal error rate	Global optimum non guarantee	Optimal estimation of SOFC model parameters	[130]	2024
Lvy Flight HGSO	LB-HGSO	Good local search ability; avoiding local optima; good convergence speed	More process time	Benchmark functions and two engineering problems	[129]	2022
	SFS-HGSO	Good accuracy	Lack of compared algorithms	Feature selection problem	[128]	2023
	IHGSO	Best parameter values; good accuracy	More computational complexity; additional processing time	Optimal SVM parameters	[127]	2023
	E-HGSO	Optimal statistical results; high precision level	Excessive exploration	Feature selection problem	[126]	2024
Opposition-Based	OBL/HGO	Optimal PID parameters found; good control performance	Absence of statistical analysis; few compared algorithms	DC motor speed regulation	[109]	2021
HGSO	DOLHGSO	Efficient population diversity; expand global search ability	More process time	Global optimization problems	[125]	2022
Multation HGSO	MHGSO	Good results in classification	Additional processing time and cost	Optimization of the DenseNet-121 hyperparameters	[106]	2022
Quantum-Based HGSO	QHGSO	Good statistical results	Only one convergence analysis	Global optimization problems	[124]	2021

Table 4 (continued)

	Name	Pros	Cons	Application	Study	Year
Fuzzy-Based HGSO	HGSO-ANFIS	Low error rate	Absence of convergence analysis; no statistical evaluation	Prediction of soil shear strength	[123]	2021
	ANFIS-MLP-HGSO	Good accuracy; low error rate	Only two algorithms used for comparison	Prediction of copper grade in Kerman province, Iran	[122]	2021
	RHGSO-FC	High segmentation quality	Only one dataset used	Image segmentation	[121]	2022
	HGSO-ANFIS	Good prediction results	Few approaches used for comparison	Prediction of mine blast-induced flyrock	[120]	2023
Improved HGSO	LR-HGSO	Optimal operating cost	Weak convergence speed in some cases	Unit commitment problem	[119]	2020
	MHGSO	Good statistical results; high classification accuracy	Complex structure	DNA motif discovery problem	[111]	2020
	HHGSO			Feature extraction	[118]	2021
	IHGSO	Reduced number of selected features	Only two datasets used	Histopathological image classification	[117]	2021
	Taylor HGSO	Significant classification accuracy	Few datasets used	Fuel consumption vehicle routing problem	[116]	2022

3.1.3 Adaptive Henry Gas Solubility Optimization Algorithm

Zamli et al. [131] suggested a new variant of the HGSO algorithm (HHGSO) for solving the team formation problem and the combinatorial t-way test suite generation. The adaptive switching strategy based on a penalized and reward technique was integrated into the original HGSO algorithm to control the cluster mappings. Experimental results demonstrated that the proposed HHGSO model provides superior performance against other competitor algorithms such as the Jaya Algorithm (JA), Sooty Tern Optimization Algorithm (STOA), Butterfly Optimization Algorithm (BOA), and Owl Search Algorithm (OSA).

Ghadimi et al. [110] suggested an improved version of the HGSO algorithm (cHGSO) for optimization and sensitivity analysis of a combined energy source based on a photovoltaic (PV), diesel generator (DG), and batteries system. The self-adaptive weighting mechanism and chaos strategy were integrated into the original HGSO algorithm to control its convergence speed and improve its efficiency. The cHGSO's performance was validated considering three objectives including CO2 emissions, entire cost of the system, and permissible emission. Simulation results demonstrated the superiority of the cHGSO algorithm compared to PSO and HOMER algorithms.

A self-adaptive HGSO algorithm (SAHGSO) was proposed in the work of Xu and Razmjooy [130] for optimal estimation of solid oxide fuel cell (SOFC) model parameters. A self-adaptation strategy was incorporated into the HGSO algorithm to remove the stochastic behavior of the individuals and enhance its convergence speed. The proposed SAGSHO algorithm was validated using 96-cell SOFC stack under various temperature and pressure values. Experimental results demonstrated that the SAHGSO algorithm is more effective than other well-known approaches with the lowest error value.

3.1.4 Lévy Flight-Based Henry Gas Solubility Optimization Algorithm

In the work of Li et al. [129], three enhanced versions of the HGSO algorithm were proposed: Lévy-HGSO, based on the Lévy flight operator; Brown-HGSO, based on the Brownian motion operator; and LB-HGSO, which combines both the Lévy flight operator and Brownian motion operator. The proposed algorithms were evaluated on 40 benchmark functions and two engineering problems, demonstrating superior performance compared to SCA, WOA, lightning search algorithm (LSA), WCA, and the original HGSO, with faster convergence and higher precision.

Zhang et al. [128] introduced an enhanced HGSO algorithm (SFS-HGSO) for solving the feature selection problem. The proposed SFS-HGSO incorporated the Lévy flight strategy, Gaussian mechanism, and Brownian motion concept into the HGSO algorithm to enhance its performance. The efficiency of the proposed SFS-HGSO method was validated using 20 standard UCI benchmark datasets and comparative results demonstrated its superiority compared to well-known meta-heuristic optimization techniques such as HBA, WOA, and HHO.

Yu et al. [127] proposed an improved version of the HGSO algorithm (IHGSO) for optimizing the Support Vector Machines (SVM) penalty factor and kernel function parameters. Lévy flight mechanism, Brownian motion operator, and Tangent flight motion were integrated into the HGSO algorithm to enhance its global and local search abilities. Simulation experiments demonstrated that optimizing SVM parameters using the IHGSO algorithm can effectively enhance the classification accuracy.

Wang et al [126] introduced an enhanced version of the HGSO algorithm (E-HGSO) for solving the feature selection problem. Lévy flight mechanism and search factor mechanism were integrated into the HGSO algorithm to improve the efficiency, diversity, and randomness of the search process. The effectiveness of the proposed E-HGSO algorithm was evaluated using eight standard datasets obtained from the UCI Machine Learning Repository in comparison with eight well-regarded meta-heuristics methods. Comparison results showed the competitive performance of the proposed E-HGSO algorithm considering convergence precision, convergence speed, and accuracy metrics.

3.1.5 Opposition-Based Learning Henry Gas Solubility Optimization Algorithm

Ekinci et al. [109] introduced a novel optimization approach (OBL/HGO) by integrating the OBL strategy into the HSGO algorithm for DC motor speed regulation. The proposed OBL/HGO algorithm was assessed taking into account the time multiplied absolute error (ITAE) as the objective function in comparison with some other well-regarded optimization methods such as GWO, SCA, Stochastic Fractal Search (SFS), and Atom Search Optimization (ASO). Conducted experimental results demonstrated that the proposed OBL/HGO algorithm provides superior control performance and excellent robustness to disturbances.

An improved version of the HGSO algorithm, called DOLHGSO, was proposed in the work of Bi and Zhang [125] to solve global optimization problems. The enhancements include dynamic opposite-based learning (OBL) to increase population diversity and sine-cosine strategy for improved position updates and better balance between exploration and exploitation. The performance of the DOLHGSO algorithm was validated on CEC2017 benchmark functions and three real-world engineering design problems. Statistical analyses confirm that the DOLHGSO algorithm outperforms existing methods, demonstrating enhanced diversity and strategic coordination.

3.1.6 Mutation-Based Henry Gas Solubility Optimization Algorithm

In the work of Nandhini and Ashokkumar [106], a mutation-based HGSO (MHGSO) algorithm was introduced to optimize hyperparameters of the DenseNet-121 architecture for automatic plant leaf disease identification. The proposed MHGSO was used mainly to reduce the computational complexity and the error rate of the Convolutional Neural Network (CNN). Experiment results revealed the MHGSO's impressive performance in terms of accuracy, precision, and recall scores.

3.1.7 Quantum-Based Henry Gas Solubility Optimization Algorithm

An improved version of the HGSO algorithm, named Quantum HGSO (QHGSO), was proposed by Mohammadi et al. [124] for solving global optimization problems. A quantum theory was integrated into the original HGSO algorithm to enhance its performance and create a good counterbalance between intensification and diversification. The QHGSO's performance was validated in three well-known engineering problems and results demonstrated its superiority compared to nine well-regarded optimization methods including the standard HGSO, SSA, GOA, WOA, DA, SCA, GWO, MFO, and ALO algorithms.

3.1.8 Fuzzy-Based Henry Gas Solubility Optimization Algorithm

Ding et al. [123] proposed a new hybrid model (HGSO-ANFIS) based on the hybridization of HGSO and adaptive neuro-fuzzy inference system (ANFIS) for the prediction of soil shear strength. The performance of the proposed HGSO-ANFIS model was validated with real data considering the root mean square error (RMSE) and the coefficient of determination (R^2). Simulation results showcased superior performance of the proposed HGSO-ANFIS model compared to other ANFIS-based models, providing R^2 of 0.954 RMSE of 0.1891.

A hybrid ANFIS-MLP-HGSO model was proposed in the work of Abbaszadeh et al. [122], integrating the HGSO algorithm, the ANFIS model, and Multi-Layer Perceptron (MLP) model, to predict copper grade in Kerman province, Iran. Three input scenarios were tested: the first included the latitude and altitude of boreholes, the second used longitude and altitude, and the third combined latitude, longitude, and altitude. Simulation results showed the superiority of the ANFIS-MLP-HGSO model among all the models tested by exhibiting the least uncertainty.

Yadav and Saraswat [121] introduced a new method for image segmentation, called RHGSO-FC, which integrates fuzzy clustering and random strategies into the HGSO algorithm. The efficiency of the RHGSO-FC was evaluated using the NYU-depth V2 RGBD and CEC2017 benchmarks. Simulation results demonstrated the superiority of the proposed approach compared to state-of-the-art algorithms.

Ye et al. [120] introduced a new hybrid model based on the combination of HGSO and ANFIS for predicting the mine blast-induced flyrock. The HGSO-ANFIS algorithm uses HGSO to provide major solutions and achieve a high level of performance. Simulation results showcased the efficiency of the HGSO compared to the basic and hybrid ANFIS-based models, achieving the coefficient of determination and a system error of 0.924 and 18.112, respectively.

3.1.9 Other Improved Henry Gas Solubility Optimization Algorithm

Saranya and Saravanan [119] suggested a modified HGSO algorithm (LR-HGSO) based on the integration of Lagrange Relaxation strategy for solving the unit commitment problem in a superconducting magnetic energy storage (SMES) based thermal system. The efficiency of the proposed LR-HGSO algorithm was assessed to find the optimal sizing of SMES in IEEE 10-unit 24-hour test system with the main objective of minimizing the operating costs and emissions. Experimental results showed the superiority of the proposed LR-HGSO algorithm when compared with other well-known conventional methods.

A Modified HGSO (MHGSO) algorithm was proposed in the work of Hashim et al. [111] for DNA motif discovery (MD) problem, incorporating a new stage to capture motif characteristics for accurate detection. Validation was conducted using the ABS database, which includes CREB, CAAT, SP1, SRF, USF, and TBP across three species–Rat (RN), Mouse (MM), and Human (HS). Results showed that the MHGSO algorithm outperforms state-of-the-art algorithms, achieving superior results in correlation, recall, precision, and F-score.

Utama et al. [118] suggested an improved version of the HGSO algorithm (HHGSO) based on the integration of neighborhood Exchange rules procedure for solving the Fuel Consumption Vehicle Routing Problem (FCVRP). The HGSO's effectiveness was assessed using two data instances with 12 and 22 nodes, considering the variation of population parameters, the variable Kilometers per liter, and the number of iterations. Experiments showed that the proposed HHGSO provides better results compared to the hybrid PSO, SA, and TS algorithms in terms of fuel consumption and computational time.

Vishnoi and Jain [117] proposed an improved version of the HGSO algorithm (IHGSO) for histopathological image classification. A new position update equation was introduced into the standard HGSO to obtain a good balance between global and local search. The efficiency of the proposed IHGSO algorithm was assessed using 23 benchmark functions and testing over two datasets (i.e. the breast cancer cell and ICIAR grand challenge). Experimental results revealed the IHGSO's superiority over alternative approaches.

Jaffino et al. [116] proposed a modified version of the HGSO algorithm, called Taylor-HGSO, based on the integration of Taylor series into traditional HGSO algorithm for solving the feature extraction in the epilepsy detection problem. The improved approach was evaluated using the TUEP and CHB-MIT datasets. Simulation results demonstrated the efficiency of the proposed Taylor-HGSO in terms of accuracy, sensitivity, specificity, F1 score, and MCC metrics.

3.2 Multi-objective Henry Gas Solubility Optimization Algorithm

The multi-objective versions of the HGSO algorithm are highlighted in this section, and their summary is given in Table 5. Sukpancharoen and Prasartkaew [140] proposed a multi-objective HGSO (MOO-HGSO) algorithm for optimizing the combined heat and power plant (CHPP) system. The MOO-HGSO algorithm's performance was validated using four scenarios under varied conditions, considering the cost and energy consumption metrics. Simulation results revealed the efficiency of the proposed MOO-HGSO for improving CHPP performance.

Kahloul et al. [141] proposed a multi-objective version of the HGSO algorithm (MHGSO) for solving engineering design problems. In the proposed MHGSO approach, effective archiving and leader selection strategies based on the crowding distance were used to guide the population

Table 5 Multi-objective versions of the HGSO algorithm

	Name	Pros	Cons	Application	Study	Year
Multi-objective HGSO	MOO-HGSO	Minimizing energy and cost; good convergence	Increased computational time	Combined heat and power plant system	[140]	2021
	MHGSO	Good fitness cost and Pareto optimal fronts	Increased execution time	Engineering design problems	[141]	2022

towards a well-distributed Pareto front and enhance the diversity of solutions. Experiments showed the ability of the proposed MHGSO to achieve interesting results in comparison with three well-known multi-objective meta-heuristics, such as MOEA/D, MOGWO, and MSSA.

3.3 Hybridized Versions of Henry Gas Solubility Optimization Algorithm

In this section, the hybridization of the HGSO algorithm with other algorithms are presented as shown in Table 6 and Figs. 11, 12.

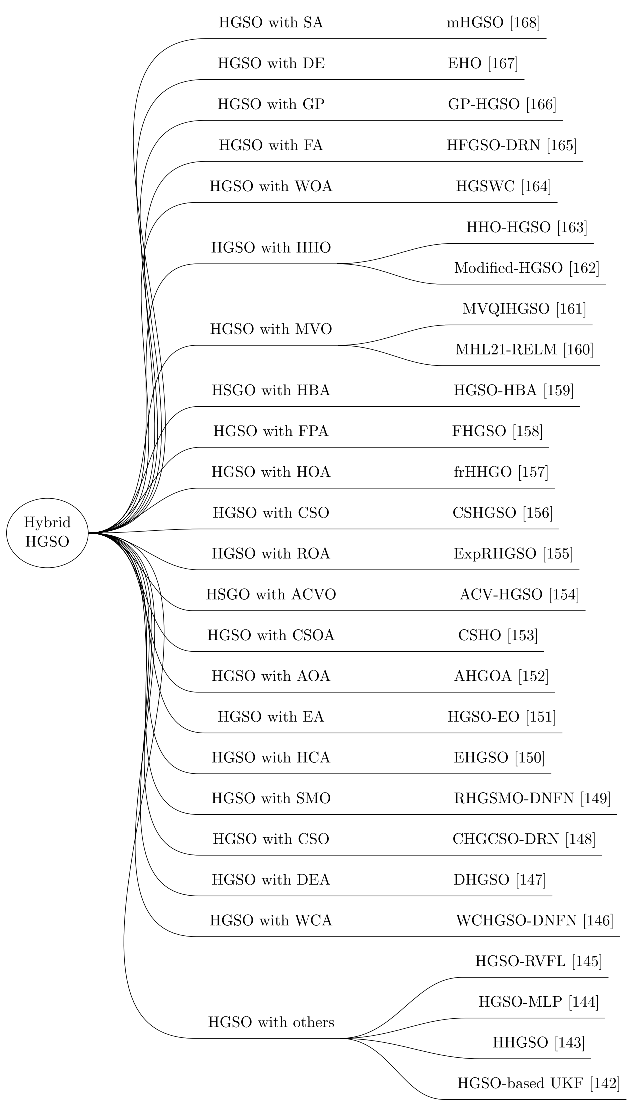

Fig. 11 Taxonomy of the hybrid HGSO

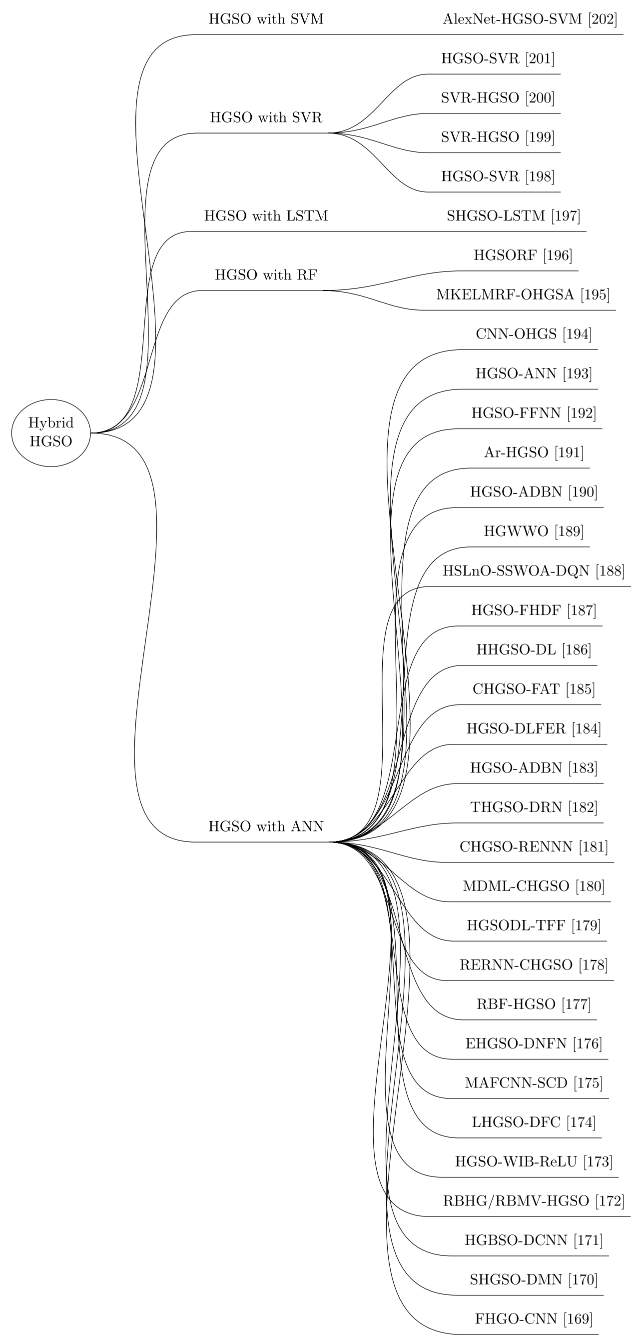

Fig. 12 Taxonomy of the hybrid HGSO

3.3.1 Hybridization with Simulated Annealing Algorithm

Abdel-Mawgoud et al. [168] suggested a hybrid approach (mHGSO) based on the hybridization of HGSO and SA algorithms to obtain the best size of solar photovoltaic (PV) and battery energy storage (BES) in radial distribution systems (RDS). IEEE 69-bus RDS consisting of 68 branches and 69 buses was used to study the effectiveness of the proposed mHGSO algorithm. Simulation results proved the

Table 6 Hybrid versions of the HGSO algorithm

	Name	Pros	Cons	Application	Study	Year
HGSOHGSO + SA	mHGSO	Good transition from exploration to exploitation; good convergence	Compared only with HGSO; no statistical analysis	Radial distribution system	[168]	2021
HGSO + DE	EHO	Good stability; enhanced exploitation ability	Complex space search; more running time	Pressure retarded osmosis system	[167]	2022
HGSO + GP	GP-HGSO	optima antenna length	Unbalanced exploration search	Plate-wire antenna capacitance optimization	[166]	2022
HGSO + FA	HFGSO-DRN	High detection accuracy	Complex structure	Prostate cancer detection system	[165]	2024
HGSO + WOA	HGSWC	Improved exploration and exploitation abilities	Computational complexity	Cloud task scheduling problem	[164]	2021
HGSO + HHO	HHO-HGSO	Good fitness results; optimal number of features	Extended process cost	Global optimization and engineering problems	[163]	2020
	Modified-HGSO	Good local search	Computation time	Feature selection problem	[162]	2021
	HGHHC	Good statistical results; population diversity	Only one algorithm used for comparison	Task Scheduling in Cloud Computing	[203]	2025
HGSO + MVO	MHL21-RELM	Espace from local optima	One dataset used	Fabric defect classification	[160]	2023
	MVQIHGSO	Low error rate; optimal hyperparameters	Not good in exploration	Deriving operating rules of hydropower reservoirs	[161]	2023
HGSO + HBA	HGSO-HBA	Optimal hyperparameters; high recognition rate	Extended computational cost	Kannada character scripts recognition	[159]	2024
HGSO + FPA	FHGSO	High accuracy rate	Only one dataset used	Image classification	[158]	2023
HGSO + HOA	frHHGO	Optimized energy cost and delay	Complex structure	E-waste management in the IoT-cloud architecture	[157]	2023
HGSO + CSO	CSHGSO	Good accuracy and privacy performance	One dataset used	Secure data publishing	[156]	2023
HGSO + ROA	ExpRHGSO	Good classification performance	Extended process time	Rice plant disease detection and classification	[155]	2022
HGSO + ACVO	ACV-HGSO	Optimal network parameters	Complex architecture	Lung cancer detection	[154]	2022
HGSO + CSOA	CSHO	Efficient energy cost	Not focusing on other metrics like delay	Intrusion detection in IoT environments	[153]	2022
HGSO + AOA	AHGOA	High detection results; good fitness value	Quick transition exploration/exploitation	Feature selection problem	[152]	2024
HGSO+ EO	HGSO-EO	Optimal number of features	Few approaches for comparison	Twitter spam detection	[151]	2024
HGSO + HCA	EHGSO	Good exploitation ability; escape local optima	Process time	Feature selection problem	[150]	2025
HGSO + SMO	RHGSMO-DNFN	Low interference and error rate	Additional training time	Designing m-user MIMO interference channel	[149]	2023
HGSO + CSO	CHGCSO-DRN	Good routing performance	No statistical analysis	Plant disease categorization in IoT	[148]	2025
HGSO + DEA	DHGSO	Good classification performance	Global optima no guarantee	Lung cancer classification	[147]	2022
HGSO+ WCA	WCHGSO-DNFN	Optimized model's parameters	lack used datasets	Facial expression recognition	[146]	2022
HGSO + SVM	AlexNet-HGSO-SVM	Optimal visual works; large scale approach	No convergence analysis	Soil image classification	[202]	2022

Table 6 (continued)

	Name	Pros	Cons	Application	Study	Year
HGSO + SVR	HGSO-SVR	Good model's parameter; low error rates	One approach for comparison	Compressive strength prediction	[201]	2022
	GMDH-HGSO	Low prediction errors	additional computation time	Sediment transport prediction	[200]	2022
	SVR-HGSO	Optimized cost and error rates	Compared only with one algorithm	Pile settlement prediction	[199]	2022
	HGSO-SVR	Good estimation performance	No new approach for comparison	Compressive strength prediction of high-performance concrete	[198]	2023
HGSO + LSTM	SHGSO-LSTM	Good convergence; high accuracy	running time	Lipoprotein detection	[197]	2022
HGSO + RF	HGSORF	High classification performance	Computational complexity	Classification	[196]	2022
	MKELMRF-OHGSA	Good accuracy	High complexity	DoS attacks in WSNs	[195]	2022
HGSO + ELM	ELM-HGSO	Improved model; low error rate	Single study site; absence of crucial data	Suspended sediment load prediction	[204]	2025
HGSO + ANN	CNN-OHGS	Optimized attack prevention	Convergence instability	Autonomous vehicle control system	[194]	2021
	HGSO-ANN	Relevant feature identification	Complex structure	Bearing faults identification	[193]	2022
	HGSO-FFNN	Good statistical results; high accuracy	One tested dataset	Alcoholic EEG signals recognition problem	[192]	2022
	Ar-HGSO	Avoid local optima; optimal model's weights	High complexity and cost	Diabetic retinopathy detection	[191]	2022
	HGSO-ADBN	Effective feature selection	process time	Aeroengine sensor fault diagnosis	[190]	2022
	HGWWO	Optimal model's weight; space from local optima	No statistical analysis	COVID-19 detection	[189]	2022
	HSLnO-SSWOA-DQN	Optimal feature selection	Computational cost and time	Medical data classification	[188]	2022
	HGSO-FHDF	Good detection accuracy	One dataset	Automated brain cancer classification	[187]	2022
	HHGSO-DL	Optimal hyperparameters	process time	LED driver system design	[186]	2023
	CHGSO-FAT	Optimal statistical results; low execution time	No recent approaches for comparison; Undefined chaotic map	FOPID controller system	[185]	2023
	HGSO-DLFER	Tune hyperparameter; high performance	One dataset	Facial emotion recognition	[184]	2023
	HGSO-ADBN	Optimal hidden neurons and learning rate	Process cost	Enhancing the Group Recommender System	[183]	2023
	THGSO-DRN	Reliable fruit detection	Local optima trapping	Fruit ripeness classification	[182]	2023
	CHGSO-RENNN	Population diversity; enhanced gain parameters	Gradient vanishing	PI controller gain parameters	[181]	2023
	MDML-CHGSO	QoS based secure model	Complex structure	Fog-based Vehicular networks	[180]	2023
	HGSODL-TFF	Accurate hyperparameter	Lack of flexibility	6G enabled vehicular networks	[179]	2023
	RERNN-CHGSO	Maximum power extraction	Gradient vanishing	Photovoltaic systems	[178]	2023
	RBF-HGSO	Optimal model	One approach for comparison	Compressive strength prediction of high-performance concrete	[177]	2023
	EHGSO-DNFN	High QoS performance	Instable in large scale network	Intrusion detection for MANETs	[176]	2023

Table 6 (continued)

	Name	Pros	Cons	Application	Study	Year
	MAFCNN-SCD	Enhaced model's hyperparameter	Process time	Detection and classification of skin cancer	[175]	2023
	LHGSO-DFC	Realible feature extraction	Process cost	Feature extraction	[174]	2023
	HGSO-WIB-ReLU	Optimal hyperparameter tuning	Unstability	DDoS Attack Detection	[173]	2023
	RBHG/RBMV	Low prediction error	One approach for comparison; one dataset	High-Performance Concrete properties prediction	[172]	2023
	HGBSO-DCNN	Optimal feature selection	No focus on model's parameter	Brain tumor classification	[171]	2023
	DCNN-HGS	Secured disease detection	Local optima trapping	Disease prediction in data from WSNs	[205]	2023
	SHGSO-DMN	High accuracy	Reduced interpretability	Image forgeries detection	[170]	2024
	FHGO-CNN	Optimized energy cost; optimal parameter	complex architecture; scalability	E-waste management in IoT applications	[169]	2024
	DMN-AHGSO	High accuracy	Complex model	Multilevel-thermoplastic waste segregation	[206]	2024
	ANN-HGSO	Reduced error rate	Computational complexity	Aluminum alloy's tensile strength prediction	[207]	2025
HGSO + Other	HGSO-RVFL	Optimal model's parameter; good performance	Process cost and time	AA6061-T6 aluminium alloy joints prediction	[145]	2020
methods	HGSO-MLP	High accuracy; fast convergence	Not the first best algorithm	Stream-flow time series forecasting	[144]	2021
	HHGSO	Good statistical results	Domain specific approach	Search-based Software Engineering Problem	[143]	2021
	HGSO-based UKF	Optimal multi-object tracking; high accuracy	Process time	Multi-object tracking	[142]	2022

efficiency of the mHGSO algorithm compared to the original HGSO.

3.3.2 Hybridization with Differential Evolution

Chen et al. [167] proposed a hybrid algorithm (EHO) based on the combination of HGSO and DE for the dynamic performance of the pressure retarded osmosis (PRO) system. The efficiency of the proposed EHO approach was validated in complex operational environments considering the draw concentrations, variations in temperature, and flow rate levels. Experiments indicated that the proposed method gives better performance compared to the classical HGSO and some well-known meta-heuristics in terms of accuracy, cost-efficiency, and tracking speed.

3.3.3 Hybridization with Genetic Programming

Janairo et al. [166] proposed three techniques based on the integration of GP with HGSO (GP-HGSO), AOA (GP-AOA), and LA (GP-LA) for the plate-wire antenna capacitance optimization through Geometry Modeling. The proposed techniques were validated using various wire antenna and dipole plate dimensions and results proved the validity of the proposed techniques for more accurate determination of the optimal antenna geometry.

3.3.4 Hybridization with Firefly Algorithm

Reddy and Kalaivani [165] developed a suitable and accurate prostate cancer detection system (HFGSO-DRN) by combining HGSO, FA, and the deep residual network (DRN). Prostate cancer identification was executed with DRN, and then trained using the HFGSO algorithm. Simulation results demonstrated increased performance of the proposed HFGSO-DRN system with specificity, sensitivity, and accuracy of 0.9130, 0.9367, and 0.9263, respectively.

3.3.5 Hybridization with Whale Optimization Algorithm

A hybrid algorithm (HGSWC) was proposed in the work of Abd Elaziz and Attia [164] for solving the cloud task scheduling problem. The HGSWC algorithm integrates WOA for local search and Opposition-Based Learning (COBL) mechanisms to enhance solution quality. Validated on 36 benchmark functions and 15 scheduling problems, the HGSWC algorithm outperforms six metaheuristic algorithms including SSA, FA, MFO, PSO, WOA, and HGSO, achieving near-optimal solutions without computational overhead.

3.3.6 Hybridization with Harris Hawks Optimization Algorithm

Xie et al. [163] suggested a hybrid approach (HHO-HGSO) based on the hybridization of HGSO and HHO algorithms for solving global optimization problems. CEC2005 and CEC2017 benchmark test functions and four real engineering design problems were used to assess the performance of the proposed HHO-HGSO algorithm. Comparative experiments demonstrated that the proposed approach has strong optimization ability compared to HGSO, HHO, MPA, WOA, WCA, and Lightning search algorithm (LSA).

Abd Elaziz and Yousri [162] proposed a modified HGSO algorithm, named Modified-HGSO, by hybridizing HGSO with an improved version of the HHO algorithm for solving the feature selection problem. The efficiency of the proposed method was assessed using a set of eighteen UCI datasets and two real-world datasets in the discovery field and drug design. Comparison results demonstrated the high quality of the proposed algorithm when compared with eight well-known meta-heuristic methods in terms of fitness value, number of selected features, and accuracy.

3.3.7 Hybridization with Multi-Verse Optimizer Algorithm

In [161], a hybrid approach (MVQIHGSO) based on the combination of HGSO and MVO algorithms was introduced for Deriving operating rules of hydropower reservoirs. The MVQIHGSO approach was tested on 23 classical benchmark functions and employed to optimize hyperparameters of SVM model for deriving operation rules. Statistical results indicated the efficiency of the proposed MVQIHGSO algorithm compared to most of the well-known metaheuristic algorithms in terms of convergence accuracy and speed.

A hybrid model (MHL21-RELM) based on the hybridization of HGSO, MVO, and regularized extreme learning machine (RELM) was proposed by Zhou et al. [160] to enhance the fabric defect classification. This hybridization aims to solve the issue of low classification accuracy of the traditional ELM and prevent the traditional HGSO from falling into local optimal. Experimental results across various fabric defect datasets validated the effectiveness of the proposed MHL21-RELM approach, achieving 97.29% accuracy on the Textile Texture Database–outperforming traditional methods by 6–30% and demonstrating strong generalization capabilities.

3.3.8 Hybridization with Honey Badger Algorithm

A hybrid approach was developed in the work of Parashivamurthy and Rajashekararadhya [159] for Kannada handwritten script recognition. The method begins with image preprocessing using CLAHE and filtering techniques, followed by segmentation with an active contour approach. Feature extraction is performed using Adaptive Local Tetra Pattern (LTrP) and Freeman Chain Code Histogram, where Hybrid Honey Badger Henry Gas Solubility Optimization (HGSO-HBA) fine-tunes the parameters. Experimental results demonstrate an improved recognition accuracy of 96%, proving the effectiveness of the proposed approach.

3.3.9 Hybridization with Flower Pollination Optimization Algorithm

In the work of Deepa and Rasi [158], a combined method (FHGSO) based on the hybridization of HGSO with FPA algorithms was developed for image classification. The efficiency of the proposed FHGSO method was validated using the Stanford background dataset in comparison with some well-regarded image classification models. Experiments showed the performance of the proposed FHGSO algorithm obtaining the values of 0.907, 0.955, and 0.938 for specificity, sensitivity, and testing accuracy, respectively.

3.3.10 Hybridization with Horse Herd Optimization Algorithm

In [157], a hybrid approach (frHHGO) based on the hybridization of the Fractional HGSO with the Horse Herd Optimization Algorithm (HOA) was introduced to optimize the E-waste management in the Internet of Things (IoT)-cloud architecture. The frHHGO approach was evaluated using the Gofile dataset and compared to various optimization approaches such as Cuckoo search-based neural networks and Fractional HGSO. By analyzing the results, the proposed frHHGO algorithm obtained optimal energy consumption and classification metrics including accuracy, sensitivity, and specificity.

3.3.11 Hybridization with Cat Swarm Optimization Algorithm

A hybrid algorithm (CSHGSO) was developed by Kulkarni et al. [156] to enhance privacy-preserving data publishing (PPDP) while minimizing data loss and improving security. The CSHGSO algorithm combines HGSO with Cat Swarm

Optimization (CSO) to generate secure encryption keys based on objective measures. The CSHGSO method was evaluated on the Heart Disease Dataset using the JAVA tool, demonstrating its effectiveness in secure data publishing. Experimental results indicated that the CSHGSO algorithm achieves higher conditional privacy of 1.338 (database-1), maximum accuracy of 0.965 (database-4), and NMI value of 0.927 (database-4), outperforming existing approaches in preserving privacy and data utility.

3.3.12 Hybridization with Rider Optimization Algorithm

A hybrid model (ExpRHGSO) based on the hybridization of HGSO and Rider Optimization Algorithm (ROA) was introduced by Daniya and Vigneshwari [155] for rice plant disease detection and classification. Experiments showed good performance of the developed ExpRHGSO model achieving superior testing sensitivity, specificity, and accuracy with the maximum values of 0.923, 0.919, and 0.916.

3.3.13 Hybridization with Anti-Corona Virus Optimization

A hybrid algorithm, called ACV-HGSO, was developed in the work of Ramkumar et al. [154] for lung cancer detection in a smart IoT environment using medical data. The proposed approach integrates Anti-Corona Virus Optimization (ACVO) with HGSO to enhance detection performance. The ACV-HGSO algorithm effectively removes noise from medical data and extracts dimension-reduced features to minimize complexity. Experimental results demonstrated that the ACV-HGSO algorithm achieves a testing accuracy of 0.910, sensitivity of 0.914, and specificity of 0.912, outperforming existing techniques in IoT-based lung cancer detection.

3.3.14 Hybridization with Competitive Swarm Optimization Algorithm

Boopathi [153] developed a hybrid approach (CSHO) based on combining HGSO and Competitive Swarm Optimization Algorithm (CSOA) for robust intrusion detection in IoT environments. The main objective of the proposed CSHO algorithm is to offer security as a service and provide evidence in terms of scalability. Simulation results revealed the good performance of the proposed CSHO algorithm by obtaining F-measure, energy, recall, and precision of 0.9001, 0.1610, 0.8993, and 0.9052, respectively.

3.3.15 Hybridization with Archimedes Optimization Algorithm

Nalluri and Sasikala [152] proposed a hybrid HGSO with Archimedes Optimization algorithm (AOA), called AHGOA, for enhancing the feature selection in the Pneumonia Detection application. The efficiency of the hybrid AHGOA approach was evaluated using one collected dataset. Results showed that the AHGOA algorithm outperforms AOA, HGSO, HGS, PRO, and BES approaches in terms of precision, accuracy, sensitivity, and specificity metrics.

3.3.16 Hybridization with Equilibrium Optimizer

In the work of Legoui et al. [151], a hybrid algorithm (HGSO-EO) was proposed for Twitter spam detection, combining the HGSO algorithm with the Equilibrium Optimizer (EO). The HGSO-EO algorithm was evaluated using a modified Social Honeypot dataset, with performance comparisons made against individual HGSO, EO, classical filter, and wrapper-based methods, as well as other metaheuristic algorithms. The experimental results demonstrated that the HGSO-EO algorithm outperformed existing methods in both accuracy and effectiveness for feature selection in spam detection.

3.3.17 Hybridization with Hill Climbing Algorithm

Elgazzar et al. [150] developed a hybrid HGSO with Hill Climbing algorithms for solving the feature selection problem. The efficiency of the proposed EHGSO approach was evaluated using the U.S. Census Bureau's American Community Survey data. According to simulation results, the proposed EHGSO algorithm improved significantly the accuracy and fitness value compared to the traditional HGSO.

3.3.18 Hybridization with Spider Monkey Optimization

Reddy and Ravi Kumar [149] proposed a hybrid technique (RHGSMO-DNFN) based on the combination of HGSO, spider monkey optimization, conditional autoregressive value at risk (CAViaR), and deep neuro-fuzzy network (DNFN) for designing m-user MIMO interference channel. The proposed technique was applied with zero-forcing maximum likelihood detection for initial signal estimates. With the lowest bit error rate (BER), signal-to-interference and noise ratio (SINR), and symbol error rate (SER), the proposed RHGSMO-DNFN technique provides better performance than existing optimization approaches.

3.3.19 Hybridization with Chicken Swarm Optimization

Saini et al. [148] proposed a hybrid model (CHGCSO-DRN) based on the hybridization of HGSO, Chicken Swarm Optimization (CSO), and Deep Residual Network (DRN) for Plant disease categorization in IoT environments. The efficiency of the proposed CHGCSO-DRN model was validated based on rice crops images which are preprocessing using median filtering. Simulation results demonstrated the superiority of the proposed CHGCSO-based DRN model over other existing models achieving an accuracy of 94.3%, a maximum specificity of 92%, a maximum sensitivity of 93.3%, and an F1-score of 93%.

3.3.20 Hybridization with Dolphin Echolocation Algorithm

Patra et al. [147] introduced a hybrid model called DHGSO, by integrating HGSO with the Dolphin Echolocation algorithm (DEA), to enhance lung cancer classification using histopathological images. This hybrid model optimizes the training of the Deep Maxout Network (DMN), ensuring improved feature learning and classification accuracy. By effectively balancing exploration and exploitation, DHGSO enhances model performance, leading to an accuracy of 93.08%, sensitivity of 94.81%, and specificity of 94.59%, outperforming other comparative methods.

3.3.21 Hybridization with Water Cycle Algorithm

Borgalli et al. [146] proposed a hybrid model (WCHGSO-DNFN), based on the combination of HGSO, Water Cycle Algorithm (WCA), and Deep Neuro Fuzzy Network (DNFN), for facial expression recognition (FER) and pain intensity measurement. The WCHGSO-DNFN model utilizes dataset-2 for compound FER and dataset-1 for pain intensity assessment. Experimental results demonstrate the model's effectiveness, achieving a testing accuracy of 81.4%, sensitivity of 81.9%, and specificity of 80.6% on dataset-1, while attaining 81.5, 75.8, and 84.8% on dataset-2.

3.3.22 Hybridization with Support Vector Machine

The authors in [202] presented a hybrid model (AlexNet-HGSO-SVM) which integrates AlexNet, HGSO, and SVM for soil image classification. The proposed model was evaluated on a soil image dataset with seven classes and compared with other metaheuristic-based models, including DE, GWO, WOA with SA, and GOA. Experimental results confirmed that the proposed AlexNet-HGSO-SVM model outperforms these methods in terms of classification accuracy and robustness.

3.3.23 Hybridization with Support Vector Regression

Chen et al. [201] proposed a hybrid model (HGSO-SVR), which integrates the HGSO algorithm with the Support Vector Regression (SVR) model, to predict the compressive strength of admixed concrete containing fly ash and microsilica. Comparative analysis demonstrated that the HGSO-SVR model significantly outperformed the PSO-SVR model, achieving fitness values of 1.4156 and 1.5419, respectively, thereby confirming the superior accuracy of the HGSO-SVR model in compressive strength prediction.

The hybrid models (SVR-HGSO, SVR-EO, GMDH-EO, and GMDH-HGSO) were developed in the work of Javadi et al. [200] to predict sediment discharge (Qs) in free-flow flushing by integrating SVR and Group Method of Data Handling (GMDH) with HGSO and EO. Using 160 datasets from Janssen's experimental study, the models were trained with input parameters including reservoir water level, bed level, inflow, outflow, and flushing time. Performance evaluation based on RMSE, MAE, R^2, and MARE showed that HGSO and EO improved GMDH accuracy by up to 26 and 22%, respectively. Among all models, SVR-EO and SVR-HGSO achieved the highest accuracy ($R^2 = 0.98$ training, $R^2 = 0.96$ validation), while GMDH-HGSO demonstrated the best overall performance ($R^2 = 0.96$, RMSE = 22.37), making it the most recommended model for sediment transport prediction.

Two hybrid models, SVR-HGSO and SVR-PSO, were proposed in the work of Kumar and Robinson [199] to predict pile settlement (PS) accurately. The SVR-HGSO model is based on SVR coupled HGSO, while the SVR-PSO model integrates SVR with PSO to fine-tune model parameters. Performance evaluation using five metrics demonstrated the superiority of SVR-HGSO, achieving an RMSE of 0.29 mm (compared to 0.46 mm for SVR-PSO), and an MAE of 0.278 mm–57.10% lower than SVR-PSO. The OBJ value further validated the accuracy of SVR-HGSO at 0.283 mm, confirming its effectiveness for precise pile settlement estimation.

Wu and Yang [198] proposed two hybrid models, HGSO-SVR and CSO-SVR, for predicting the compressive strength (CS) of high-performance concrete (HPC) incorporating blast furnace slag (BFS) and fly ash (FA). SVR was employed for regression, while HGSO and CSO optimize its parameters to enhance predictive accuracy. Both models were trained on 1030 experiments and eight input variables, including admixtures, aggregates, and curing age. The findings confirm the best performance of the HGSO-SVR model by achieving superior accuracy and a significantly lower RMSE compared to the CSO-SVR model.

3.3.24 Hybridization with Long Short-Term Memory

A hybrid model (SHGSO-LSTM) based on the combination of HGSO, Long Short-Term Memory (LSTM), and Gated Recurrent Unit (GRU) was proposed in the work of Kathavate et al. [197] for lipoprotein detection, addressing sequence prediction challenges in spirochaetes. The model extracts correlation features, enhanced log energy entropy, raw features, and semantic similarity features. The proposed approach improves prediction accuracy, overcoming limitations in existing bacterial lipoprotein detection methods.

3.3.25 Hybridization with Random Forest

Islam et al. [196] developed a novel optimized classifier (HGSORF) based on the hybridization of the HGSO algorithm with Random Forest (RF) model for C-Section (CS) and non-CS classes classification. The efficiency of the proposed HGSORF classifier was assessed using noisy Real-world CS datasets such as the Pakistan Demographic and Health Survey (PDHS) datasets. Experiments revealed that the HGSORF method provides the highest accuracy of 98.33% compared with other frequently used optimization algorithms.

In the work of Jeyalakshmi et al. [195], a hybrid model (MKELMRF-OHGSA) was proposed for detecting and isolating Denial-of-Service (DoS) attacks in WSNs. This model integrates Oppositional HGSO (OHGSO), Random Forest, and Mixed Kernel Extreme Learning Machine (MKELM). The MKELMRF-OHGSA model was evaluated using six performance metrics including detection rate, network lifetime, packet delivery ratio, accuracy, false alarm rate, and throughput. Experimental results show that the proposed MKELMRF-OHGSA algorithm achieves an average detection rate of 98%, outperforming other existing methods.

3.3.26 Hybridization with Artificial Neural Networks

Rabikumar and Kavitha [194] developed a hybrid approach (CNN-OHGS) that combined the HGSO algorithm with the CNN model for an autonomous vehicle control system. The CNN-OHGS approach was used to minimize the distance variations among the vehicles and ensure safety. Conducted simulations demonstrated the CNN-OHGS's performance compared to other existing optimization approaches.

A hybrid model (HGSO-ANN), based on the combination of HGSO with ANN, was proposed in the work of Mishra et al. [193] for early detection of bearing faults in rotating machines. The performance of the proposed HGSO-ANN approach was evaluated under constant and varying speed conditions. Experimental validations confirm the hybrid model's effectiveness in preventing unplanned bearing failures, showcasing its reliability and potential.

Sadiq et al. [192] proposed a combined approach (HGSO-FFNN) based on the integration of the HGSO algorithm with the feed-forward neural network (FFNN) for solving the alcoholic EEG signals recognition problem. The hybrid approach was validated in comparison with 11 well-known classifiers such as FFNN, SVM, RF, Recurrent Neural Network (RNN), Linear Discriminate Analysis (LDA), and K-nearest Neighbor (KNN) with Euclidean distance, KNN with city block distance, Generalized Regression Neural Network (GRNN), Neural Network (NN) and Multilayer NN (MNN). Simulation results demonstrated the efficiency of the hybrid algorithm compared to existing approaches in the literature in terms of evaluation metrics used in classification.

Elwin et al. [191] proposed a hybrid Autoregressive-Henry Gas Sailfish Optimization algorithm with a deep learning approach, called Ar-HGSO, for solving the diabetic retinopathy detection problem. The performance of the Ar-HGSO algorithm was tested using both IDRID and DDR datasets. Compared to CNN, Synergic Deep learning, Deep-CNN, DNN, and EWKPC + HGSO-based DCNN methods, the Ar-HGSO achieves the best results in terms of accuracy, specificity, and sensitivity metrics.

Li et al. [190] developed a hybrid model (HGSO-ADBN) combining HGSO with an adaptive deep belief network (ADBN) for enhancing aero-engine sensor fault diagnosis. The HGSO-ADBN model was assessed using measured and simulated aero-engine data considering convergence speed and accuracy metrics. Experimental validations confirm the superiority of the proposed approach, achieving a diagnostic accuracy of 98.1% and reducing computation time to 98 s.

A hybrid model (HGWWO) based on the combination of HGSO, CNN, Deep Generative Adversarial Network (Deep GAN), U-Net, and Water Wave Optimization (WWO), was developed in the work of Kalpana et al. [189] for COVID-19 detection. The HGWWO approach integrates image pre-processing using the Region of Interest (RoI) and median filtering, lung lobe segmentation with U-Net, and feature extraction via CNN. Experimental results showed the HGWWO model's effectiveness, achieving a testing accuracy of 91.69%, sensitivity of 93.28%, and specificity of 90.32%.

Patra et al. [188] introduced a hybrid approach (HSLnO-SSWOA-DQN) based on the combination of HGSO with Deep Q Network (DQN) and two optimization algorithms for medical data classification. The proposed HSLnO-SSWOA-DQN approach integrates data normalization for pre-processing and classification with a DQN optimized by SSWOA. Experimental results demonstrated the effectiveness of the proposed approach, providing a maximum accuracy of 95.41%, specificity of 95.36%, and sensitivity of 95.65%.

A hybrid model (HGSO-FHDF) was developed by Ragab et al. [187] for automated brain cancer classification by integrating handcrafted and deep features. The proposed HGSO-FHDF model employs Gabor filtering (GF) for noise reduction and Tsallis entropy-based segmentation to identify tumor regions in MRI images. Feature extraction was performed using a fusion of handcrafted features and deep features from a Residual Network (ResNet). The performance of the hybrid model was evaluated on the BRATS 2015 dataset, demonstrating its effectiveness in brain tumor detection and classification.

Fayaz et al. [186] introduced a new hybrid approach (HHGSO-DL), based on the hybridization of the HGSO algorithm with Deep Learning model, for LED driver system design. The performance of the proposed HHGSO-DL approach was investigated on ED luminaire and LED chip packaging with thermal aging loading. Conducted experimental results showed the promising performance of the proposed HHGSO-DL compared to state-of-the-art approaches.

Arivalahan et al. [185] proposed a hybrid approach, called CHGSO-FAT, based on the hybridization of the Chaotic HGSO and FeedBack Artificial Network for optimizing the Fractional Order Proportional Integral Derivative (FOPID) controller system. The robustness of the CHGSO-FAT approach was evaluated using 100, 150, 200, 250, and 500 trails. Results revealed that the CHGSO-FAT algorithm outperforms both PSO and GA algorithms in terms of computation time and fitness value metrics.

The authors in [184] proposed a hybrid model (HGSO-DLFER) integrating HGSO with deep learning for facial emotion recognition (FER) in human-computer interaction (HCI). The HGSO algorithm performs hyperparameter optimization, while adaptive fuzzy filtering (AFF) removes noise and MobileNet extracts features. Experimental validations confirm the superiority of the HGSO-DLFER model, achieving a maximum accuracy of 98.65%, outperforming conventional FER techniques.

Roy and Dutta [183] developed a hybrid method (HGSO-ADBN), based on the combination of the Adaptive Deep Belief Network (ADBN) and HGSO algorithm, for enhancing the Group Recommender System. The HGSO-ADBN method was evaluated using four different datasets and compared to the SVM, DNN, NN, and DBN models. Simulation results proved the superiority of the proposed model in terms of MAP metric.

Arumugasamy and Arokiasamy [182] proposed a hybrid model (THGSO-DRN), based on the hybridization of HGSO and Deep Residual Network (DRN), for fruit ripeness classification. The effectiveness of the THGSO-DRN model was validated based on fruit images which are preprocessed with Gaussian filtering. The proposed THGSO-DRN provided maximum accuracy of 92.5%, specificity of 90.5%, and sensitivity of 93.5% demonstrating enhanced fruit ripening classification performance and prediction capabilities.

Karthika et al. [181] introduced a novel hybrid control technique (CHGSO-RENNN) for small signal stability analysis for microgrids under uncertainty. The proposed CHGSO-RENNN technique is based on the combination of chaotic HGSO and recalling-enhanced recurrent neural network (RENNN), which is used to optimally predict the internal and external current loop control parameters. Experimental results revealed the efficiency of the proposed CHGSO-RENNN for optimal tuning of PI controller gain parameters.

Tripathi and Sharma [180] proposed an optimal trust and secure (MDML-CHGSO) approach for fog-based Vehicular ad hoc network (VANET). The proposed MDML-CHGSO approach is based on the combination of chaotic HGSO algorithm and modified deep metric learning model. Experiments showed the MDML-CHGSO's effectiveness to provide a trust-based security design in terms of average latency, throughput, and packet delivery ratio metrics.

Escorcia-Gutierrez et al. [179] developed a new traffic flow forecasting model (HGSODL-TFF), based on the hybridization of HGSO with Deep Belief Network (DBN), for 6G enabled vehicular networks. The performance of the proposed HGSODL-TFF model was validated on test data under several aspects and results reported the superiority of the HGSODL-TFF model when compared to other recent optimization approaches.

A hybrid control system (RERNN-CHGSO) based on the combination of Recalling Enhanced Recurrent Neural Network (RERNN) with Chaotic HGSO algorithm was developed in the work of Meenalochini et al. [178] for an extended switched coupled inductor quasi-z-source inverter in grid-connected photovoltaic (PV) systems. The proposed RERNN-CHGSO system was evaluated under various conditions taking into account the parameters of power, voltage, current, and total harmonic distortion (THD). Simulation results demonstrated the efficiency of the hybrid RERNN-CHGSO system compared to other existing control models.

Two hybrid models, RBF-HGSO and RBF-PSO, were proposed in the work of Li [177] to predict the compressive strength of high-performance concrete. The RBF-HGSO model combines the Radial Basis Function (RBF) neural network with HGSO, while the RBF-PSO model integrates the RBF neural network with PSO. The RBF-HGSO model outperformed RBF-PSO, achieving a RMSE of 2.5629 compared to 2.6583, demonstrating its superior accuracy in predicting the compressive strength of high-performance concrete.

Ninu [176] proposed an intrusion detection system (EHGSO-DNFN) for Mobile Ad hoc Networks (MANETs) based on Exponential-HGSO algorithm (EHGSO) and Deep Neuro Fuzzy Network. The Exponential Weighted Moving Average strategy was integrated into The HGSO algorithm for optimal route selection. Simulation results demonstrated the high performance of the proposed EHGSO-DNFN system compared to other existing optimization methods considering the metrics of packet drop, energy, throughput, jitter, recall, and precision.

A hybrid model (MAFCNN-SCD) was proposed in the work of Obayya et al. [175] for the detection and classification of skin cancer. The model integrates three advanced methods: Multi-Attention Fusion Convolutional Neural Networks (MAFNet), HGSO, and Deep Belief Networks (DBN). The effectiveness of the MAFCNN-SCD model was validated on two benchmark datasets including the ISIC 2017 database and the HAM10000 database. Simulation results demonstrated the superior performance of the MAFCNN-SCD model compared to other state-of-the-art techniques.

A novel approach, LHGSO-DFC, was introduced by Kumar et al. [174] to enhance image retrieval efficiency. LHGSO-DFC integrates the Lion HGSO algorithm with the Deep Fuzzy Clustering (DFC) model. Experimental results showed significant improvements in retrieval performance, achieving F-measure, precision, and recall values of 0.887, 0.891, and 0.882, respectively.

A novel hybrid model, HGSO-WIB-ReLU, integrating HGSO algorithm with CNN architecture featuring the Weight Initialization-Based Rectified Linear Unit (WIB-ReLU), was proposed by Lakshmanan et al. [173] to detect various types of DoS attacks, including HTTP, DNS, and ICMP flood attacks. Experimental evaluations on benchmark datasets (BUET-DDoS2020, CIC-DoS Attacks, and Low Rate DDoS) showcased exceptional performance, achieving accuracy rates of 97, 96.67, and 96%, respectively. These results highlight the model's effectiveness and superiority over state-of-the-art methods in accurately identifying low-rate DoS attacks.

The authors in [172] developed two hybrid models, RBHG and RBMV, to enhance the prediction of High-Performance Concrete (HPC) properties. RBHG integrates the Radial Basis Function Neural Network (RBFNN) with HGSO, while RBMV combines RBFNN with MVO. Experimental validations on 181 HPC mixtures confirm the superiority of RBMV, achieving an RMSE of 3.7 mm for slump (43.2% lower than RBHG) and 3.66 MPa for compressive strength (compared to 5 MPa for RBHG). With an R^2 of 98.25%, RBMV surpasses RBHG (96.86%), demonstrating a more efficient and accurate approach for modeling HPC hardness properties.

Ponnupila Omana et al. [171] proposed a hybrid approach (HGBSO-DCNN) that integrates HGSO algorithm with Deep Convolutional Neural Network (DCNN) to address the brain tumor classification. Data augmentation was used for enhanced classification accuracy. The proposed HGBSO-DCNN approach demonstrated superior performance, achieving 92.21% accuracy, 93.24% sensitivity, and 92.95% specificity, showcasing its effectiveness and reliability in accurately classifying brain tumors.

A hybrid model (SHGSO-DMN), combining the Squirrel HGSO algorithm with the Deep Maxout Network (DMN), was proposed by Nirmala Priya [170] for detecting image forgeries. The SHGSO-DMN model demonstrated outstanding performance, achieving an accuracy of 95.07%, a True Negative Rate (TNR) of 95.68%, and a True Positive Rate (TPR) of 95.17%, surpassing existing forgery detection techniques.

A hybrid approach (FHGO-CNN), which integrates fractional HGSO with CNN, was proposed in the work of Ramya et al. [169] for E-waste management in IoT applications. When compared to existing methods such as traditional deep learning, TensorFlow-based deep learning, Cuckoo Search-based neural networks, and machine learning, the proposed FHGO-CNN approach demonstrates superior accuracy, achieving improvements of 19.49, 18.05, 12.77, and 7.89%, respectively.

3.3.27 Hybridization with Other Methods

A hybrid model named HGSO-RVFL, combining the HGSO algorithm with the Random Vector Functional Link (RVFL) network, was proposed in the work of Shehabeldeen et al. [145]. The HGSO-RVFL model was used to predict the ultimate tensile strength (UTS) of AA6061-T6 aluminum alloy joints. The validity of the HGSO-RVFL model was tested, demonstrating its effectiveness in accurately predicting the UTS of friction stir welded (FSW) joints.

Ahmed et al. [144] presented an innovative approach for streamflow time series forecasting problem by integrating physics-inspired metaheuristic algorithms: Henry Gas Solubility Optimization-Multi-Layer Perceptron (HGSO-MLP), Equilibrium Optimization-Multi-Layer Perceptron (EO-MLP), and Nuclear Reaction Optimization-Multi-Layer Perceptron (NRO-MLP). A 130-year dataset from the High Aswan Dam (HAD) was employed to assess model performance against conventional neural networks (MLP, RNN) and nine hybrid MLP-based metaheuristic models. The findings reveal that Physics-MLP models outperform both Swarm-MLP and evolutionary-MLP models in accurately capturing streamflow patterns.

Zamli et al. [143] proposed a hybrid approach, called HHGSO, based on the hybridization of the HGSO algorithm with dynamic cluster-to-algorithm mapping for solving the Search-based Software Engineering Problems. The performance of the HHGSO algorithm was evaluated using IMDB and DBLB datasets using various number of required skills. Compared to Jaya Algorithm (JA), Sooty Tern Optimization Algorithm (STOA), Butterfly Optimization Algorithm (BOA), Owl Search Algorithm (OSA), and traditional HGSO algorithm, the HHGSO approach obtained the best cost, number of team members, average cost, and average time.

A hybrid model (HGSO-based UKF) was developed in the work of Aganathan et al. [142] for multi-object tracking. The HGSO-based UKF was utilized to improve tracking precision by modifying the Unscented Kalman Filter (UKF) with Henry Gas Solubility Optimization (HGSO). Experimental results demonstrated the effectiveness of the HGSO-based UKF model, achieving an accuracy of 92%, multiple object tracking precision (MOTP) of 87.6%, sensitivity of 91.7%, and specificity of 92%, outperforming conventional methods.

4 Applications of the Henry Gas Solubility Optimization Algorithm

4.1 Engineering

This section investigates the applications of the HGSO algorithm as summarized in Table 7. Yildiz et al. [112] applied the HGSO algorithm for the optimum shape and design of vehicle components in the automotive industry. The HGSO algorithm was assessed based on a finite element analysis taking into account the mass objective function under a stress constraint. Experimental results showed the ability of the HGSO algorithm to design better optimal vehicle components compared to other optimizers in the literature.

The HGSO algorithm was utilized in the work of Ekinci et al. [208] for optimizing the parameters of a FOPID controller. Its efficiency was demonstrated through box plots and convergence analyses. Performance comparisons with other methods, including SSA, Stochastic Fractal Search (SFS), and Improved Kidney Algorithm (IKA), based on transient and frequency response analyses, revealed that the HGSO algorithm outperformed the alternatives in simulation results.

In [140], the authors applied the HGSO algorithm to optimize the Combined Heat and Power Plant (CHPP) system. The HGSO algorithm's performance was validated in four scenarios using different external exchangers. Simulation results showed that the HGSO algorithm achieved good results considering the metrics of energy, exergy, and cost.

Ekinci et al. [209] applied the HGSO algorithm to obtain optimal parameters for a power system stabilizer (PSS) and enhance its dynamic performance. The HGSO algorithm was validated using a single-machine infinite-bus system and compared with ASO and conventional PSS controllers. Experimental results showed that HGSO gives better statistical performance and convergence ratio in tuning the PSS parameters.

Nguyen et al. [210] used the HGSO algorithm to search for optimum parameters of a landslide susceptibility application in Vietnam's mountainous regions. The performance of the HGSO algorithm was assessed using 13 features taken from Ha Giang mountain with RMSE as the objective function. Simulation results showed that the HGSO algorithm can be considered as a promising and alternative solution for adaptive weights of the deep neural network.

Ebrahim et al. [211] used the HGSO algorithm to optimize the Microgrid Droop Controller parameters. The HGSO algorithm was tested in two different cases, such as Fixed Cyclic Load in Islanding Mode, and Continuous Cyclic Load in Islanding Mode. Compared to both PSO and ALO algorithms, the HGSO algorithm obtained the best results regarding the fitness value.

Idir et al. [212] suggested a high-performance FOPID controller based on the HGSO algorithm for the direct current (DC) motor control. The performance of the HGSO-FOPID controller was assessed considering disturbance rejection analyses, transient and frequency responses, and index of performance and compared with various well-known controller approaches such as PSO-PID, ASOA-PID, SCA-PID, GWO-PID, IWO-PID, SFS-PID. Results revealed that the proposed HGSO-FOPID controller gives better performance with lower settling time.

Mousakazemi [213] applied the HGSO algorithm to control and optimize PID gains for the load-following operation of a nuclear power plant reactor. The HGSO's performance was validated using the integral of the time-weighted square error (ITSE) index as the fitness (cost) function, which was constrained by a stability condition based on a Lyapunov synthesis. Simulation results showed that the HGSO algorithm provides good accuracy with the least error compared to GA.

The HGSO algorithm was applied in the study of Qi et al. [214] to optimize a multi-cell Linear Parameter Varying (LPV) model. The main principle is based on selecting the best steady-state points, thereby enhancing model accuracy and reducing redundancy. Simulation results validate the effectiveness of the HGSO algorithm, demonstrating a strong correlation between the LPV and nonlinear models, ensuring robust and efficient aero-engine control.

The HGSO algorithm was used in the work of Liu et al. [215] to optimize the PI controller parameters for the trajectory planning of a 9-DOF redundant manipulator. Experimental validation on the 9-DOF redundant manipulator demonstrates superior trajectory tracking accuracy, confirming the efficiency and effectiveness of the proposed approach.

The authors in [120] applied the HGSO algorithm to enhance flyrock distance (FD) prediction in mine blasting. Evaluated on 222 blast records, the HGSO model outperformed baseline and hybrid ANFIS models, achieving a determination coefficient of 0.924 and a system error of 18.112. Sensitivity analysis identified blast hole diameter (0.97%) as the most influential parameter. The results confirm the superior efficiency of the HGSO model, making it a reliable tool for predictive modeling in blasting operations.

Kumar and Kumar [216] applied the HGSO algorithm for optimal routing in heterogeneous wireless sensor networks. The main objective is to ensure performance regarding energy efficiency, scalability, self-healing, and self-reconfigurability. Experimental results showcased the effectiveness of the HGSO algorithm over other methods in terms of throughput and energy consumption.

4.2 Power and Energy

The HGSO algorithm was used in the work of [113] to address Maximum Power Point Tracking (MPPT) in Photovoltaic (PV) systems. The HGSO technique was validated in five different weather and operating conditions and compared with several state-of-the-art methods, including Perturb and Observe (P&O), PSO, DOA, CSA, and GOA. The results showed that the HGSO technique improves power efficiency by 1-4%, reduces tracking time by 15-30%, settling time by 20%, and oscillation by 80% compared to other methods, with strong performance across seasons.

In [118], authors presented the HGSO algorithm to optimize the fuel consumption for the Vehicle Routing Problem. Simulation results proved the superiority of the HHGSO algorithm compared to SA, TS, and hybrid PS in terms of fuel consumption, computational time under various numbers of gas, iteration, and KPL on fuel consumption and computation time.

Singh and Sandhu [217] applied the HGSO algorithm for estimating Proton Exchange Membrane Fuel Cell (PEMFC) parameters. The algorithm's performance was evaluated using ten benchmark functions and compared with five other methods. Additionally, validation was carried out on three PEMFC models (SR-12, BCS-500 W, and NedStack PS-6), with results compared to real data. The findings show that the HGSO algorithm provides superior performance, with faster convergence, reduced errors, and shorter processing times compared to other algorithms.

The authors in [218] applied the HGSO algorithm for optimal Phasor Measurement Unit (PMU) placement in power systems. The HGSO algorithm minimizes the number of PMUs while ensuring full observability by considering system topology and Zero Injection Buses (ZIBs). Experimental validation on IEEE 14-bus and 30-bus systems demonstrates that incorporating ZIBs reduces the required PMUs while maintaining full network observability. Additionally, a state estimation analysis confirms the effectiveness of the HGSO algorithm in reducing estimation errors, outperforming conventional placement strategies.

Haider et al. [219] applied the HGSO algorithm for optimal load scheduling in smart grids. The HGSO's performance was evaluated under various pricing schemes taking into account adaptive consumption level pricing and time-of-use, compared with other works existing in the literature. Experiments demonstrated the efficiency of the HGSO algorithm in terms of peak power demand reduction and substantial energy cost savings.

Hemeida et al. [220] applied the HGSO algorithm to optimally tune PI controller parameters for a Static VAR Compensator (SVC), enhancing voltage and angle stability in power systems. Experimental validation under three-phase short circuit faults and mechanical disturbances demonstrates the superiority of the HGSO-optimized SVC over conventional PI controllers.

In the work of Mousakazemi [221], the HGSO algorithm was applied to enhance the pressurized light-water nuclear reactor (PWR) parameters model. The HGSO algorithm was evaluated in short and long-term operations and compared to the standard PSO algorithm. Simulation results demonstrated that the HGSO algorithm enhanced significantly PWR usage by obtaining the best least overshoot/undershoot and steady-state error.

In [222], authors adapted the HGSO algorithm to optimize the water transportation delay and penstock head loss in the short-term hydrothermal scheduling problem. The performance of the HGSO algorithm was validated using seven hydro units and eight thermal units. Results showed that the HGSO algorithm outperforms the SOS, IMO, SCA, and CSA approaches in terms of cost and computational time.

In the work of Rishehri and Ansarifar [223], the HGSO algorithm was used for optimizing the small modular reactor core loading with dual-cooled fuel. The performance of the HGSO algorithm was validated considering safety and dynamic parameters such as convective heat transfer coefficients and temperature reactivity feedback coefficients. Experiments showcased the efficiency of the HGSO algorithm when compared with PSO, GA, and GWO algorithms.

4.3 Classification

In [105], the HGSO algorithm was applied to tackle the feature selection problem. The efficiency of the HGSO approach was validated using over eighteen datasets with a wide range of feature sizes (small, medium, and high) and five evaluation criteria. Experimental results showed that the proposed HGSO algorithm obtained superior results versus five competitor meta-heuristics methods such as GWO, GOA, DA, SSA, and WOA.

Cao et al. [224] applied the HGSO algorithm for optimizing SVR parameters and obtaining good prediction stability. The HGSO algorithm was validated using ten low- and high-dimensional benchmark datasets in terms of prediction accuracy, convergence performance, and computational complexity. Experimental results revealed that the HGSO algorithm gives optimal comprehensive performance compared with six well-known algorithms such as HHO, SSA, DA, ALO, PSO, and FA.

The HGSO algorithm was applied in the work of Elwin et al. [191] for Diabetic Retinopathy (DR) detection and severity classification based on color fundus images. Evaluated on the IDRID and DDR datasets, the HGSO approach outperforms existing methods, achieving testing accuracy of 0.9142, sensitivity of 0.9254, and specificity of 0.9142 on the IDRID dataset.

In [225], authors applied HGSO to solve the feature selection problem. The efficiency of the HGSO algorithm was assessed using ten datasets considering two main objectives such as Error Rate (ER) and feature Reduction Rates (RR). Results showed that the HGSO algorithm provides higher performance compared to EO, FA, and PSO algorithms in terms of accuracy and number of features

Elden et al. [226] adapted the HGSO algorithm to enhance the feature selection process in the pediatric sepsis detection problem. The effectiveness of the HGSO algorithm was evaluated using the GSE66099 microarray dataset and compared to various meta-heuristics such as SCA, Tree Growth Optimization (TGO), EO, Atom Search Optimization (ASO), SSO, PSO, GWO, Poor and Rich Algorithm (PRA), and GA. Results showed that, using the HGSO, the SVM classifier achieved the best results in terms of accuracy, specificity, sensitivity, and AUC metrics.

Authors in [227], used the HGSO algorithm for solving the feature selection problem in the maintenance prediction system. The robustness of the HGSO algorithm was evaluated using five different datasets. Simulation results demonstrated the efficiency of the HGSO algorithm based Serial Cascaded deep learning model obtained the best performance compared to state-of-the-art classifiers.

Devi and Sriramya [228] applied the HGSO algorithm for designing a blockchain to perform traceability of drugs. The main principle is the registration of drugs in the blockchain, which then generates a secret key obtained using the HGSO algorithm. Simulation results demonstrated the superiority of the HGSO algorithm achieving the memory, response time, privacy, and normalized variance of 84 MB, 32.678 sec, 0.958, and 0.958, respectively.

4.4 Image Processing

The HGSO algorithm was applied in the work of Kurban et al. [229] for multilevel color image thresholding. The study compared six nature-inspired algorithms, including HGSO, EO, PO, TFWO, MPA, and SMA, using aerial images obtained by drones. The segmentation results were evaluated using Structural Similarity Index Measure (SSIM), Peak Signal-to-Noise Ratio (PSNR), Blind/Referenceless Image Spatial Quality Evaluator (BRISQUE), Perception-Based Image Quality Evaluator (PIQE), Natural Image Quality Evaluator (NIQE), and CPU time consumption. Experimental analysis showed that MPA and TFWO outperformed other algorithms in terms of image quality metrics and computational efficiency.

Mishra and Pal [230] used the HGSO algorithm for bi-level thresholding-based image segmentation to detect COVID-19 infections in CT images. The HGSO method's efficiency was validated on publicly available COVID-19 CT images using Peak Signal-to-Noise Ratio (PSNR), Mean Squared Error (MSE), Structural Similarity Index Measure (SSIM), and Feature Similarity Index Measure (FSIM). Comparative analysis with SCA, SSA, GWO, CPSOGSA, and MFO-based segmentation methods demonstrated the superiority of the HGSO algorithm in medical image segmentation.

Authors in [231] utilized the HGSO to optimize the extraction of phenolic compounds from Haloxylon scoparium using ultrasound-assisted extraction (UAE). The HGSO-optimized UAE achieved a maximum phenolic compound yield of 191.88 mg GAE/g DM, significantly exceeding the 105.87 mg GAE/g DM obtained through maceration. This optimized extraction method demonstrates strong potential for pharmaceutical and food applications.

5 Results and Comparison

In this section, we assess the efficiency of HGSO by comparing it with fourteen well-known optimization algorithms including FA, BA, GWO, MFO, MVO, SCA, SAO, LCA, ALO, BBO, CSO, FPA, PSO, AOA algorithms. The experiments are conducted using 30 search agents over 500 iterations. The parameter settings for each algorithm are provided in Table 8.

The performance of HGSO is assessed using 23 IEEE CEC benchmark functions, which are categorized into three groups: unimodal, multimodal, and fixed-dimension numerical optimization problems. The details of these functions, including their search range, dimension (Dim), and theoretical optimum ($f_{\min}$), are summarized in Tables 9, 10, and 11. Additionally, a 2D visualization of these 23 benchmark functions is provided in Fig. 13.

Six performance metrics are used to comprehensively evaluate the optimization results, assessing the effectiveness and reliability of the algorithms:

- **Mean**: The average objective function value over multiple runs, indicating the algorithm's central tendency and overall performance.
- **Standard Deviation (SD)**: Measures the dispersion of results. A lower SD signifies greater consistency and stability, while a higher SD suggests increased variability.
- **Minimum (Min)**: The best (lowest) objective function value obtained across all runs, reflects the algorithm's optimal performance.
- **Maximum (Max)**: The worst (highest) objective function value obtained across all runs, representing the upper bound of performance variability.
- **Rank**: The relative ranking of each algorithm based on performance, with lower ranks indicating superior results.

- **P-value**: Assesses statistical significance; lower values suggest stronger evidence of a meaningful difference in performance.
- **Convergence Speed**: The rate at which an algorithm approaches the optimal solution. Faster convergence demonstrates an algorithm's efficiency in achieving high-quality solutions with fewer iterations, reducing computational cost.

The simulation results are detailed in Tables 11, 12, 13, and 14. For each function, the HGSO algorithm achieves the best or among the best values in terms of minimum (Best), maximum (Worst), mean, and standard deviation (Std), indicating both accuracy and robustness. Notably, for unimodal functions such as F_1 to F_7, the HGSO algorithm effectively converges to the global optimum with minimal variance, showcasing its strong exploitation capabilities. For multimodal functions (F_8 to F_{13}), the algorithm maintains a high level of performance despite the increased complexity and number of local optima, reflecting a well-balanced exploration-exploitation strategy. Although HGSO does not achieve the best performance on all composite and hybrid functions (F_{14} to F_{23}), it remains competitive, often ranking among the top-performing algorithms. In many cases, it outperforms or matches the performance of well-established metaheuristics such as BA, FA, GWO, MFO, and MVO based on statistical indicators. The relatively consistent top rankings of the HGSO algorithm across most functions, supported by low p-values (typically < 0.05), confirm the statistical significance of its performance. Overall, these results validate the effectiveness, stability, and generalization ability of HGSO across a diverse set of optimization problems.

The box plots in Fig. 14 depict the performance distribution of the optimization algorithms across the 23 benchmark functions $F_1 - F_{23}$. For unimodal functions (F1–F7), the HGSO algorithm consistently achieves superior performance with minimal variance, particularly evident in F1, F3, F5, and F6 where it reaches near-zero optimal values while other algorithms show considerably higher scores and greater variability. For multimodal functions (F8–F23), the performance landscape becomes more complex, with HGSO maintaining competitive performance but showing occasional challenges in functions like F9, F16, and F19 where other algorithms like GWO or MVO demonstrate better convergence. Overall, the HGSO algorithm exhibits the most consistent performance across the majority of benchmark functions, demonstrating its robustness and effectiveness as an optimization algorithm for diverse problem landscapes.

As illustrated in Fig. 15, for unimodal functions (F1–F12), the HGSO algorithm demonstrates exceptional convergence behavior, consistently achieving rapid descent to near-optimal values within the first 50-100 iterations and maintaining stable solutions thereafter. Most competing algorithms show significantly slower convergence rates and often stagnate at suboptimal fitness levels, with several algorithms failing to achieve meaningful improvement beyond the initial iterations. The convergence gap between the HGSO algorithm and other algorithms is particularly pronounced in functions F1, F2, F3, and F6, where HGSO reaches fitness values several orders of magnitude better than its competitors. For multimodal functions (F13–F23), the performance landscape becomes more competitive, with several algorithms showing comparable convergence trajectories. While the HGSO algorithm maintains strong performance across most functions, algorithms like MFO, FA, and BBO demonstrate competitive convergence in certain cases, particularly in F15, F17, and F21. The convergence curves reveal that multimodal functions present greater challenges for all algorithms, with more gradual descent patterns and occasional premature convergence. Overall, the HGSO algorithm exhibits superior consistency and convergence speed across the majority of benchmark functions, establishing its effectiveness for both unimodal and multimodal optimization problems.

Figure 16 illustrates the Friedman test results performed on the mean fitness value for each compared algorithm across the 23 benchmark functions. Based on the mean rank, we can notice that the HGSO offers a mean rank of 6.65 against the highest rank of 14.83 provided by BA and the lowest one given by GWO. Thus, we can conclude that, the HGSO algorithm provides an average score. Results showed that, the p-value is less than 0.05, which means that their is at least, one significant difference between the HGSO and the other algorithms.

To further validate the efficiency of the HGSO algorithm, several HGSO variants were developed and evaluated as follows:

- **CHGSO**: HGSO enhanced using chaotic maps to improve population diversity and search ergodicity.
- **LHGSO**: HGSO integrated with Lévy flight to enable large exploratory jumps for better global search.
- **OHGSO**: HGSO improved by incorporating opposition-based learning to guide the search toward better regions.
- **MHGSO**: HGSO modified with mutation operators to enhance exploitation and local refinement.
- **CLHGSO**: Combines chaotic maps and Lévy flight in HGSO to balance exploration and randomness.
- **COHGSO**: Combines chaotic maps and opposition-based learning to boost population initialization and search direction.
- **CMHGSO**: Uses chaotic maps and mutation operators in HGSO to reinforce both diversity and refinement.
- **LOHGSO**: Integrates Lévy flight and opposition-based learning to merge exploration strength with guided search.

Table 7 Applications of HGSO algorithm

Class	Problem	Research works
Engineering	Optimum shape and design of vehicle components	Yildiz et al. [112]
	FOPID controller optimization	Ekinci et al. [208]
	Welded beam design, tension/compression spring design, and speed reducer design problems	Hashim et al. [104]
	Power system stabilizer parameters optimization	Ekinci et al. [209]
	Landslide susceptibility application in Vietnam's mountainous regions	Nguyen et al. [210]
	Microgrid Droop Controller parameters optimization	Ebrahim et al. [211]
	Direct current motor control	Idir et al. [212]
	PID gains control and optimization	Mousakazemi [213]
	Detecting fake reviews in Social Media	Purohit et al. [232]
	Echo suppression in synthetic aperture radar	Chukka and Battula [233]
	Multi-cell linear parameter varying model optimization	Qi et al. [214]
	Fractional PID controllers in fuel cell choppers	Güven and Mengi [234]
	Trajectory planning of 9-DOF redundant manipulator	Liu et al. [215]
	Flyrock distance prediction in mine blasting	Ye et al. [120]
	Facial emotion recognition	Aleisa et al. [184]
	Forecasting Soil Friction Gradient	Lone et al. [235]
	Anomaly Detection in Rotary Equipments	Sangeetha et al. [236]
	Fractional Order PI-PD Controller for DC Motor Speed	Yaseen Taha and Oglah [237]
	Routing in heterogeneous wireless sensor networks	GKumar and Kumar [216]
	Mechanical design optimization	Mehta et al. [238]
	Optimal design of large-scale truss structures	Bodalal [239]
	Combined Heat and Power Plant system	Sukpancharoen and Prasartkaew [140]
Power and Energy	Maximum Power Point Tracking in Photovoltaic systems	Mirza et al. [113]
	Fuel consumption for the Vehicle Routing Problem	Utama et al. [118]
	Proton Exchange Membrane Fuel Cell (PEMFC) parameters estimation	Singh and Sandhu [217]
	Optimal Phasor Measurement Unit placement in power systems	Selim et al. [218]
	Optimal load scheduling in smart grids	Haider et al. [219]
	Voltage and angle stability in power systems	Hemeida et al. [220]
	Power conversion systems.	Mohd Zawawi et al. [240]
	Pressurized light-water nuclear reactor optimization	Mousakazemi [221]
	short-term hydrothermal scheduling problem	Das et al. [222]
	Optimal dual-cooled fuel configuration	Rishehri and Ansarifar [223]
	Wind and green hydrogen production optimization	Idriss et al. [241]
Classification	Feature Selection	Neggaz et al. [105], Legoui et al. [225], Chinta et al. [227], Elgazzar et al. [242]
	SVR parameters optimization	Cao et al. [224]
	Diabetic Retinopathy detection and severity classification	Elwin et al. [191]
	Pediatric sepsis detection and classification	Elden et al. [226]
	Optimal values of SVR key parameters	Esmaeili-Falak et al. [243]
	Disease detection and classification	Gokiladevi et al. [244]
	Multilevel thermoplastic waste segregation and classification	Vignesh and Monica Subashini [245]
	Brain tumour classification	Jegan et al. [246]
	Prostate cancer detection and classification	Reddy and Kathirvelu [247]
	COVID-19 detection	Ali et al. [248]
	Scalable bearing fault diagnosis	Nayana et al. [249]
	Blockchain with drug traceability	Devi and Sriramya [228]

Table 7 (continued)

Class	Problem	Research works
Image Processing	Multilevel color image thresholding	Kurban et al. [229]
	Bi-level thresholding-based image segmentations	Mishra and Pal [230]
	Automated brain cancer classification in MRI images	Ragab et al. [187]
	Extraction of phenolic compounds from Haloxylon scoparium	Ragab et al., Hamdellou et al. [231]

– **LMHGSO**: Applies Lévy flight and mutation operators to jointly promote wide search and local adjustment.
– **CLOHGSO**: Combines chaotic maps, Lévy flight, and opposition-based learning to provide strong global exploration with guided intensification.
– **CLMHGSO**: Incorporates chaotic maps, Lévy flight, and mutation operators to maintain diversity while supporting both exploration and exploitation.

Figure 17 illustrates the convergence of the HGSO and its variants. As shown, for the unimodal functions (F1–F12), the HGSO and its variants attain the near-optimal solution in the earlier iteration stage, which demonstrates the strength of the HGSO-based algorithms in the exploitation search. As for multimodal functions, the convergence gap between HGSO and its variants is clearly noticed. The OHGSO algorithm consistently exhibits robust performance across the majority of benchmark functions from F13–F23, while the CHGSO variant provides the worst performance in terms of convergence speed and efficiency.

The box plots of HGSO and its variants are represented in Fig. 18. Based on the figure, the HGSO, CHGSO, OHGSO, MHGSO, COHGSO, and CMHGSO algorithms provide the lowest median score, indicating better overall performance in the case of unimodal functions. While the other variants exhibit several outliers and a wider interquartile range. For multimodal functions, the HGSO and its variants show an irregularity in their behaviour, where we can notice a similarity of behaviour with the best performance in function F16.

Figure 19 shows the Friedman test results of HGSO and its variants. By analyzing the mean rank, we can notice that the best rank is given by MHGSO against the worst performance provided by the CLOHGSO algorithm.

6 Discussion and Future Works

The Henry Gas Solubility Optimization (HGSO) algorithm is a metaheuristic algorithm inspired by Henry's law, designed to effectively balance exploration and exploitation. It simulates the huddling behavior of gas molecules, which helps mitigate premature convergence and prevents the algorithm from getting trapped in local optima. To further enhance exploration, HGSO divides the population into clusters, each corresponding to an independent instance of the algorithm, thereby improving solution diversity. Additionally, it dynamically updates Henry's constant $\left(H_j\right)$ and gas solubility $\left(S_{ij}\right)$ using temperature-dependent equations derived from Van't Hoff's law, ensuring adaptability across iterations. As a result, experimental evaluations demonstrate that HGSO outperforms several well-established metaheuristic algorithms, including PSO, GWO, and WOA, in solving benchmark functions and real-world optimization problems [104].

However, the HGSO algorithm has several limitations. Firstly, its static cluster mapping restricts dynamic adjustments during iterations, which consequently reduces optimization efficiency in evolving search spaces. Secondly, its reliance on fixed parameter settings limits adaptability, especially in dynamic environments where real-time adjustments are crucial. Moreover, the computational overhead of the cluster-based approach poses scalability challenges, particularly for large-scale problems. In addition, like many metaheuristics, the HGSO's performance is highly sensitive to initial conditions, such as the initial population distribution. As a result, poor initialization can lead to premature convergence or an ineffective exploration of the search space.

The strengths and weaknesses of the HGSO algorithm are illustrated in Table 14. To address these issues, researchers have proposed various enhancements aimed at boosting its performance and adaptability across diverse optimization challenges, including chaotic, Levy flight, OBL, fuzzy, and hybridization with other approaches.

Introducing chaotic strategies into HGSO provides incredible convergence speed and efficiency. In addition, those strategies generate a uniformly distributed initial population, offering good population diversity. This approach seeks to overcome key limitations of the original HGSO algorithm, particularly its propensity for premature convergence and insufficient exploration, thereby enhancing overall optimization effectiveness. However, chaotic HGSO increases computation complexity by generating additional computations due to the chaotic map. Mainly,

Table 8 Parameter setting of the evaluated optimization algorithms

Parameter(s)	Value(s)
HGSO	
Gases number N	30
Cluster number	5
Constants M_1 and M_2	0.1 and 0.2
Constants β, α and K	1, 1, and 1
Constants $l_1, l_2, and\ l_3$	$5E-03$, 100, and $1E-02$
FA	
Minimum frequency f_{Min}	0
Maximum frequency f_{Max}	2
Initial loudness A_0	1
Initial pulse emission rate r_0	1
Loudness constant α	0.5
Emission rate constant γ	0.5
BA	
Frequency min f_{min}	0
Frequency max f_{max}	2
Loudness constant	0.5
Emission rate constant	0.5
Initial Loudness A_0	Random
GWO	
Control parameter $a1_{max}$	2
Control parameter $a1_{min}$	0
MFO	
Control parameter b	1
Convergence factor a_{min}	-2
Convergence factor a_{max}	-1
MVO	
Minimum of Wormhole Existence Probability WEP_{Min}	0.2
Maximum of Wormhole Existence Probability WEP_{Max}	1
BBO	
Keep rate	0.2
Migration influence α	0.9
Mutation Probability p_{mutation}	0.1
Parameter $c1$ in updating velocity	2
Parameter $c2$ in updating velocity	2
FPA	
Switch probability p	0.8
AOA	
Local interaction constant C_1	2
Global interaction constant C_2	6
Transfer control constant C_3	1
Direction switch constant C_4	2
Upper bound of normalized acceleration u	0.9
Lower bound of normalized acceleration l	0.1
Transfer function TF	Increasing from 0.36 to 1
Exploration-exploitation balance d	decreasing from 2.71 to 0
LCA	
Growth Power p	$\frac{2}{3}$

Table 9 Unimodal benchmark functions

Function	Description	Dimension	Range	$f_{\min}$
F1	$f(x) = \sum_{i=1}^{n} x_i^2$	10	[−100, 100]	0
F2	$f(x) = \sum_{i=0}^{n} \lvert x_i \rvert + \prod_{i=0}^{n} \lvert x_i \rvert$	10	[−10, 10]	0
F3	$f(x) = \sum_{i=1}^{d} \left(\sum_{j=1}^{i} x_j \right)^2$	10	[−100, 100]	0
F4	$f(x) = \max_i \left\{ \lvert x_i \rvert, 1 \le i \le n \right\}$	10	[−100, 100]	0
F5	$f(x) = \sum_{i=1}^{n-1} \left[100\left(x_i^2 - x_{i+1}\right)^2 + \left(1 - x_i\right)^2 \right]$	10	[−30, 30]	0
F6	$f(x) = \sum_{i=1}^{n} \left(\lvert x_i + 0.5 \rvert \right)^2$	10	[−100, 100]	0
F7	$f(x) = \sum_{i=0}^{n} i x_i^4 + \text{random}\,[0, 1)$	10	[−1.28, 1.28]	0

Table 10 Multimodal benchmark functions

Function	Description	Dimension	Range	$f_{\min}$
F_8	$f(x) = \sum_{i=1}^{n} \left(-x_i \sin\left(\sqrt{\lvert x_i \rvert} \right) \right)$	10	[−500, 500]	$-418.9829 \times n$
F_9	$f(x) = \sum_{i=1}^{n} \left[x_i^2 - 10\cos\left(2\pi x_i\right) + 10 \right]$	10	[−5.12, 5.12]	0
F_{10}	$f(x) = -20\exp\left(-0.2\sqrt{\frac{1}{n} \sum_{i=1}^{n} x_i^2} \right)$	10	[−32, 32]	0
F_{11}	$f(x) = 1 + \frac{1}{4000} \sum_{i=1}^{n} x_i^2 - \prod_{i=1}^{n} \cos\left(\frac{x_i}{\sqrt{i}} \right) + \exp\left(\frac{1}{n} \sum_{i=1}^{n} \cos\left(2\pi x_i\right) \right) + 20 + e$	10	[−600, 600]	0
F_{12}	$f(x) = \sum_{i=1}^{n-1} \left(y_i - 1\right)^2 \left[1 + 10\sin^2(\pi y_1)\right] + \sum_{i=1}^{n} u\left(x_i, 10, 100, 4\right)$, where $y_i = 1 + \frac{x_i + 1}{4}$	10	[−50, 50]	0
F_{13}	$f(x) = 0.1\left[\sin^2(3\pi x_1) + \sum_{i=1}^{n} (x_i - 1)^2 (1 + \sin^2(3\pi x_{i+1})) \right] + (x_n - 1)^2 (1 + \sin^2(2\pi x_n)) + \sum_{i=1}^{n} u(x_i, 5, 100, 4)$ $u(x_i, a, k, m) = \begin{cases} k(x_i - a)^m & x_i > a \\ 0 & -a \le x_i \le a \\ k(-x_i - a)^m & x_i < -a \end{cases}$	10	[−50, 50]	0

the adaptive HGSO-based methods aim to achieve a balance between the exploration and exploitation phases, which is one of the HGSO limitations. The balance is attained when the control parameters are adjusted dynamically as proposed in [110, 130], etc. However, this adjustment may lead to over-adaptation, causing a convergence instability. Lévy flight is a random walk distribution in which the step lengths are drawn from a heavy-tailed probability distribution that follows a power-law. This characteristic allows the HGSO's population to perform large jumps, discovering far areas and escaping from local optima. Despite that, the Lévy flight exhibits an instability in convergence and is highly sensitive to initial parameters. In the opposition-based learning HGSO algorithm, every candidate solution and its opposite are evaluated; only the best of the two is retained. The OBL guides the HGSO algorithm toward the promiscuous area where the probability of finding the global optimal solution is high. This strategy increases the accuracy and convergence efficiency. Despite that, the OBL-HGSO is not without limitations. One of the OBL-HGSO variant's drawbacks is the increased computational time and complexity due to the evaluation of both candidate and opposite solutions. Moreover, like other meta-heuristics, the OBL-HGSO-based approaches are highly problem-dependent and

Table 11 Fixed-dimension multimodal benchmark functions

Function	Description	Dimension	Range	$f_{\min}$
F_{14}	$f(x)=\left(\frac{1}{500}+\sum_{j=1}^{25}\frac{1}{j+\sum_{i=1}^{2}(x_i-a_{ij})}\right)^{-1}$	2	$[-65, 65]$	1
F_{15}	$f(x)=\sum_{i=1}^{11}\left[a_i-\frac{x_1(b_i^2+b_ix_2)}{b_1^2+b_ix_3+x_4}\right]^2$	4	$[-5, 5]$	0.00030
F_{16}	$f(x)=4x_1^2-2.1x_1^4+\frac{1}{3}x_1^6+x_1x_2-4x_2^2+4x_2^4$	2	$[-5, 5]$	-1.0316
F_{17}	$\left(x_2-\frac{5.1}{4\pi^2}x_1^2+\frac{5}{\pi}x_1-6\right)^2+10\left(1-\frac{1}{8\pi}\right)\cos x_1+10$	2	$[-5, 5]$	0.398
F_{18}	$f(x)=\left[1+(x_1+x_2+1)^2(19-14x_1+3x_1^2-14x_2+6x_1x_2+3x_2^2)\right] \times \left[30+(2x_1-3x_2)^2(18-32x_1+12x_1^2+48x_2-36x_1x_2+27x_2^2)\right]$	2	$[-2, 2]$	3
F_{19}	$f(x)=-\sum_{i=1}^{4}c_i\exp\left(-\sum_{j=1}^{3}a_{ij}(x_j-p_{ij})^2\right)$	3	[1][3]	−3.86
F_{20}	$f(x)=-\sum_{i=1}^{4}c_i\exp\left(-\sum_{j=1}^{6}a_{ij}(x_j-p_{ij})^2\right)$	6	[1]	−3.32
F_{21}	$f(x)=-\sum_{i=1}^{5}\left[(X-a_i)(X-a_i)^{\top}+c_i\right]^{-1}$	4	[10]	−10.1532
F_{22}	$f(x)=-\sum_{i=1}^{7}\left[(X-a_i)(X-a_i)^{\top}+c_i\right]^{-1}$	4	[10]	−10.4028
F_{23}	$f(x)=-\sum_{i=1}^{10}\left[(X-a_i)(X-a_i)^{\top}+c_i\right]^{-1}$	4	[10]	−10.5363

the choice of the opposite strategy is a challenging task. The mutated variant of the HGSO is inspired by the mutation operation employed and introduced in the evolutionary algorithms, such as the GA and DE algorithms. The mutation-based HGSO variants offer more robustness and diversity than the original HGSO, with local optimal avoidance and the risk of premature convergence. Compared to traditional HGSO, the Quantum-HGSO offers a good exploration ability due to the quantum principles, resulting in faster convergence in the earlier stage of the process. Similar to OBL, the Q-HGSO algorithm explores larger regions than the HGSO, which enhances the population diversity. However, this variant of the HGSO suffers from parameter sensitivity and computational complexity. Similar to adaptive HGSO, the Fuzzy-HGSO based algorithms enhances the performance of HGSO through dynamic control of the control parameters. The Fuzzy-HGSO variants achieve the exploration/exploitation balance by the fuzzy logic control mechanisms such as Fuzzy Interference System. Nevertheless, this enhancement generates additional time and presents some sensitivity to parameters. The multi-objective HGSO (MO-HGSO) algorithm is mainly applied for solving multi-objective optimization problems. The MO-HGSO calculates and evaluates solutions based Pareto dominance principles. The major strength of the MO-HGSO-based algorithm is the accuracy in solving complex and multi-criteria problems with or without many objectives and constraints. However, the performance of the MO-HGSO algorithms may decrease in large-scale problems, especially when the number of objectives increases. According to the current research conducted in this paper, the HGSO algorithm demonstrated promising results in addressing complex optimization problems. However, the standards HSGO suffers from local optima stagnation and weak exploitation ability. Thus, several hybridizations with other meta-heuristics were proposed such as SA, FA, etc. This type of hybridization attempts to achieve a good balance between exploration and exploitation to attain the global optimal solution. Furthermore, hybrid meta-heuristics with HGSO algorithms prevent from premature convergence and local optimal escaping, which are one of the important HGSO limitations. However, hybrid HGSO-based approaches do not guarantee the optimality of the solution, which is one of the characteristic and limitation of the meta-heuristics. In machine learning [250], feature selection and both models' parameter and hyperparameters tuning are fundamental tasks in the development of accurate AI models. These tasks can be classified as NP-hard optimization problems, which can be solved by nature-inspired optimization algorithms. The HGSO algorithm is an efficient algorithm able de determine the optimal features of datasets, and the model's parameter/hyperparemeter, that maximizes the model accuracy. Despite that, this architecture is a problem-dependent solution, which cannot be generalized.

Figure 20 illustrates the classification of algorithmic modifications based on the type of enhancement applied. Notably, chaotic mechanisms (24.1%) form the largest category, as they leverage chaotic maps to improve both exploration and exploitation in optimization. Following closely, improved versions (17.2%) incorporate refined techniques to enhance algorithmic performance. Equally significant, the

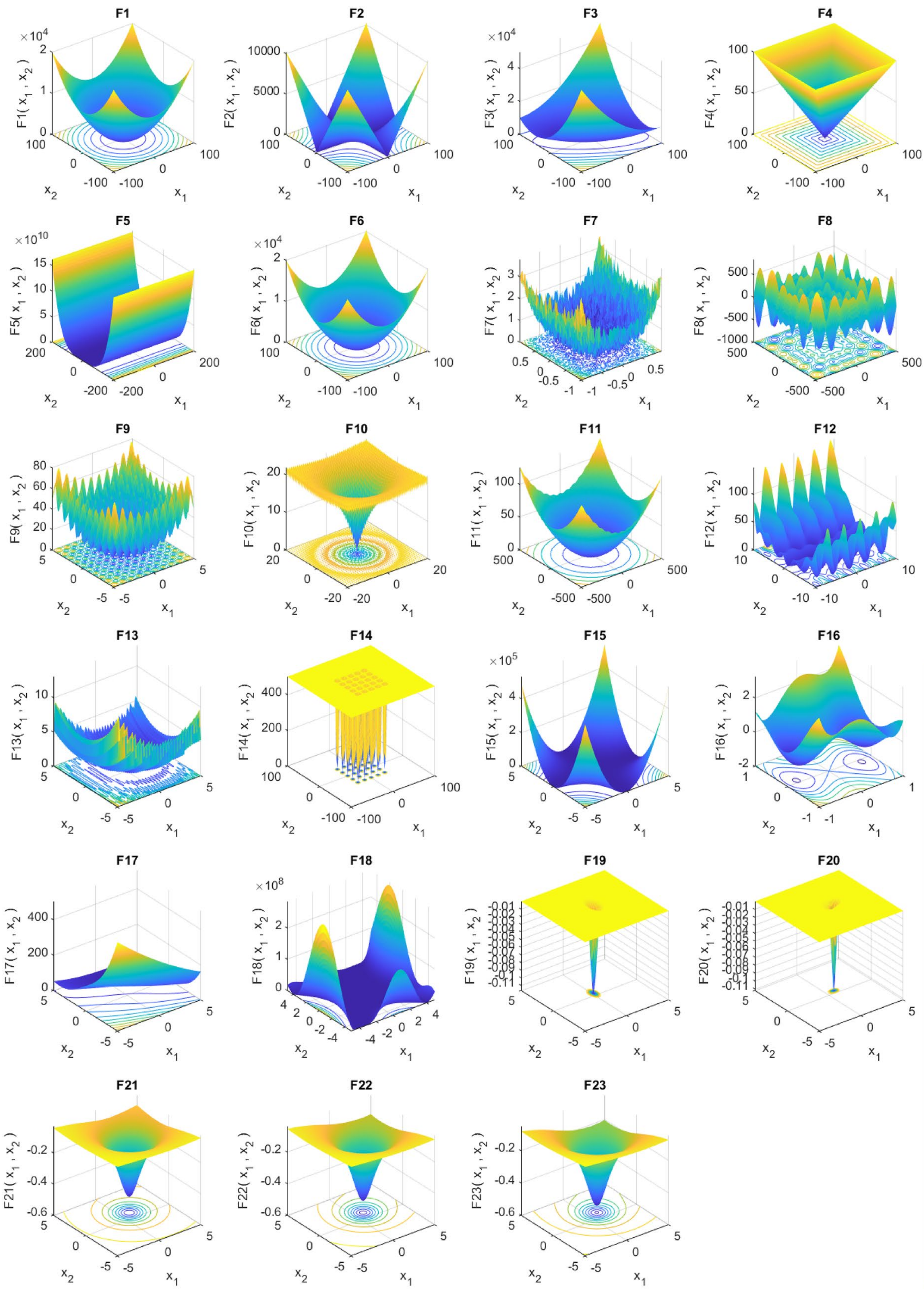

Fig. 13 2D representation of 23 IEEE CEC benchmark functions

Table 12 Fitness results

Function	Metric	HGSO	BA	FA	GWO	MFO	MVO	SCA	SAO	LCA	ALO	BBO	CSO	FPA	PSO	AOA
F_1	Best	8.99E−235	4.89E+03	3.18E−09	2.34E−61	7.80E−16	6.51E−03	1.01E−16	3.11E−30	7.96E−04	1.99E−09	4.73E−05	4.05E−66	1.12E+01	7.52E−54	2.30E−133
	Worst	5.96E−206	1.50E+04	7.60E−09	6.81E−54	1.59E−12	3.34E−02	5.76E−12	1.09E−24	4.34E−01	8.76E−08	8.60E−04	1.08E−55	3.87E+01	3.03E−43	2.10E−96
	Mean	2.98E−207	8.85E+03	5.44E−09	3.42E−55	3.55E−13	1.34E−02	9.28E−13	9.96E−26	6.43E−02	1.30E−08	1.88E−04	5.98E−57	2.17E+01	1.52E−44	1.05E−97
	Std	0.00E+00	2.45E+03	1.17E−09	1.52E−54	4.89E−13	5.85E−03	1.87E−12	2.75E−25	1.16E−01	1.82E−08	1.89E−04	2.40E−56	8.58E+00	6.77E−44	4.70E−97
	Rank	1	15	9	4	7	12	8	6	13	10	11	3	14	5	2
	P−value	0.00E+00	6.80E−08	6.80E−08	6.80E−08	6.80E+00	6.80E−08	6.80E−08	6.80E−08	6.80E−08	6.80E−08	6.80E−08	6.80E−08	6.80E−08	6.80E−08	6.80E−08
F_2	Best	1.55E−117	1.83E+01	1.34E−05	9.57E−35	4.36E−10	2.14E−02	7.22E−12	9.21E−17	7.52E−03	2.14E−05	6.40E−04	6.48E−41	2.16E+00	2.37E−28	1.25E−70
	Worst	1.28E−104	2.22E+01	2.21E−05	2.13E−32	3.41E−08	7.20E−02	2.07E−09	2.82E−14	1.32E−01	2.60E+00	3.13E−03	1.52E−36	7.32E+00	7.26E−14	4.70E−51
	Mean	6.40E−106	2.08E+01	1.76E−05	3.92E−33	3.63E−09	4.16E−02	7.28E−10	5.10E−15	7.06E−02	3.21E−01	1.94E−03	1.69E−37	3.79E+00	3.63E−15	2.37E−52
	Std	2.86E−105	8.94E−01	2.74E−06	4.91E−33	7.38E−09	1.46E−02	7.82E−10	8.15E−15	3.64E−02	7.92E−01	6.31E−04	4.46E−37	1.31E+00	1.62E−14	1.05E−51
	Rank	1	15	9	4	8	11	7	6	12	13	10	3	14	5	2
	P-value	0.00E+00	6.80E−08	6.80E−08	6.80E−08	6.80E−08	6.80E−08	6.80E−08	6.80E−08	6.80E−08	6.80E−08	6.80E−08	6.80E−08	6.80E−08	6.80E−08	6.80E−08
F_3	Best	1.10E−220	2.68E+03	4.56E−09	5.37E−31	8.41E−04	3.93E−02	9.49E−08	9.16E−13	3.74E−02	4.67E−05	2.39E−02	2.26E−25	4.65E+00	1.78E−08	1.18E−116
	Worst	3.63E−165	6.90E+03	1.02E−08	1.46E−22	1.63E−01	3.70E−01	1.38E+01	2.31E−08	1.41E+01	1.43E−02	5.90E−01	3.80E−05	3.98E+01	6.77E−05	1.10E−82
	Mean	1.82E−166	5.45E+03	7.06E−09	7.64E−24	2.86E−02	1.44E−01	6.94E−01	4.27E−09	2.95E+00	2.17E−03	2.41E−01	1.90E−06	1.64E+01	1.44E−05	5.66E−84
	Std	0.00E+00	1.35E+03	1.21E−09	3.27E−23	4.20E−02	9.10E−02	3.08E+00	5.94E−09	4.54E+00	3.18E−03	1.71E−01	8.49E−06	1.06E+01	2.07E−05	2.46E−83
	Rank	1	15	5	3	9	10	12	4	13	8	11	6	14	7	2
	P-value	0.00E+00	6.80E−08	6.80E−08	6.80E−08	6.80E−08	6.80E−08	6.80E−08	6.80E−08	6.80E−08	6.80E−08	6.80E−08	6.80E−08	6.80E−08	6.80E−08	6.80E−08
F_4	Best	5.34E−112	3.46E+01	2.99E−05	9.73E−21	3.76E−03	4.47E−02	1.86E−06	1.75E−11	9.83E−03	1.28E−04	2.70E−02	2.08E−21	3.99E+00	1.52E−07	1.13E−68
	Worst	6.25E−100	5.79E+01	4.89E−05	2.43E−17	4.75E+01	1.90E−01	1.06E−02	1.00E−09	2.24E−01	1.06E−02	7.14E−02	3.02E−15	1.14E+01	1.79E−04	2.07E−44
	Mean	3.12E−101	5.40E+01	4.07E−05	2.62E−18	4.77E+00	1.06E−01	1.73E−03	1.50E−10	8.08E−02	2.62E−03	4.00E−02	2.86E−16	6.73E+00	3.23E−05	1.93E−45
	Std	1.40E−100	6.24E+00	5.02E−06	5.41E−18	1.09E+01	4.94E−02	3.05E−03	2.18E−10	6.03E−02	2.60E−03	1.09E−02	7.68E−16	1.65E+00	5.68E−05	5.96E−45
	Rank	1	15	7	3	13	12	8	5	11	9	10	4	14	6	2
	P-value	0.00E+00	6.80E−08	6.80E−08	6.80E−08	6.80E−08	6.80E−08	6.80E−08	6.80E−08	6.80E−08	6.80E−08	6.80E−08	6.80E−08	6.80E−08	6.80E−08	6.80E−08
F_5	Best	6.90E+00	3.01E+06	8.16E−03	5.33E+00	6.61E−01	3.43E+00	6.62E+00	9.70E−01	3.49E−03	6.77E−02	1.16E−01	6.99E+00	2.01E+02	1.34E−01	8.11E+00
	Worst	8.74E+00	2.39E+07	7.03E+00	8.70E+00	9.00E+04	2.10E+03	8.20E+00	9.51E+00	2.22E+00	9.59E+00	2.14E+02	8.72E+00	1.49E+03	7.84E+00	8.94E+00
	Mean	7.58E+00	1.25E+07	8.99E−01	6.71E+00	9.05E+03	3.36E+02	7.32E+00	4.47E+00	3.97E−01	5.82E+00	1.57E+01	7.49E+00	5.97E+02	4.56E+00	8.73E+00
	Std	5.10E−01	6.13E+06	1.54E+00	8.00E−01	2.77E+04	6.56E+02	3.37E−01	1.74E+00	5.86E−01	2.83E+00	4.68E+01	4.88E−01	3.50E+02	1.94E+00	2.04E−01
	Rank	9	15	2	6	14	12	7	3	1	5	11	8	13	4	10
	P-value	0.00E+00	6.80E−08	7.90E−08	5.90E−05	1.00E+00	1.23E−03	1.81E−01	6.67E−06	6.80E−08	4.11E−02	6.04E−03	3.37E−01	6.80E−08	6.01E−07	3.42E−07
F_6	Best	1.14E−01	4.32E+03	2.46E−09	1.28E−06	1.78E−15	5.94E−03	1.56E−01	1.66E−31	1.87E−04	3.41E−09	7.07E−06	4.57E−02	9.55E+00	0.00E+00	4.78E−01
	Worst	9.62E−01	1.15E+04	7.71E−09	2.50E−01	1.42E−12	2.24E−02	8.60E−01	2.48E−25	2.78E−01	1.75E−08	4.76E−04	7.72E−01	5.64E+01	1.54E−32	1.43E+00
	Mean	4.98E−01	8.82E+03	5.70E−09	1.25E−02	2.25E−13	1.45E−02	4.61E−01	1.50E−26	5.86E−02	8.35E−09	1.47E−04	3.52E−01	2.60E+01	4.93E−33	1.02E+00
	Std	2.56E−01	2.25E+03	1.36E−09	5.60E−02	3.96E−13	5.28E−03	1.65E−01	5.54E−26	6.82E−02	3.73E−09	1.34E−04	1.78E−01	1.26E+01	5.51E−33	2.78E−01
	Rank	12	15	4	7	3	8	11	2	9	5	6	10	14	1	13
	P-value	0.00E+00	6.80E−08	6.80E−08	1.06E−07	6.80E−08	6.80E−08	9.03E−01	6.80E−08	1.66E−07	6.80E−08	6.80E−08	9.62E−02	6.80E−08	5.63E−08	9.75E−06

Table 12 (continued)

Function	Metric	HGSO	BA	FA	GWO	MFO	MVO	SCA	SAO	LCA	ALO	BBO	CSO	FPA	PSO	AOA
F_7	Best	2.47E−05	2.61E−01	5.80E−05	2.47E−04	2.08E−03	7.45E−04	1.33E−04	1.09E−03	1.38E−05	4.75E−03	1.50E−03	2.94E−04	1.45E−02	5.40E−04	2.23E−05
	Worst	6.21E−04	2.43E+00	5.30E−04	2.40E−03	1.54E−02	9.97E−03	7.29E−03	9.35E−03	1.28E−03	4.54E−02	9.68E−03	3.72E−03	5.71E−02	6.01E−03	1.53E−03
	Mean	1.76E−04	1.95E+00	2.07E−04	7.83E−04	7.99E−03	3.02E−03	1.85E−03	4.24E−03	4.21E−04	2.48E−02	4.36E−03	1.50E−03	2.89E−02	2.57E−03	5.05E−04
	Std	1.50E−04	8.22E−01	1.23E−04	5.17E−04	4.08E−03	2.12E−03	1.93E−03	1.92E−03	3.41E−04	1.27E−02	2.37E−03	8.73E−04	1.15E−02	1.30E−03	4.32E−04
	Rank	1	15	2	5	12	9	7	10	3	13	11	6	14	8	4
	P-value	0.00E+00	6.80E−08	2.08E−01	1.05E−06	6.80E−08	6.80E−08	6.67E−06	6.80E−08	2.23E−02	6.80E−08	6.80E−08	1.23E−07	6.80E−08	7.90E−08	3.34E−03
F_8	Best	−2.49E+03	−5.16E+03	−3.83E+03	−3.22E+03	−3.83E+03	−3.40E+03	−2.50E+03	−3.71E+03	−4.19E+03	−3.54E+03	−3.72E+03	−3.57E+03	−3.83E+03	−2.75E+03	−2.55E+03
	Worst	−1.66E+03	−1.04E+03	−2.53E+03	−1.99E+03	−2.40E+03	−2.25E+03	−1.87E+03	−2.88E+03	−1.02E+03	−1.93E+03	−2.95E+03	−2.44E+03	−2.78E+03	−2.02E+03	−1.69E+03
	Mean	−2.04E+03	−2.00E+03	−3.47E+03	−2.58E+03	−3.22E+03	−2.84E+03	−2.18E+03	−3.27E+03	−2.85E+03	−2.20E+03	−3.28E+03	−3.05E+03	−3.03E+03	−2.41E+03	−2.09E+03
	Std	2.24E+02	1.18E+03	3.13E+02	2.96E+02	3.26E+02	3.62E+02	1.70E+02	2.31E+02	1.04E+03	3.79E+02	2.30E+02	3.01E+02	2.29E+02	1.80E+02	2.42E+02
	Rank	14	15	1	9	4	8	12	3	7	11	2	5	6	10	13
	P-value	0.00E+00	4.99E−02	6.80E−08	2.69E−06	9.13E−08	3.42E−07	2.39E−02	6.78E−08	1.23E−03	1.02E−01	6.80E−08	9.17E−08	6.80E−08	1.81E−05	3.79E−01
F_9	Best	0.00E+00	7.04E+01	2.98E+00	0.00E+00	1.19E+01	4.98E+00	0.00E+00	2.98E+00	1.32E−04	1.19E+01	2.99E+00	0.00E+00	1.95E+01	2.98E+00	0.00E+00
	Worst	0.00E+00	8.69E+01	2.19E+01	5.78E+00	3.28E+01	2.89E+01	1.32E+01	1.99E+01	6.07E+01	3.58E+01	2.59E+01	1.85E+01	3.72E+01	1.89E+01	2.97E+01
	Mean	0.00E+00	8.45E+01	9.25E+00	7.14E−01	2.14E+01	1.43E+01	1.10E+00	6.17E+00	3.06E+00	2.30E+01	1.32E+01	1.24E+00	2.91E+01	1.06E+01	6.14E+00
	Std	0.00E+00	5.84E+00	4.14E+00	1.77E+00	5.53E+00	6.10E+00	3.44E+00	3.69E+00	1.36E+01	7.61E+00	6.44E+00	4.30E+00	4.96E+00	4.27E+00	9.83E+00
	Rank	1	15	8	2	12	11	3	7	5	13	10	4	14	9	6
	P-value	0.00E+00	8.01E−09	8.01E−09	4.02E−02	7.98E−09	8.01E−09	2.99E−08	7.55E−09	8.01E−09	8.01E−09	8.01E−09	1.63E−01	8.01E−09	7.95E−09	2.09E−03
F_{10}	Best	8.88E−16	1.49E+01	2.25E−05	4.44E−15	3.38E−08	2.48E−02	1.10E−09	4.44E−15	8.88E−03	2.06E−05	2.31E−03	8.88E−16	3.56E+00	4.44E−15	8.88E−16
	Worst	8.88E−16	1.99E+01	3.27E−05	7.99E−15	3.96E−07	2.33E+00	1.81E−06	1.04E−13	2.75E−01	1.65E+00	8.41E−03	4.44E−15	6.97E+00	7.99E−15	4.44E−15
	Mean	8.88E−16	1.76E+01	2.80E−05	7.28E−15	1.33E−07	2.25E−01	3.18E−07	1.99E−14	9.00E−02	8.24E−02	4.73E−03	4.26E−15	5.09E+00	6.57E−15	1.24E−15
	Std	0.00E+00	1.36E+00	2.63E−06	1.46E−15	1.08E−07	5.55E−01	4.75E−07	2.31E−14	7.89E−02	3.68E−01	1.49E−03	7.94E−16	1.03E+00	1.79E−15	1.09E−15
	Rank	1	15	9	5	7	13	8	6	12	11	10	3	14	4	2
	P-value	0.00E+00	8.01E−09	8.01E−09	2.04E−09	8.01E−09	8.01E−09	8.01E−09	7.59E−09	8.01E−09	8.01E−09	8.01E−09	3.13E−09	8.01E−09	3.95E−09	1.62E−01
F_{11}	Best	0.00E+00	4.50E+01	2.21E−02	0.00E+00	2.71E−02	1.21E−01	1.55E−13	7.40E−03	1.07E−02	7.87E−02	1.20E−02	0.00E+00	9.54E−01	7.40E−03	0.00E+00
	Worst	0.00E+00	1.31E+02	1.21E−01	8.00E−02	2.93E−01	7.18E−01	6.22E−01	5.78E−01	6.62E−01	4.92E−01	1.19E−01	2.76E−01	1.56E+00	1.25E−01	6.74E−02
	Mean	0.00E+00	8.96E+01	5.65E−02	2.44E−02	1.34E−01	3.34E−01	9.52E−02	2.04E−01	2.07E−01	2.30E−01	5.78E−02	2.65E−02	1.22E+00	6.96E−02	5.97E−03
	Std	0.00E+00	2.57E+01	2.83E−02	2.22E−02	9.19E−02	1.50E−01	1.94E−01	2.11E−01	1.86E−01	1.10E−01	3.15E−02	7.10E−02	1.60E−01	3.62E−02	1.85E−02
	Rank	1	15	5	3	9	13	8	10	11	12	6	4	14	7	2
	P-value	0.00E+00	8.01E−09	8.01E−09	3.31E−06	8.01E−09	8.01E−09	8.01E−09	8.01E−09	8.01E−09	8.01E−09	8.01E−09	8.06E−02	8.01E−09	7.99E−09	1.63E−01
F_{12}	Best	3.14E−02	8.75E+05	2.74E−11	5.51E−07	8.63E−17	3.40E−04	3.91E−02	4.81E−32	3.53E−05	1.18E−08	1.41E−07	4.75E−03	8.90E−01	4.71E−32	1.09E−01
	Worst	2.66E−01	7.30E+07	5.94E−11	5.83E−02	3.11E−01	3.14E−01	1.82E−01	3.11E−01	1.49E−02	8.74E+00	8.16E−05	7.16E−02	6.42E+00	8.20E−32	7.38E−01
	Mean	8.78E−02	2.25E+07	4.64E−11	9.83E−03	7.78E−02	4.81E−02	9.36E−02	1.56E−02	2.26E−03	2.98E+00	9.43E−06	3.75E−02	2.98E+00	4.97E−32	3.60E−01
	Std	5.30E−02	2.13E+07	9.05E−12	1.62E−02	1.38E−01	1.14E−01	3.83E−02	6.95E−02	3.50E−03	2.80E+00	2.02E−05	1.66E−02	1.47E+00	7.66E−33	1.75E−01
	Rank	10	15	2	5	9	8	11	6	4	14	3	7	13	1	12
	P-value	0.00E+00	6.80E−08	6.80E−08	1.92E−07	7.11E−03	1.61E−04	2.98E−01	1.20E−06	6.80E−08	1.23E−03	6.80E−08	1.60E−05	6.80E−08	5.27E−08	3.42E−07

Table 12 (continued)

Function	Metric	HGSO	BA	FA	GWO	MFO	MVO	SCA	SAO	LCA	ALO	BBO	CSO	FPA	PSO	AOA
F_{13}	Best	1.70E−01	8.51E+06	1.31E−10	3.31E−06	5.99E−16	9.82E−04	1.29E−01	1.07E−31	9.57E−06	2.48E−08	2.04E−06	5.39E−02	8.89E−01	1.35E−32	2.95E−01
	Worst	6.62E−01	3.08E+08	4.27E−10	9.75E−02	1.87E−01	2.96E−02	4.69E−01	1.10E−02	2.58E−02	1.10E−02	2.50E−05	4.81E−01	4.26E+00	1.10E−02	9.93E−01
	Mean	4.38E−01	8.61E+07	2.61E−10	9.60E−03	1.26E−02	8.56E−03	3.22E−01	2.75E−03	8.51E−03	1.10E−03	6.70E−06	1.85E−01	2.97E+00	5.49E−04	6.53E−01
	Std	1.57E−01	7.95E+07	8.08E−11	2.95E−02	4.13E−02	7.23E−03	8.20E−02	4.88E−03	8.56E−03	3.38E−03	5.45E−06	1.06E−01	9.34E−01	2.46E−03	2.02E−01
	Rank	12	15	1	8	9	7	11	5	6	4	2	10	14	3	13
	P-value	0.00E+00	6.80E−08	6.80E−08	6.80E−08	9.17E−08	6.80E−08	1.67E−02	6.61E−08	6.80E−08	6.80E−08	6.80E−08	9.75E−06	6.80E−08	4.36E−08	3.34E−03
F_{14}	Best	9.98E−01	2.01E+00	9.98E−01	9.98E−01	9.98E−01	9.98E−01	9.98E−01	9.98E−01	9.98E−01	9.98E−01	9.98E−01	9.98E−01	9.98E−01	9.98E−01	9.98E−01
	Worst	2.99E+00	3.98E+02	1.99E+00	2.98E+00	3.97E+00	9.98E−01	2.98E+00	1.08E+01	2.94E+01	7.87E+00	8.84E+00	2.98E+00	9.98E−01	1.27E+01	3.97E+00
	Mean	1.83E+00	1.46E+02	1.05E+00	2.09E+00	1.84E+00	9.98E−01	1.69E+00	3.12E+00	5.47E+00	2.63E+00	6.16E+00	1.44E+00	9.98E−01	5.86E+00	1.35E+00
	Std	6.51E−01	1.76E+02	2.22E−01	9.60E−01	1.21E+00	4.90E−11	9.69E−01	2.80E+00	7.37E+00	2.31E+00	2.32E+00	8.19E−01	3.03E−05	3.57E+00	7.38E−01
	Rank	7	15	3	9	8	1	6	11	12	10	14	5	2	13	4
	P-value	0.00E+00	3.94E−07	1.63E−07	9.68E−01	6.31E−02	6.80E−08	1.90E−01	3.78E−01	9.46E−01	2.17E−01	5.87E−05	1.45E−03	7.90E−08	1.77E−03	5.63E−04
F_{15}	Best	3.24E−04	2.27E−03	3.07E−04	3.07E−04	3.10E−04	4.30E−04	4.75E−04	3.07E−04	9.63E−04	6.71E−04	4.42E−04	3.28E−04	4.07E−04	3.07E−04	4.02E−04
	Worst	4.52E−04	2.43E−03	4.26E−04	2.04E−02	1.66E−03	1.34E−03	1.52E−03	6.57E−04	2.40E−03	1.77E−03	9.09E−04	8.45E−04	1.03E−03	4.97E−04	3.14E−03
	Mean	3.69E−04	2.42E−03	3.18E−04	1.43E−03	7.95E−04	7.27E−04	9.87E−04	4.50E−04	1.55E−03	1.01E−03	5.73E−04	6.06E−04	6.72E−04	3.40E−04	8.81E−04
	Std	3.44E−05	3.55E−05	3.02E−05	4.46E−03	3.17E−04	1.78E−04	3.46E−04	1.36E−04	3.29E−04	2.75E−04	1.29E−04	1.46E−04	1.33E−04	5.10E−05	6.27E−04
	Rank	3	15	1	13	9	8	11	4	14	12	5	6	7	2	10
	P-value	0.00E+00	6.80E−08	5.17E−06	9.89E−01	1.20E−06	7.90E−08	6.80E−08	5.08E−01	6.80E−08	6.80E−08	9.17E−08	1.58E−06	9.17E−08	3.34E−03	1.06E−07
F_{16}	Best	−1.03E+00	−1.02E+00	−1.03E+00	−1.03E+00	−1.03E+00	−1.03E+00	−1.03E+00	−1.03E+00	−1.02E+00	−1.03E+00	−1.03E+00	−1.03E+00	−1.03E+00	−1.03E+00	−1.03E+00
	Worst	−1.03E+00	2.11E+00	−1.03E+00	−1.03E+00	−1.03E+00	−1.03E+00	−1.03E+00	−1.03E+00	−2.26E−01	−1.03E+00	−1.03E+00	−1.03E+00	−1.03E+00	−1.03E+00	−1.03E+00
	Mean	−1.03E+00	−3.06E−01	−1.03E+00	−1.03E+00	−1.03E+00	−1.03E+00	−1.03E+00	−1.03E+00	−6.54E−01	−1.03E+00	−1.03E+00	−1.03E+00	−1.03E+00	−1.03E+00	−1.03E+00
	Std	1.52E−04	6.82E−01	2.10E−14	2.12E−08	2.28E−16	4.96E−07	5.61E−05	2.28E−16	2.01E−01	3.29E−14	3.29E−14	2.43E−05	6.79E−08	2.04E−16	8.13E−05
	Rank	13	15	4	7	1	9	11	1	14	6	5	10	8	1	12
	P-value	0.00E+00	6.80E−08	6.79E−08	6.80E−08	8.01E−09	6.80E−08	1.67E−02	8.01E−09	6.80E−08	6.79E−08	6.73E−08	3.66E−07	6.80E−08	2.40E−08	8.35E−03
F_{17}	Best	3.98E−01	4.00E−01	3.98E−01	3.98E−01	3.98E−01	3.98E−01	3.98E−01	3.98E−01	1.10E+00	3.98E−01	3.98E−01	3.98E−01	3.98E−01	3.98E−01	3.98E−01
	Worst	4.13E−01	1.10E+00	3.98E−01	3.98E−01	3.98E−01	3.98E−01	4.11E−01	3.98E−01	1.10E+00	3.98E−01	3.98E−01	3.98E−01	3.98E−01	3.98E−01	5.74E−01
	Mean	4.01E−01	1.06E+00	3.98E−01	3.98E−01	3.98E−01	3.98E−01	4.00E−01	3.98E−01	1.10E+00	3.98E−01	3.98E−01	3.98E−01	3.98E−01	3.98E−01	4.27E−01
	Std	3.98E−03	1.56E−01	1.01E−14	4.74E−06	0.00E+00	4.48E−07	3.13E−03	0.00E+00	4.56E−16	1.13E−13	5.23E−08	4.19E−06	3.96E−06	0.00E+00	4.53E−02
	Rank	12	14	4	10	1	7	11	1	15	5	6	8	9	1	13
	P-value	0.00E+00	2.56E−07	6.66E−08	6.80E−08	8.01E−09	6.80E−08	3.10E−01	8.01E−09	8.01E−09	6.80E−08	6.80E−08	6.28E−08	6.80E−08	8.01E−09	3.85E−02
F_{18}	Best	3.00E+00	3.00E+00	3.00E+00	3.00E+00	3.00E+00	3.00E+00	3.00E+00	3.00E+00	3.00E+01	3.00E+00	3.00E+00	3.00E+00	3.00E+00	3.00E+00	3.00E+00
	Worst	3.00E+00	3.01E+01	3.00E+00	3.00E+00	3.00E+00	3.00E+00	3.00E+00	3.00E+00	3.07E+01	3.00E+00	3.00E+01	3.00E+00	3.00E+00	3.00E+00	2.84E+01
	Mean	3.00E+00	2.36E+01	3.00E+00	3.00E+00	3.00E+00	3.00E+00	3.00E+00	3.00E+00	3.06E+01	3.00E+00	1.25E+01	3.00E+00	3.00E+00	3.00E+00	5.98E+00
	Std	1.37E−04	1.12E+01	1.15E−13	8.32E−05	2.35E−15	3.27E−06	1.37E−04	1.24E−15	1.45E−01	3.13E−13	1.32E+01	1.89E−04	3.07E−08	7.69E−16	6.69E+00
	Rank	11	14	4	8	3	7	10	2	15	5	13	9	6	1	12
	P-value	0.00E+00	6.80E−08	6.80E−08	1.06E−02	6.56E−08	7.95E−07	2.56E−02	2.95E−08	1.51E−08	6.80E−08	1.08E−01	4.10E−05	6.80E−08	3.93E−08	7.58E−06

Table 12 (continued)

Function	Metric	HGSO	BA	FA	GWO	MFO	MVO	SCA	SAO	LCA	ALO	BBO	CSO	FPA	PSO	AOA
F_{19}	Best	−3.86E+00	−3.83E+00	−3.86E+00	−3.86E+00	−3.86E+00	−3.86E+00	−3.86E+00	−3.86E+00	−3.34E+00	−3.86E+00	−3.86E+00	−3.86E+00	−3.86E+00	−3.86E+00	−3.86E+00
	Worst	−3.85E+00	−3.68E+00	−3.86E+00	−3.85E+00	−3.86E+00	−3.86E+00	−3.85E+00	−3.86E+00	−3.34E+00	−3.86E+00	−3.86E+00	−3.86E+00	−3.86E+00	−3.86E+00	−3.62E+00
	Mean	−3.86E+00	−3.69E+00	−3.86E+00	−3.86E+00	−3.86E+00	−3.86E+00	−3.85E+00	−3.86E+00	−3.34E+00	−3.86E+00	−3.86E+00	−3.86E+00	−3.86E+00	−3.86E+00	−3.84E+00
	Std	3.90E−03	3.37E−02	5.20E−15	2.24E−03	2.28E−15	2.29E−06	2.61E−03	2.28E−15	1.37E−15	7.03E−13	1.78E−15	1.06E−03	3.03E−09	2.24E−15	5.84E−02
	Rank	11	14	5	10	1	8	12	1	15	6	1	9	7	1	13
	P-value	0.00E+00	6.80E−08	6.63E−08	3.07E−06	8.01E−09	6.80E−08	1.48E−01	8.01E−09	8.01E−09	6.80E−08	4.67E−08	1.66E−07	6.80E−08	1.51E−08	7.35E−01
F_{20}	Best	−3.16E+00	−2.44E+00	−3.20E+00	−3.32E+00	−3.20E+00	−3.20E+00	−3.11E+00	−3.32E+00	−1.36E+00	−3.20E+00	−3.32E+00	−3.32E+00	−3.31E+00	−3.32E+00	−3.16E+00
	Worst	−3.00E+00	−1.51E+00	−3.20E+00	−3.08E+00	−3.20E+00	−3.19E+00	−1.45E+00	−3.20E+00	−1.08E+00	−3.20E+00	−3.20E+00	−3.12E+00	−3.23E+00	−3.20E+00	−2.53E+00
	Mean	−3.08E+00	−1.63E+00	−3.20E+00	−3.25E+00	−3.20E+00	−3.20E+00	−2.95E+00	−3.23E+00	−1.18E+00	−3.20E+00	−3.21E+00	−3.19E+00	−3.28E+00	−3.30E+00	−2.96E+00
	Std	5.10E−02	2.62E−01	1.06E−13	8.04E−02	0.00E+00	2.64E−03	3.55E−01	4.88E−02	8.96E−02	9.77E−04	2.66E−02	6.32E−02	2.52E−02	4.88E−02	2.00E−01
	Rank	11	14	7	3	6	9	13	4	15	8	5	10	2	1	12
	P-value	0.00E+00	6.80E−08	6.80E−08	6.01E−07	8.01E−09	6.80E−08	6.22E−04	2.40E−08	6.80E−08	6.80E−08	6.80E−08	7.95E−07	6.80E−08	2.40E−08	2.39E−02
F_{21}	Best	−5.01E+00	−1.92E+00	−1.02E+01	−1.02E+01	−1.02E+01	−1.02E+01	−6.37E+00	−1.02E+01	−8.36E+00	−1.02E+01	−1.02E+01	−1.01E+01	−1.02E+01	−2.68E+00	−9.68E+00
	Worst	−4.41E+00	−9.63E−01	−2.63E+00	−3.12E+00	−2.63E+00	−5.06E+00	−8.77E−01	−2.63E+00	−5.04E+00	−2.63E+00	−2.63E+00	−2.52E+00	−1.01E+01	−2.68E+00	−4.33E+00
	Mean	−4.70E+00	−1.10E+00	−9.40E+00	−9.55E+00	−3.91E+00	−8.63E+00	−3.17E+00	−4.24E+00	−5.55E+00	−4.74E+00	−4.66E+00	−7.96E+00	−1.01E+01	−2.68E+00	−7.75E+00
	Std	1.79E−01	2.66E−01	2.31E+00	1.89E+00	2.74E+00	2.38E+00	1.39E+00	1.83E+00	8.78E−01	2.17E+00	3.30E+00	3.02E+00	1.38E−02	1.02E−16	1.40E+00
	Rank	9	15	3	2	12	4	13	11	7	8	10	5	1	14	6
	P-value	0.00E+00	6.80E−08	1.60E−05	1.20E−06	1.04E−03	6.80E−08	3.29E−05	5.94E−01	6.80E−08	1.08E−01	3.14E−02	2.56E−03	6.80E−08	1.13E−08	1.20E−06
F_{22}	Best	−5.01E+00	−1.55E+00	−1.04E+01	−1.04E+01	−1.04E+01	−1.04E+01	−4.96E+00	−1.04E+01	−5.09E+00	−1.04E+01	−1.04E+01	−1.04E+01	−1.04E+01	−5.09E+00	−1.04E+01
	Worst	−4.10E+00	−1.20E+00	−1.04E+01	−5.09E+00	−2.77E+00	−2.77E+00	−4.25E+00	−3.72E+00	−5.07E+00	−1.84E+00	−2.77E+00	−2.73E+00	−1.00E+01	−5.09E+00	−6.39E+00
	Mean	−4.69E+00	−1.22E+00	−1.04E+01	−9.60E+00	−6.23E+00	−7.63E+00	−4.73E+00	−5.48E+00	−5.08E+00	−5.51E+00	−5.97E+00	−8.65E+00	−1.03E+01	−5.09E+00	−8.91E+00
	Std	2.40E−01	7.76E−02	2.17E−11	1.95E+00	2.54E+00	2.89E+00	2.17E−01	1.73E+00	4.88E−03	2.71E+00	2.35E+00	2.96E+00	1.05E−01	2.09E−15	1.27E+00
	Rank	14	15	1	3	7	6	13	10	12	9	8	5	2	11	4
	P-value	0.00E+00	6.80E−08	6.80E−08	6.80E−08	1.36E−05	1.20E−06	3.65E−01	1.21E−05	6.80E−08	3.15E−02	1.55E−05	2.75E−04	6.80E−08	2.86E−08	6.80E−08
F_{23}	Best	−5.10E+00	−2.52E+00	−1.05E+01	−1.05E+01	−1.05E+01	−1.05E+01	−5.87E+00	−1.05E+01	−6.38E+00	−1.05E+01	−1.05E+01	−1.05E+01	−1.05E+01	−1.05E+01	−1.03E+01
	Worst	−4.54E+00	−9.66E−01	−3.84E+00	−2.42E+00	−2.43E+00	−1.86E+00	−9.43E−01	−2.42E+00	−5.11E+00	−1.68E+00	−2.42E+00	−2.34E+00	−9.75E+00	−2.42E+00	−3.38E+00
	Mean	−4.81E+00	−1.08E+00	−9.93E+00	−1.01E+01	−8.74E+00	−6.67E+00	−3.85E+00	−6.91E+00	−5.19E+00	−6.53E+00	−5.58E+00	−6.55E+00	−1.04E+01	−5.18E+00	−5.83E+00
	Std	1.63E−01	3.51E−01	1.87E+00	1.81E+00	3.24E+00	4.02E+00	1.49E+00	3.16E+00	2.81E−01	3.48E+00	3.78E+00	3.35E+00	1.79E−01	3.65E+00	1.78E+00
	Rank	13	15	3	2	4	6	14	5	11	8	10	7	1	12	9
	P-value	0.00E+00	6.80E−08	1.20E−06	1.20E−06	1.09E−03	5.98E−01	1.23E−02	1.42E−04	6.80E−08	2.85E−01	2.85E−01	1.20E−01	6.80E−08	1.07E−01	4.39E−02

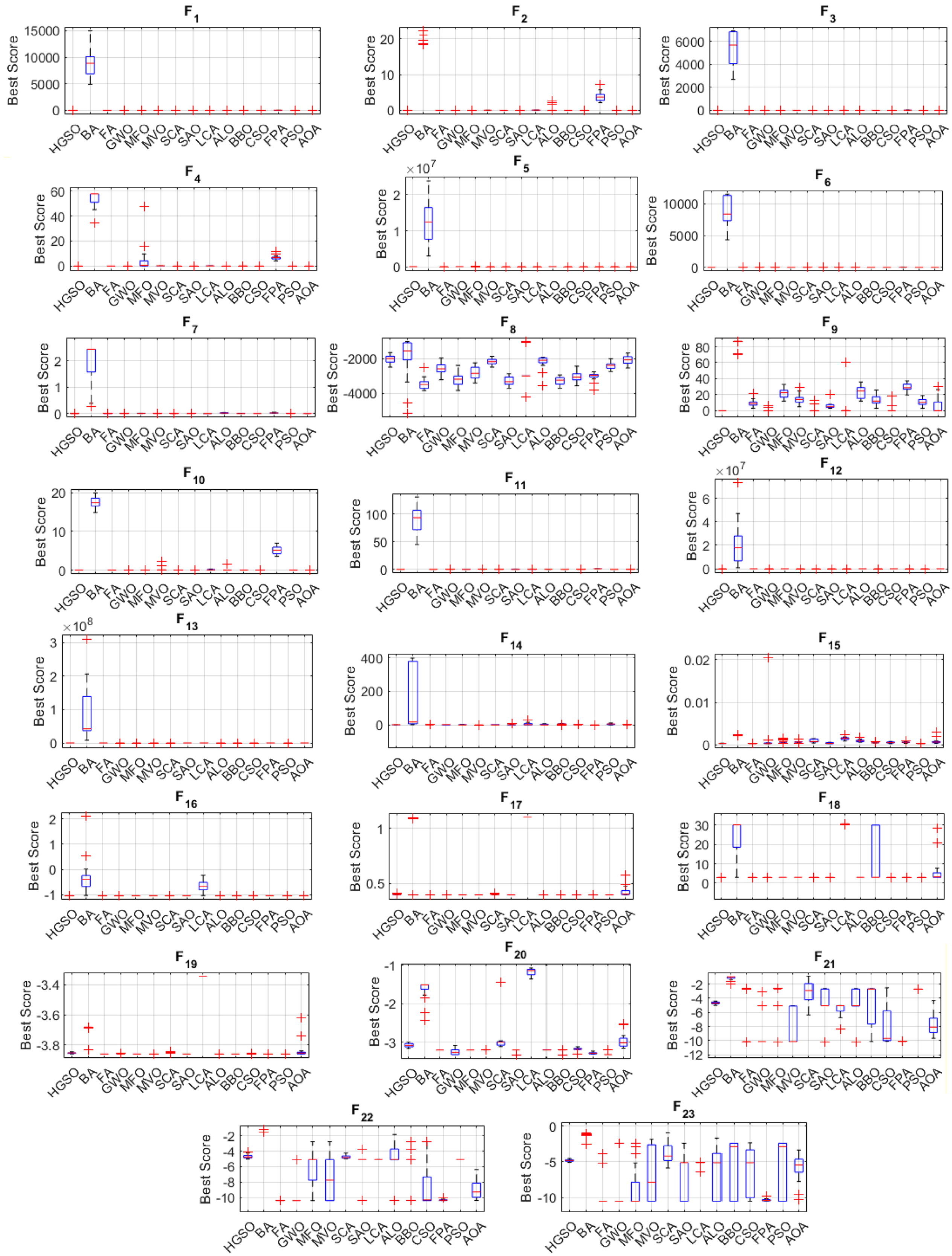

Fig. 14 Box plots of all algorithms across 23 benchmark functions

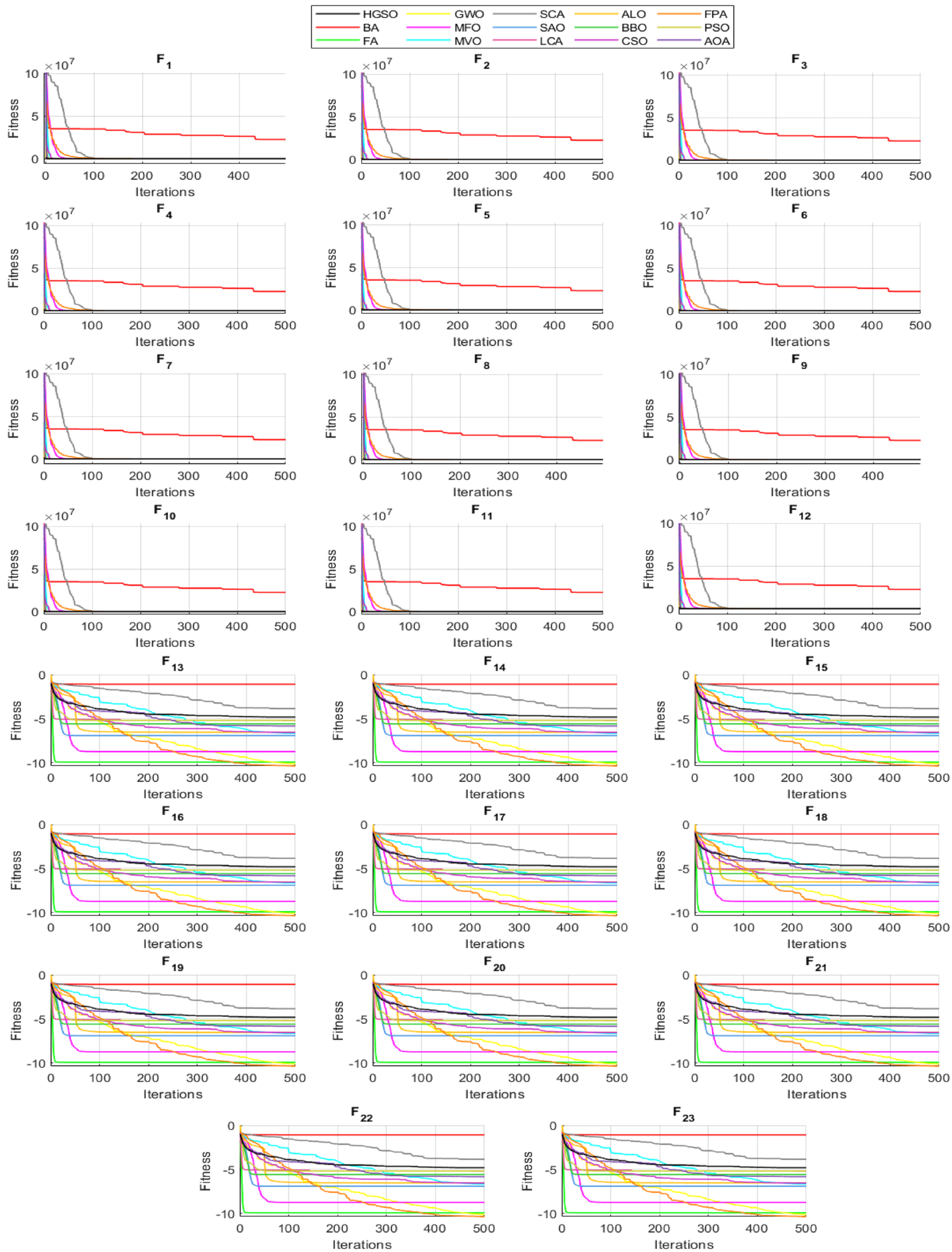

Fig. 15 Convergence of all algorithms across 23 benchmark functions

	N	Mean	STD	Minimum	Maximum	Percentiles 25e	50e	75e
HGSO	23	-8,9058E+001	4,25299E+002	-2,04E+003	7,58E+000	-3,0800E+000	6,4000E-106	4,0100E-001
BA	23	5,2662E+006	1,83871E+007	-2,00E+003	8,61E+007	-1,0800E+000	2,0800E+001	5,4500E+003
FA	23	-1,5188E+002	7,23338E+002	-3,47E+003	9,25E+000	-3,2000E+000	7,0600E-009	5,6500E-002
GWO	23	-1,1324E+002	5,37750E+002	-2,58E+003	6,71E+000	-3,2500E+000	7,2800E-015	2,4400E-002
MFO	23	2,5368E+002	2,03147E+003	-3,22E+003	9,05E+003	-3,2000E+000	7,9500E-004	3,9800E-001
MVO	23	-1,0936E+002	5,99387E+002	-2,84E+003	3,36E+002	-3,2000E+000	1,4500E-002	3,3400E-001
SCA	23	-9,4974E+001	4,54527E+002	-2,18E+003	7,32E+000	-2,9500E+000	1,7300E-003	4,6100E-001
SAO	23	-1,4249E+002	6,81779E+002	-3,27E+003	6,17E+000	-3,2300E+000	1,5000E-010	2,0400E-001
LCA	23	-1,2291E+002	5,94526E+002	-2,85E+003	3,06E+001	-1,1800E+000	5,8600E-002	3,9700E-001
ALO	23	-9,5060E+001	4,58896E+002	-2,20E+003	2,30E+001	-3,2000E+000	2,1700E-003	3,9800E-001
BBO	23	-1,4157E+002	6,84178E+002	-3,28E+003	1,57E+001	-3,2100E+000	5,7300E-004	2,4100E-001
CSO	23	-1,3335E+002	6,35817E+002	-3,05E+003	7,49E+000	-3,1900E+000	1,9000E-006	3,5200E-001
FPA	23	-1,0224E+002	6,50161E+002	-3,03E+003	5,97E+002	-3,2800E+000	1,2200E+000	6,7300E+000
PSO	23	-1,0464E+002	5,02563E+002	-2,41E+003	1,06E+001	-2,6800E+000	6,5700E-015	6,9600E-002
AOA	23	-9,1115E+001	4,35760E+002	-2,09E+003	8,73E+000	-2,9600E+000	1,2400E-015	6,5300E-001

RANK

	Mean rank :
HGSO	6,65
BA	14,83
FA	4,65
GWO	5,24
MFO	8,17
MVO	8,33
SCA	9,52
SAO	6,20
LCA	10,30
ALO	8,98
BBO	8,11
CSO	5,89
FPA	9,20
PSO	6,41
AOA	7,52

a

N	23
Chi-square	109,360
df	14
Asymp. sig	,000

a. Friedman test

Fig. 16 The Friedman tests of the fitness value

fuzzy-based and Lévy Flight modifications (13.8% each) improve optimization performance by handling uncertainty through fuzzy logic while enhancing global search efficiency via stochastic random walks. Additionally, adaptive techniques (10.3%) improve performance by dynamically adjusting parameters in response to changing environments. Meanwhile, binary optimization and opposition-based learning (6.9% each) focus on discrete search spaces and accelerating convergence through opposition-based strategies. Finally, quantum-based and mutation-based approaches (3.4% each) represent the smallest categories, indicating that

Table 13 Comparison of HGSO and its variants on F_1 to F_{23}

Function	Metric	HGSO	CHGSO	LHGSO	OHGSO	MHGSO	CLHGSO	COHGSO	CMHGSO	LOHGSO	LMHGSO	CLOHGSO	CLMHGSO
F_1	Best	1.38E−234	7.06E−123	5.29E−05	3.04E−231	1.72E−226	4.52E−05	9.91E−124	6.20E−124	4.84E−05	3.72E−05	1.23E−04	3.73E−05
	Worst	2.97E−205	2.84E−58	1.26E−04	4.61E−193	7.86E−199	1.59E−04	6.48E−70	9.68E−72	1.28E−04	1.11E−04	3.10E−04	1.76E−04
	Mean	2.14E−206	1.42E−59	8.54E−05	2.30E−194	4.27E−200	1.06E−04	3.24E−71	4.84E−73	8.27E−05	8.01E−05	2.15E−04	1.07E−04
	Std	0.00E+00	6.36E−59	1.84E−05	0.00E+00	0.00E+00	3.02E−05	1.45E−70	2.16E−72	1.72E−05	1.89E−05	4.79E−05	3.42E−05
	Rank	1	6	9	3	2	10	5	4	8	7	12	11
	P-value	0.00E+00	6.80E−08	6.80E−08	7.56E−01	1.08E−01	6.80E−08	6.80E−08	6.80E−08	6.80E−08	6.80E−08	6.80E−08	6.80E−08
F_2	Best	1.08E−118	2.73E−63	1.92E−02	8.71E−117	3.98E−120	1.87E−02	1.68E−63	1.87E−63	1.45E−02	1.67E−02	2.74E−02	2.10E−02
	Worst	4.83E−94	2.33E−42	2.64E−02	9.11E−103	2.09E−103	3.22E−02	4.32E−39	1.99E−37	3.08E−02	2.63E−02	4.75E−02	3.02E−02
	Mean	2.41E−95	1.17E−43	2.28E−02	4.60E−104	1.05E−104	2.53E−02	2.56E−40	1.03E−38	2.25E−02	2.29E−02	3.78E−02	2.56E−02
	Std	1.08E−94	5.21E−43	1.99E−03	2.04E−103	4.68E−104	3.80E−03	9.74E−40	4.44E−38	4.03E−03	2.85E−03	4.92E−03	2.74E−03
	Rank	3	4	8	2	1	10	5	6	7	9	12	11
	P-value	0.00E+00	6.80E−08	6.80E−08	2.73E−01	1.40E−01	6.80E−08	6.80E−08	6.80E−08	6.80E−08	6.80E−08	6.80E−08	6.80E−08
F_3	Best	2.06E−223	9.61E−122	6.50E−05	3.02E−222	3.94E−215	4.16E−05	3.86E−122	2.33E−121	5.73E−05	6.47E−05	1.50E−04	1.08E−04
	Worst	4.89E−172	1.09E−69	1.31E−04	1.24E−172	3.65E−165	2.89E−04	1.19E−61	1.85E−75	1.66E−04	1.65E−04	4.77E−04	4.03E−04
	Mean	2.44E−173	5.46E−71	9.90E−05	6.18E−174	1.83E−166	1.78E−04	5.94E−63	9.24E−77	1.02E−04	1.08E−04	3.01E−04	2.05E−04
	Std	0.00E+00	2.43E−70	1.83E−05	0.00E+00	0.00E+00	5.82E−05	2.66E−62	4.13E−76	2.89E−05	3.14E−05	9.38E−05	6.86E−05
	Rank	2	5	7	1	3	10	6	4	8	9	12	11
	P-value	0.00E+00	6.80E−08	6.80E−08	4.25E−01	3.51E−01	6.80E−08	6.80E−08	6.80E−08	6.80E−08	6.80E−08	6.80E−08	6.80E−08
F_4	Best	3.52E−118	2.92E−61	4.70E−03	3.80E−116	7.68E−116	3.71E−03	2.20E−61	1.95E−61	3.88E−03	3.93E−03	6.26E−03	4.28E−03
	Worst	7.95E−101	6.43E−40	6.15E−03	2.05E−93	3.59E−93	7.12E−03	9.55E−40	8.36E−36	6.46E−03	6.00E−03	1.10E−02	6.92E−03
	Mean	5.67E−102	3.30E−41	5.36E−03	1.03E−94	1.88E−94	5.44E−03	7.68E−41	4.18E−37	5.24E−03	4.96E−03	9.14E−03	5.68E−03
	Std	1.89E−101	1.44E−40	4.90E−04	4.59E−94	8.02E−94	8.50E−04	2.27E−40	1.87E−36	7.08E−04	6.18E−04	1.23E−03	8.10E−04
	Rank	1	4	9	2	3	10	5	6	8	7	12	11
	P-value	0.00E+00	6.80E−08	6.80E−08	6.75E−01	9.03E−01	6.80E−08	6.80E−08	6.80E−08	6.80E−08	6.80E−08	6.80E−08	6.80E−08
F_5	Best	6.73E+00	8.76E+00	7.06E+00	6.95E+00	6.72E+00	7.85E+00	8.77E+00	8.30E+00	7.07E+00	7.05E+00	8.53E+00	7.86E+00
	Worst	8.08E+00	8.77E+00	7.82E+00	8.07E+00	8.11E+00	8.49E+00	8.77E+00	9.00E+00	7.64E+00	7.76E+00	8.84E+00	8.49E+00
	Mean	7.49E+00	8.76E+00	7.44E+00	7.47E+00	7.62E+00	8.16E+00	8.77E+00	8.76E+00	7.42E+00	7.44E+00	8.74E+00	8.26E+00
	Std	3.81E−01	2.03E−03	1.91E−01	3.49E−01	4.14E−01	1.95E−01	9.82E−04	1.53E−01	1.56E−01	1.74E−01	7.03E−02	1.50E−01
	Rank	5	11	3	4	6	7	12	10	1	2	9	8
	P-value	0.00E+00	6.80E−08	9.46E−01	6.75E−01	2.98E−01	1.58E−06	6.80E−08	6.80E−08	7.15E−01	9.03E−01	6.80E−08	2.22E−07
F_6	Best	6.48E−02	2.50E+00	9.11E−02	1.38E−01	5.52E−02	1.27E+00	1.53E+00	2.04E+00	5.56E−02	5.00E−02	1.16E+00	1.31E+00
	Worst	7.76E−01	2.50E+00	2.95E−01	9.01E−01	7.76E−01	1.99E+00	1.84E+00	2.50E+00	3.07E−01	3.78E−01	1.92E+00	1.88E+00
	Mean	3.56E−01	2.50E+00	1.82E−01	3.73E−01	4.04E−01	1.66E+00	1.74E+00	2.31E+00	1.65E−01	1.74E−01	1.73E+00	1.57E+00
	Std	2.08E−01	7.89E−16	6.37E−02	2.03E−01	2.14E−01	1.82E−01	8.97E−02	1.44E−01	6.86E−02	7.91E−02	1.87E−01	1.60E−01
	Rank	4	12	3	5	6	8	10	11	1	2	9	7
	P-value	0.00E+00	2.86E−08	1.78E−03	7.56E−01	3.10E−01	6.80E−08	6.80E−08	6.75E−08	4.60E−04	7.58E−04	6.80E−08	6.80E−08

Table 13 (continued)

Function	Metric	HGSO	CHGSO	LHGSO	OHGSO	MHGSO	CLHGSO	COHGSO	CMHGSO	LOHGSO	LMHGSO	CLOHGSO	CLMHGSO
F_7	Best	1.61E−05	3.50E−04	4.54E−05	3.85E−06	5.94E−06	8.07E−05	1.08E−04	6.12E−05	1.04E−05	2.57E−05	5.07E−05	1.11E−04
	Worst	4.27E−04	2.89E−03	7.66E−04	1.90E−04	4.48E−04	3.59E−03	1.30E−03	1.82E−03	3.05E−04	9.38E−04	1.07E−03	3.05E−03
	Mean	1.36E−04	1.41E−03	2.74E−04	5.18E−05	1.69E−04	1.07E−03	5.36E−04	7.80E−04	1.16E−04	2.97E−04	3.60E−04	9.44E−04
	Std	1.09E−04	6.58E−04	1.90E−04	4.53E−05	1.39E−04	9.36E−04	3.44E−04	5.24E−04	8.02E−05	2.68E−04	3.04E−04	7.49E−04
	Rank	3	12	5	1	4	11	8	9	2	6	7	10
	P-value	0.00E+00	9.17E−08	2.80E−03	1.12E−03	6.17E−01	2.92E−05	1.25E−05	1.10E−05	6.17E−01	3.85E−02	2.80E−03	6.01E−07
F_8	Best	−2.30E+03	−2.13E+03	−2.28E+03	−2.59E+03	−2.48E+03	−2.44E+03	−2.57E+03	−2.85E+03	−2.55E+03	−2.58E+03	−1.44E+03	−3.11E+03
	Worst	−1.83E+03	−1.66E+03	−1.84E+03	−1.94E+03	−2.11E+03	−1.58E+03	−1.67E+03	−2.31E+03	−1.96E+03	−2.16E+03	−1.25E+03	−2.21E+03
	Mean	−2.01E+03	−1.85E+03	−2.02E+03	−2.20E+03	−2.34E+03	−1.89E+03	−1.98E+03	−2.53E+03	−2.21E+03	−2.33E+03	−1.26E+03	−2.46E+03
	Std	1.36E+02	1.38E+02	1.02E+02	1.52E+02	1.11E+02	2.26E+02	2.23E+02	1.46E+02	1.51E+02	1.08E+02	5.30E+01	2.02E+02
	Rank	8	11	7	6	3	10	9	1	5	4	12	2
	P-value	0.00E+00	1.01E−03	7.56E−01	5.63E−04	5.23E−07	1.33E−02	3.65E−01	6.80E−08	3.05E−04	6.92E−07	1.51E−08	1.43E−07
F_9	Best	0.00E+00	0.00E+00	9.27E−03	0.00E+00	0.00E+00	1.82E−02	0.00E+00	0.00E+00	8.84E−03	1.05E−02	1.34E−02	1.61E−02
	Worst	0.00E+00	6.50E+01	2.31E−02	0.00E+00	0.00E+00	3.67E+01	6.38E+01	1.64E+01	2.82E−02	2.58E−02	1.08E−01	2.33E+01
	Mean	0.00E+00	1.28E+01	1.58E−02	0.00E+00	0.00E+00	2.55E+00	1.63E+01	2.44E+00	1.67E−02	1.85E−02	5.21E−02	2.54E+00
	Std	0.00E+00	2.12E+01	3.80E−03	0.00E+00	0.00E+00	8.25E+00	2.15E+01	5.21E+00	4.94E−03	4.49E−03	2.22E−02	5.69E+00
	Rank	1	11	4	1	1	10	12	8	5	6	7	9
	P-value	0.00E+00	6.64E−05	8.01E−09	NaN	NaN	8.01E−09	3.35E−07	2.44E−05	8.01E−09	8.01E−09	8.01E−09	8.01E−09
F_{10}	Best	8.88E−16	7.99E−15	1.07E−02	8.88E−16	8.88E−16	8.69E−03	7.99E−15	7.99E−15	7.27E−03	9.29E−03	1.19E−02	9.92E−03
	Worst	8.88E−16	4.35E−14	1.52E−02	8.88E−16	8.88E−16	1.59E−02	4.00E−14	3.29E−14	1.38E−02	1.39E−02	2.49E−02	1.68E−02
	Mean	8.88E−16	2.36E−14	1.30E−02	8.88E−16	8.88E−16	1.34E−02	2.43E−14	1.85E−14	1.15E−02	1.17E−02	1.95E−02	1.35E−02
	Std	0.00E+00	1.02E−14	1.48E−03	0.00E+00	0.00E+00	2.29E−03	9.39E−15	1.06E−14	1.78E−03	1.37E−03	3.52E−03	1.90E−03
	Rank	1	5	9	1	1	10	6	4	7	8	12	11
	P-value	0.00E+00	7.05E−09	8.01E−09	NaN	NaN	8.01E−09	7.19E−09	6.43E−09	8.01E−09	8.01E−09	8.01E−09	8.01E−09
F_{11}	Best	0.00E+00	2.55E−01	6.17E−06	0.00E+00	0.00E+00	2.43E−01	1.82E−01	2.22E−01	5.28E−06	2.42E−06	1.48E−05	8.92E−02
	Worst	0.00E+00	1.15E+00	1.51E−05	0.00E+00	0.00E+00	1.31E+00	1.04E+00	1.15E+00	1.42E−05	1.54E−05	8.38E−01	1.04E+00
	Mean	0.00E+00	7.16E−01	1.00E−05	0.00E+00	0.00E+00	7.04E−01	6.05E−01	6.03E−01	1.05E−05	8.39E−06	7.57E−02	5.79E−01
	Std	0.00E+00	2.48E−01	2.52E−06	0.00E+00	0.00E+00	2.79E−01	2.39E−01	2.61E−01	2.34E−06	3.46E−06	2.34E−01	2.32E−01
	Rank	1	12	5	1	1	11	10	9	6	4	7	8
	P-value	0.00E+00	8.01E−09	8.01E−09	NaN	NaN	8.01E−09	8.01E−09	8.01E−09	8.01E−09	8.01E−09	8.01E−09	8.01E−09

Table 13 (continued)

Function	Metric	HGSO	CHGSO	LHGSO	OHGSO	MHGSO	CLHGSO	COHGSO	CMHGSO	LOHGSO	LMHGSO	CLOHGSO	CLMHGSO
F_{12}	Best	2.07E−02	1.61E+00	1.92E−02	1.94E−02	2.28E−02	6.78E−01	5.98E−01	2.82E−01	2.49E−02	4.26E−02	2.92E−01	4.49E−01
	Worst	1.44E−01	2.65E+00	1.54E−01	1.88E−01	2.05E−01	1.67E+00	2.49E+00	2.24E+00	1.21E−01	1.10E−01	7.85E−01	9.96E−01
	Mean	8.27E−02	2.35E+00	7.47E−02	9.29E−02	1.07E−01	1.22E+00	1.62E+00	1.02E+00	7.15E−02	7.36E−02	4.58E−01	6.54E−01
	Std	3.65E−02	3.17E−01	2.75E−02	4.91E−02	5.80E−02	2.36E−01	5.81E−01	4.07E−01	3.20E−02	1.89E−02	1.39E−01	1.42E−01
	Rank	4	12	3	5	6	10	11	9	1	2	7	8
	P-value	0.00E+00	6.79E−08	3.94E−01	5.43E−01	2.98E−01	6.80E−08	6.80E−08	6.80E−08	3.51E−01	3.37E−01	6.80E−08	6.80E−08
F_{13}	Best	1.67E−01	9.21E−01	6.59E−02	1.26E−01	2.44E−01	8.05E−01	8.54E−01	8.43E−01	1.05E−01	8.15E−02	8.77E−01	7.56E−01
	Worst	6.32E−01	1.15E+00	5.67E−01	5.16E−01	6.55E−01	8.99E−01	9.59E−01	1.18E+00	4.53E−01	5.47E−01	9.59E−01	9.29E−01
	Mean	3.63E−01	9.95E−01	2.79E−01	2.96E−01	4.76E−01	8.66E−01	9.12E−01	9.70E−01	2.50E−01	3.12E−01	9.34E−01	8.54E−01
	Std	1.59E−01	7.57E−02	1.62E−01	1.41E−01	1.40E−01	3.28E−02	3.15E−02	1.07E−01	1.13E−01	1.63E−01	2.39E−02	5.30E−02
	Rank	5	12	2	3	6	8	9	11	1	4	10	7
	P-value	0.00E+00	1.83E−04	2.73E−01	3.07E−01	1.86E−01	1.83E−04	1.83E−04	1.83E−04	1.04E−01	5.21E−01	1.83E−04	1.83E−04
F_{14}	Best	1.02E+00	1.03E+00	9.98E−01	9.98E−01	9.98E−01	9.98E−01	9.98E−01	9.98E−01	1.01E+00	9.98E−01	2.19E+00	9.98E−01
	Worst	3.16E+00	6.99E+00	2.98E+00	2.98E+00	1.52E+00	8.87E+00	7.88E+00	9.99E−01	2.98E+00	1.99E+00	8.65E+00	9.98E−01
	Mean	2.00E+00	3.64E+00	1.51E+00	1.78E+00	1.06E+00	3.70E+00	3.19E+00	9.98E−01	1.89E+00	1.11E+00	5.64E+00	9.98E−01
	Std	8.27E−01	1.75E+00	6.95E−01	6.71E−01	1.63E−01	2.99E+00	2.01E+00	2.88E−04	8.79E−01	3.12E−01	2.63E+00	3.48E−05
	Rank	8	10	5	6	3	11	9	2	7	4	12	1
	P-value	0.00E+00	2.11E−02	3.76E−02	3.45E−01	7.69E−04	3.85E−01	1.86E−01	1.83E−04	7.34E−01	7.69E−04	1.31E−03	1.83E−04
F_{15}	Best	3.19E−04	1.20E−03	3.24E−04	3.21E−04	3.20E−04	4.37E−04	4.46E−04	3.73E−04	3.17E−04	3.19E−04	3.55E−04	3.38E−04
	Worst	5.14E−04	1.13E−02	4.47E−04	5.62E−04	4.88E−04	2.98E−03	4.06E−03	1.11E−03	4.41E−04	4.34E−04	2.25E−03	1.10E−03
	Mean	3.75E−04	3.42E−03	3.60E−04	3.93E−04	3.84E−04	1.30E−03	2.00E−03	7.77E−04	3.58E−04	3.65E−04	8.20E−04	5.86E−04
	Std	6.71E−05	3.10E−03	3.51E−05	6.91E−05	5.15E−05	9.18E−04	1.15E−03	2.84E−04	3.53E−05	3.71E−05	5.40E−04	2.46E−04
	Rank	4	12	2	6	5	10	11	8	1	3	9	7
	P-value	0.00E+00	1.83E−04	9.70E−01	2.73E−01	4.27E−01	3.30E−04	3.30E−04	1.01E−03	9.70E−01	7.34E−01	1.71E−03	1.13E−02
F_{16}	Best	−1.03E+00	−1.03E+00	−1.03E+00	−1.03E+00	−1.03E+00	−1.03E+00	−1.03E+00	−1.03E+00	−1.03E+00	−1.03E+00	−1.03E+00	−1.03E+00
	Worst	−1.03E+00	−9.45E−01	−1.03E+00	−1.03E+00	−1.03E+00	−1.03E+00	−9.50E−01	−1.03E+00	−1.03E+00	−1.03E+00	−9.05E−01	−1.03E+00
	Mean	−1.03E+00	−9.79E−01	−1.03E+00	−1.03E+00	−1.03E+00	−1.03E+00	−9.94E−01	−1.03E+00	−1.03E+00	−1.03E+00	−9.89E−01	−1.03E+00
	Std	7.10E−05	2.90E−02	3.72E−05	4.22E−05	3.26E−05	1.29E−03	2.90E−02	2.35E−04	5.40E−05	3.85E−05	5.01E−02	2.11E−06
	Rank	7	12	3	5	2	9	10	8	4	6	11	1
	P-value	0.00E+00	1.83E−04	2.73E−01	5.71E−01	1.40E−01	2.11E−02	1.83E−04	3.85E−01	3.45E−01	6.78E−01	1.83E−04	1.83E−04

Table 13 (continued)

Function	Metric	HGSO	CHGSO	LHGSO	OHGSO	MHGSO	CLHGSO	COHGSO	CMHGSO	LOHGSO	LMHGSO	CLOHGSO	CLMHGSO
F_{17}	Best	3.98E−01	3.99E−01	3.98E−01	3.99E−01	3.98E−01	3.98E−01	3.99E−01	3.98E−01	3.98E−01	3.98E−01	4.32E−01	3.98E−01
	Worst	4.04E−01	6.22E−01	4.01E−01	4.04E−01	4.00E−01	3.99E−01	4.25E−01	3.98E−01	4.08E−01	4.01E−01	6.94E−01	3.98E−01
	Mean	4.01E−01	4.45E−01	3.99E−01	4.00E−01	3.98E−01	3.98E−01	4.08E−01	3.98E−01	4.01E−01	3.99E−01	5.41E−01	3.98E−01
	Std	1.88E−03	6.97E−02	9.52E−04	1.92E−03	5.78E−04	4.61E−04	1.06E−02	1.38E−04	2.98E−03	9.59E−04	9.78E−02	8.75E−07
	Rank	8	11	6	7	4	3	10	2	9	5	12	1
	P-value	0.00E+00	4.59E−03	1.04E−01	9.10E−01	9.11E−03	1.71E−03	1.40E−01	4.40E−04	6.23E−01	1.40E−02	1.83E−04	1.83E−04
F_{18}	Best	3.00E+00	3.01E+00	3.00E+00	3.00E+00	3.00E+00	3.00E+00	3.00E+00	3.00E+00	3.00E+00	3.00E+00	3.00E+00	3.00E+00
	Worst	3.00E+00	4.74E+00	3.00E+00	3.00E+00	3.00E+00	3.00E+00	4.68E+00	3.00E+00	3.00E+00	3.00E+00	3.17E+00	3.00E+00
	Mean	3.00E+00	3.47E+00	3.00E+00	3.00E+00	3.00E+00	3.00E+00	3.50E+00	3.00E+00	3.00E+00	3.00E+00	3.04E+00	3.00E+00
	Std	1.36E−04	5.67E−01	4.82E−04	2.26E−04	3.17E−05	1.87E−04	5.26E−01	1.95E−04	9.06E−04	1.31E−04	5.09E−02	3.56E−05
	Rank	6	11	8	7	2	5	12	3	9	4	10	1
	P-value	0.00E+00	1.83E−04	4.52E−02	9.10E−01	4.52E−02	5.71E−01	2.11E−02	2.57E−02	1.71E−03	5.21E−01	1.83E−04	1.73E−02
F_{19}	Best	−3.86E+00	−3.81E+00	−3.86E+00	−3.86E+00	−3.86E+00	−3.86E+00	−3.85E+00	−3.86E+00	−3.86E+00	−3.86E+00	−3.85E+00	−3.86E+00
	Worst	−3.85E+00	−3.56E+00	−3.85E+00	−3.85E+00	−3.85E+00	−3.85E+00	−3.80E+00	−3.86E+00	−3.85E+00	−3.86E+00	−3.76E+00	−3.86E+00
	Mean	−3.86E+00	−3.70E+00	−3.86E+00	−3.86E+00	−3.86E+00	−3.86E+00	−3.82E+00	−3.86E+00	−3.86E+00	−3.86E+00	−3.80E+00	−3.86E+00
	Std	4.86E−03	9.20E−02	3.10E−03	2.92E−03	2.24E−03	2.78E−03	2.35E−02	1.45E−03	4.62E−03	1.70E−03	3.04E−02	2.15E−03
	Rank	7	12	6	8	5	2	10	3	9	4	11	1
	P-value	0.00E+00	1.82E−04	7.34E−01	6.78E−01	6.23E−01	2.20E−03	7.69E−04	1.01E−03	5.71E−01	2.57E−02	1.83E−04	7.69E−04
F_{20}	Best	−3.18E+00	−2.77E+00	−3.24E+00	−3.21E+00	−3.26E+00	−3.12E+00	−2.75E+00	−3.28E+00	−3.20E+00	−3.26E+00	−2.60E+00	−3.28E+00
	Worst	−2.98E+00	−2.10E+00	−3.00E+00	−3.01E+00	−3.06E+00	−2.84E+00	−2.25E+00	−3.20E+00	−2.98E+00	−3.11E+00	−2.10E+00	−3.19E+00
	Mean	−3.08E+00	−2.36E+00	−3.13E+00	−3.09E+00	−3.16E+00	−3.01E+00	−2.53E+00	−3.25E+00	−3.08E+00	−3.20E+00	−2.25E+00	−3.24E+00
	Std	7.13E−02	2.28E−01	8.26E−02	5.88E−02	6.78E−02	1.01E−01	1.66E−01	2.69E−02	6.89E−02	5.71E−02	2.29E−01	3.49E−02
	Rank	7	11	5	6	4	9	10	1	8	3	12	2
	P-value	0.00E+00	1.83E−04	1.86E−01	7.34E−01	4.52E−02	8.90E−02	1.83E−04	1.83E−04	7.34E−01	2.83E−03	1.49E−04	1.83E−04
F_{21}	Best	−4.95E+00	−4.64E+00	−4.93E+00	−6.04E+00	−5.00E+00	−3.97E+00	−4.35E+00	−1.01E+01	−7.87E+00	−5.00E+00	−7.87E+00	−1.01E+01
	Worst	−4.21E+00	−1.59E+00	−4.36E+00	−4.16E+00	−4.64E+00	−1.59E+00	−2.50E+00	−7.48E+00	−4.14E+00	−4.63E+00	−1.54E+00	−5.22E+00
	Mean	−4.60E+00	−2.85E+00	−4.66E+00	−4.79E+00	−4.78E+00	−2.43E+00	−3.00E+00	−8.97E+00	−4.88E+00	−4.85E+00	−3.36E+00	−8.99E+00
	Std	2.59E−01	1.05E+00	1.75E−01	5.21E−01	1.21E−01	7.60E−01	6.62E−01	9.15E−01	1.09E+00	1.35E−01	1.97E+00	1.41E+00
	Rank	8	11	7	5	6	12	10	2	3	4	9	1
	P-value	0.00E+00	7.69E−04	7.91E−01	6.78E−01	1.21E−01	1.83E−04	3.30E−04	1.83E−04	9.10E−01	3.12E−02	1.40E−02	1.83E−04

Table 13 (continued)

Function	Metric	HGSO	CHGSO	LHGSO	OHGSO	MHGSO	CLHGSO	COHGSO	CMHGSO	LOHGSO	LMHGSO	CLOHGSO	CLMHGSO
F_{22}	Best	−4.98E+00	−3.78E+00	−4.98E+00	−4.90E+00	−4.97E+00	−4.73E+00	−4.19E+00	−9.40E+00	−8.95E+00	−4.97E+00	−6.27E+00	−1.02E+01
	Worst	−4.30E+00	−1.65E+00	−4.39E+00	−4.22E+00	−4.70E+00	−1.93E+00	−1.75E+00	−4.57E+00	−4.67E+00	−4.70E+00	−1.38E+00	−3.34E+00
	Mean	−4.74E+00	−2.73E+00	−4.70E+00	−4.59E+00	−4.88E+00	−3.17E+00	−2.71E+00	−6.54E+00	−5.69E+00	−4.88E+00	−3.21E+00	−5.91E+00
	Std	1.99E−01	6.77E−01	2.02E−01	2.42E−01	8.59E−02	9.18E−01	7.93E−01	1.89E+00	1.60E+00	7.98E−02	1.61E+00	2.48E+00
	Rank	6	11	7	8	5	10	12	1	3	4	9	2
	P-value	0.00E+00	1.83E−04	5.71E−01	1.40E−01	1.04E−01	5.83E−04	1.83E−04	9.11E−03	1.73E−02	6.40E−02	2.57E−02	6.78E−01
F_{23}	Best	−4.94E+00	−3.12E+00	−4.94E+00	−8.14E+00	−4.98E+00	−4.47E+00	−4.16E+00	−4.85E+00	−7.27E+00	−5.03E+00	−4.81E+00	−7.82E+00
	Worst	−4.43E+00	−1.49E+00	−4.44E+00	−3.90E+00	−4.65E+00	−1.68E+00	−2.56E+00	−3.86E+00	−4.64E+00	−4.64E+00	−2.17E+00	−3.37E+00
	Mean	−4.76E+00	−2.22E+00	−4.80E+00	−5.40E+00	−4.90E+00	−3.20E+00	−3.43E+00	−4.43E+00	−5.16E+00	−4.89E+00	−3.06E+00	−5.18E+00
	Std	1.56E−01	5.65E−01	1.54E−01	1.46E+00	1.21E−01	7.74E−01	5.63E−01	2.86E−01	8.38E−01	1.37E−01	9.15E−01	1.48E+00
	Rank	7	12	6	1	4	10	9	8	3	5	11	2
	P-value	0.00E+00	1.83E−04	6.23E−01	7.91E−01	1.73E−02	2.46E−04	1.83E−04	5.80E−03	2.73E−01	3.76E−02	1.01E−03	9.70E−01

mutation operators and quantum-inspired optimization are less frequently employed in the analyzed dataset.

Figure 21 illustrates the categorization of studies on HGSO based on hybridization methods. The most prevalent approach is its integration with ANNs, which accounts for 43.9% of the methods. The second-largest category, comprising 36.4%, includes meta-heuristics such as GA, SA, and PSO, all of which exploit their capabilities to explore vast search spaces and find near-optimal solutions for complex, non-convex problems. SVR and SVM contribute 6.1% and 1.5%, respectively, underlining the significance of kernel-based techniques in regression and classification tasks. Other techniques, including Random Forest (3.0%), Long Short-Term Memory (1.5%), and Extreme Learning Machines (1.5%), hold minor portions, suggesting they are used in more specialized cases. Additionally, 6.1% is attributed to other methods, reflecting the diversity of approaches beyond those explicitly categorized.

Figure 22 illustrates the classification of related works based on their application domains. The largest category, Engineering, accounts for 41.3% of the applications, reflecting a strong focus on leveraging optimization algorithms to address real-world engineering challenges. Power and Energy follows with 21.7%, emphasizing the critical role of optimization techniques in improving efficiency and sustainability within the energy sector. Meanwhile, Classification represents 28.3% of the applications, highlighting its importance in tasks such as feature selection and data categorization. Lastly, image processing constitutes 8.7% of the applications, demonstrating the role of optimization in enhancing image analysis and processing tasks.

Future research areas for the HGSO algorithm are promising in several directions:

- Multi-objective optimization: Extending the HGSO algorithm using decomposition or Pareto-based methods to improve solution diversity and convergence in complex scenarios where multiple objectives need to be optimized simultaneously.
- Binary and discrete optimization: Adapting the HGSO algorithm for binary and discrete optimization, can tackle feature selection challenges effectively, especially in high-dimensional data like medical imaging.
- Hybridization with deep learning: Combining the HGSO algorithm with deep learning and reinforcement learning models for tasks such as hyperparameter tuning, neural architecture search, or model compression can improve feature extraction and classification accuracy.
- Parameter optimization: Investigating optimal parameter settings for the HGSO algorithm can improve its performance in various applications.

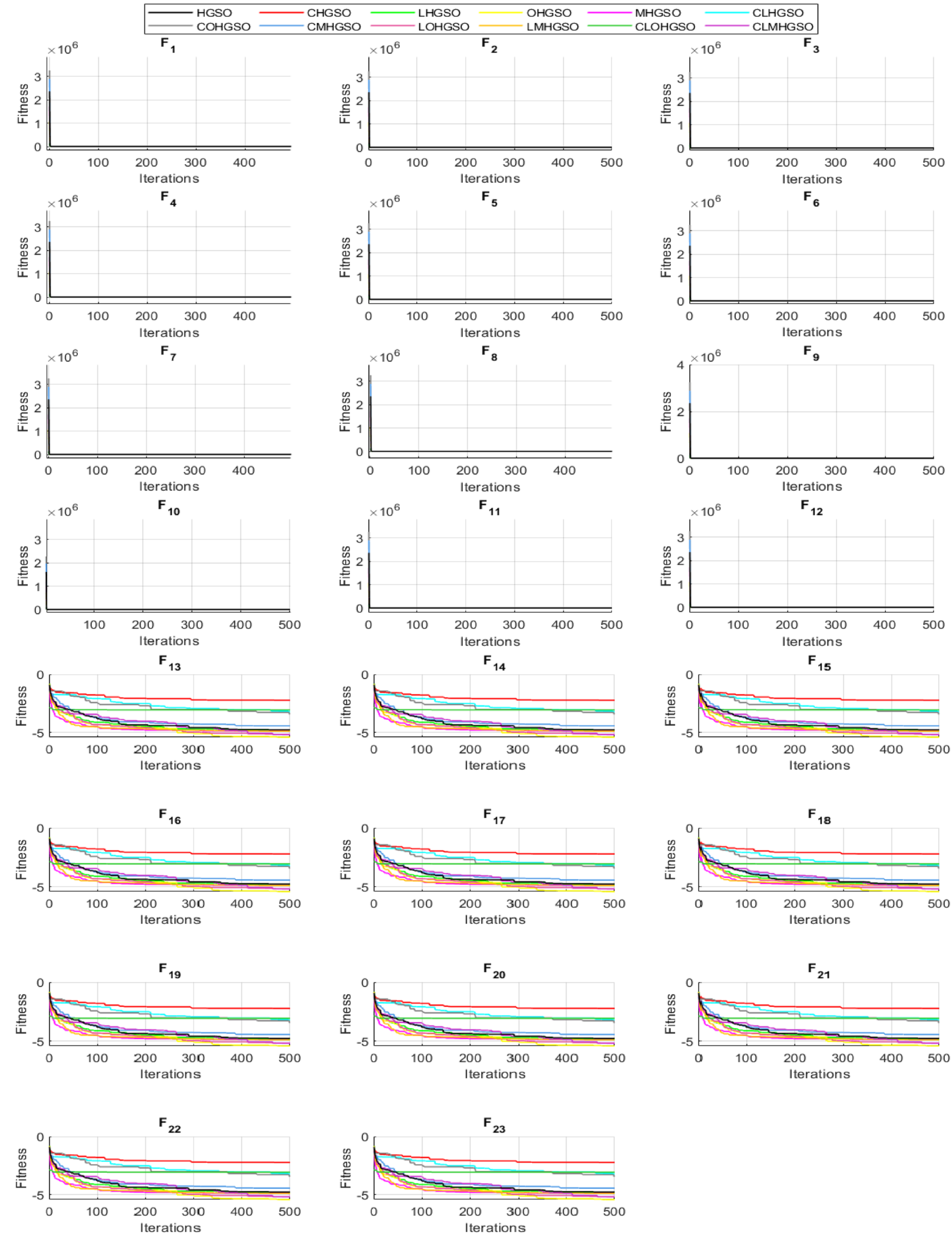

Fig. 17 Convergence of HGSO and its variants

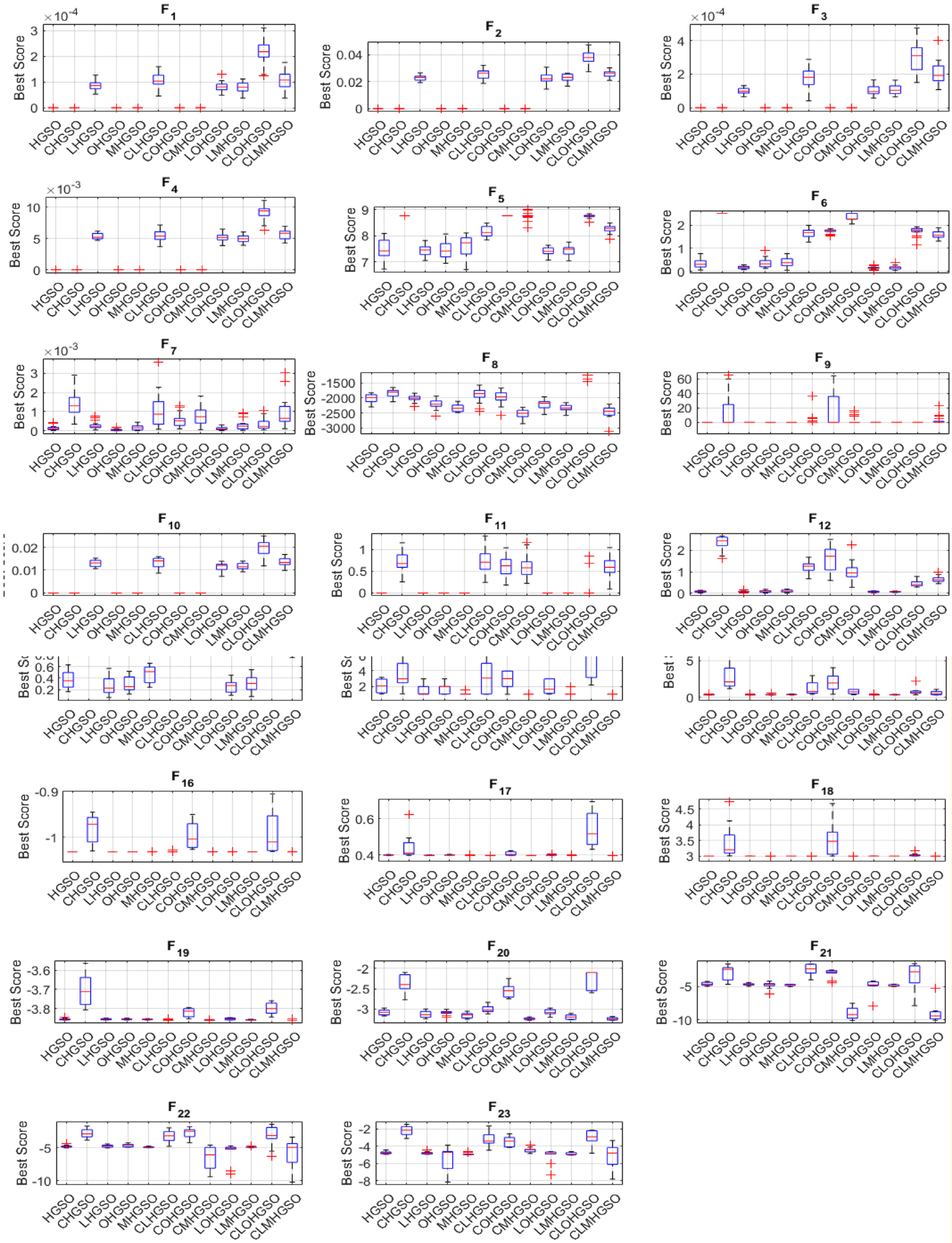

Fig. 18 Box plots of HGSO and its variants

	N	Mean	STD	Minimum	Maximum	Percentiles 25e	50e	75e
HGSO	23	-8,7756E+001	4,19043E+002	-2,01E+003	7,49E+000	-3,0800E+000	5,6700E-102	3,5600E-001
CHGSO	23	-7,9529E+001	3,85967E+002	-1,85E+003	1,28E+001	-2,2200E+000	2,3600E-014	2,3500E+000
LHGSO	23	-8,8228E+001	4,21120E+002	-2,02E+003	7,44E+000	-3,1300E+000	3,6000E-004	1,8200E-001
OHGSO	23	-9,6059E+001	4,58651E+002	-2,20E+003	7,47E+000	-3,0900E+000	4,6000E-104	2,9600E-001
MHGSO	23	-1,0215E+002	4,87841E+002	-2,34E+003	7,62E+000	-3,1600E+000	1,0500E-104	3,9800E-001
CLHGSO	23	-8,1930E+001	3,94154E+002	-1,89E+003	8,16E+000	-2,4300E+000	5,4400E-003	1,2200E+000
COHGSO	23	-8,5193E+001	4,13076E+002	-1,98E+003	1,63E+001	-2,5300E+000	2,4300E-014	1,6200E+000
CMHGSO	23	-1,1033E+002	5,27481E+002	-2,53E+003	8,76E+000	-3,2500E+000	1,8500E-014	9,9800E-001
LOHGSO	23	-9,6541E+001	4,60726E+002	-2,21E+003	7,42E+000	-3,0800E+000	3,5800E-004	1,6500E-001
LMHGSO	23	-1,0175E+002	4,85750E+002	-2,33E+003	7,44E+000	-3,2000E+000	3,6500E-004	1,7400E-001
CLOHGSO	23	-5,4582E+001	2,62787E+002	-1,26E+003	8,74E+000	-2,2500E+000	9,1400E-003	5,4100E-001
CLMHGSO	23	-1,0736E+002	5,12868E+002	-2,46E+003	8,26E+000	-3,2400E+000	5,6800E-003	8,5400E-001

Ranks

	Mean rank:
HGSO	4,61
CHGSO	9,98
LHGSO	5,48
OHGSO	4,00
MHGSO	3,91
CLHGSO	8,89
COHGSO	9,17
CMHGSO	5,72
LOHGSO	4,70
LMHGSO	4,98
CLOHGSO	10,17
CLMHGSO	6,39

a

N	23
Chi-squre	117,006
df	11
Asymp. sig	,000

a. Friedman test

Fig. 19 The Friedman tests of HGSO and its variants' the fitness value

Table 14 Strengths and weaknesses of HGSO

Strengths	Weaknesses
Effectively balances exploration and exploitation	Static cluster mapping hinders dynamic adjustments during iterations
Mitigates premature convergence and avoids local optima by simulating gas molecule huddling behavior	Sensitivity to fixed parameter settings reduces adaptability in dynamic environments
Enhances solution diversity by dividing the population into clusters, each running an independent HGSO instance	Computational overhead from the cluster-based approach introduces scalability challenges in large-scale problems
Dynamically updates Henry's constant H_j and gas solubility S_{ij} using temperature-dependent equations, improving adaptability	Its performance can be sensitive to initial conditions, such as the initial population distribution

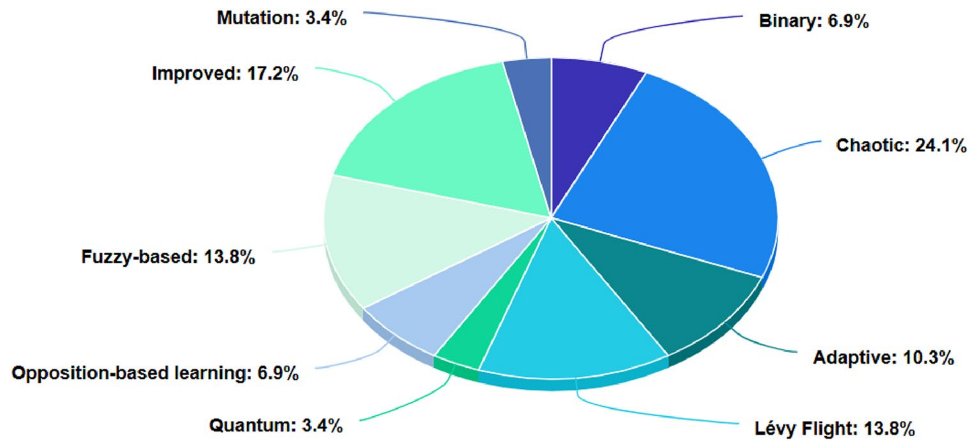

Fig. 20 The modified versions of HGSO algorithm

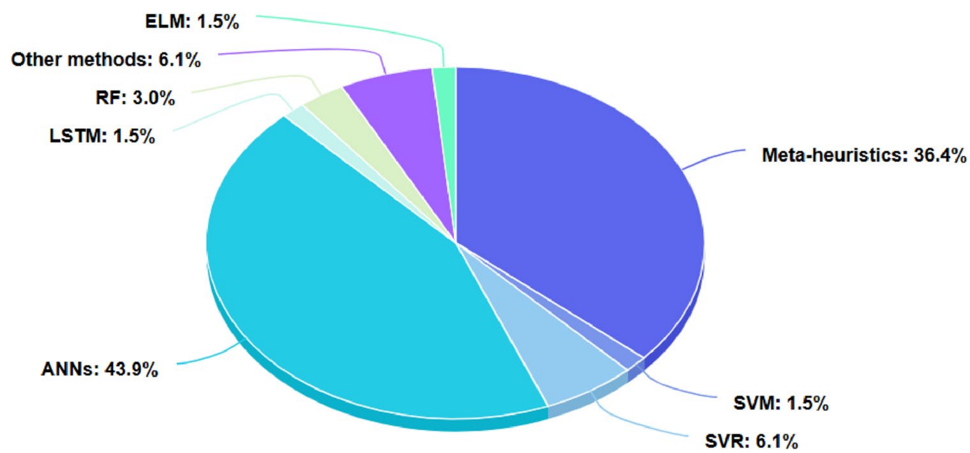

Fig. 21 The hybridized versions of HGSO algorithm

- Scalability and parallelism: Design parallel or distributed variants of the HGSO algorithm to efficiently handle large-scale and real-time optimization challenges.
- Dynamic optimization: Apply the HGSO algorithm to problems where objectives or constraints evolve over time.
- Adaptive strategies: Developing adaptive strategies to adjust the HGSO's parameters dynamically during runtime can enhance its performance in changing environments and improve its scalability for large-scale problems.
- Expansion to emerging domains: Applying the HGSO algorithm to emerging fields like quantum computing, antenna array optimization, cybersecurity, autonomous vehicles, wireless communications, and advanced manufacturing can unlock new potential applications.

7 Conclusion

The Henry Gas Solubility Optimization (HGSO) algorithm is a recent and well-known physics-based optimization algorithm inspired by the principles of Henry's law in chemistry. In this research paper, we provide an extensive and in-depth survey of the HGSO algorithm and its improved variants (multi-objective, hybridized, and modified). Since the introduction of the HGSO algorithm by Hashim et al. in 2019, over 180 HGSO papers have been published by researchers and academics. These related papers proved the emergence of the HGSO algorithm as a promising optimization meta-heuristic in tackling various optimization issues. This is due to its unique structure, its ease of implementation, its simplicity, its convergence speed, and especially its ability to easily hybridize with other optimization methods. Despite the success of the HGSO algorithm, there are still several suggestions for future research to further enhance its performance and applicability. For instance, the modification of the original HGSO algorithm requires more research by introducing new operators and strategies. Additionally, the hybridization of the HGSO algorithm with other optimization meta-heuristics and methods is recommended to enhance its exploration and exploitation. Finally, another interesting point is to expand the application of the HGSO algorithm across more dynamic, high-dimensional, and complex optimization problems.

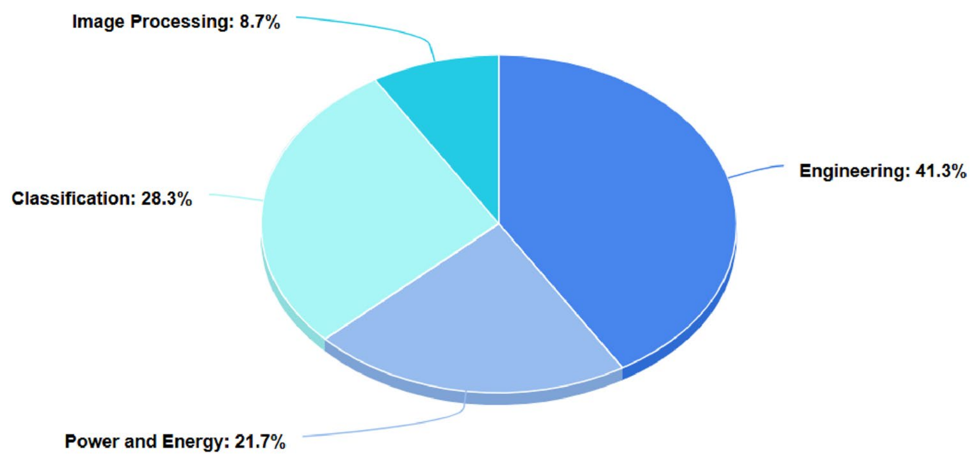

Fig. 22 The applications of HGSO algorithm

Author contributions A A S: Conceptualization, Methodology, Software, Visualization, Investigation, Validation, Writing original draft. S M T: Conceptualization, Methodology, Software, Visualization, Investigation, Validation, Writing original draft. S Y: Conceptualization, Methodology, Software, Visualization, Investigation, Validation, Writing original draft. M D: Investigation, Validation, Writing original draft. E T Y: Investigation, Validation, Writing original draft. Y M: Supervision, Methodology, Writing original draft, Writing review and editing, Visualization, Investigation. M K: Supervision, Validation, Writing review and editing. S M: Supervision, Methodology, Writing original draft, Writing review and editing, Visualization, Investigation. A R-C: Writing review and editing, Visualization, Investigation.

Data availability No datasets were generated or analysed during the current study.

Declarations

Conflict of interest The authors declare that there is no conflict of interest with any person(s) or Organization(s).

References

1. Shehab M, Sihwail R, Daoud M, Al-Mimi H, Abualigah L (2024) Nature-inspired metaheuristic algorithms: a comprehensive review. Int Arab J Inf Technol 21(5):815–831
2. Kirkpatrick S, Gelatt CD, Vecchi MP (1983) Optimization by simulated annealing. Science 220(4598):671–680
3. Glover F (1990) Tabu search: A tutorial. Interfaces 20(4):74–94
4. Feo TA, Resende MGC (1995) Greedy randomized adaptive search procedures. J Global Optim 6:109–133
5. Mladenović N, Hansen P (1997) Variable neighborhood search. Comput Oper Res 24(11):1097–1100
6. Voudouris C, Tsang E (1999) Guided local search and its application to the traveling salesman problem. Eur J Oper Res 113(2):469–499
7. Hoos Holger H, Stützle T (2004) Stochastic local search: foundations and applications. Elsevier, Amsterdam
8. Stützle T (2006) Iterated local search for the quadratic assignment problem. Eur J Oper Res 174(3):1519–1539
9. Holland J (1975) Adaptation in natural and artificial systems. University of Michigan Press, Ann Arbor
10. Koza JR (1993) Genetic programming: on the programming of computers by means of natural selection (complex adaptive systems). A Bradford Book 1:18. MIT, Cambridge
11. Baluja S (1994) Population-based incremental learning: a method for integrating genetic search based function optimization and competitive learning. School of Computer Science, Carnegie Mellon University, Pittsburgh
12. Storn R, Price K (1997) Differential evolution-a simple and efficient heuristic for global optimization over continuous spaces. J Global Optim 11:341–359
13. Salgotra R, Gandomi AH (2024) A novel multi-hybrid differential evolution algorithm for optimization of frame structures. Sci Reports 14(1):4877
14. Fogel LJ, Owens AJ, Walsh MJ (2000) Introduction to artificial intelligence through simulated evolution. Artif Intell Crit Concepts 3:259
15. De Castro LN, Von Zuben FJ (2000) The clonal selection algorithm with engineering applications. In Proceedings of GECCO, volume 2000, pp. 36–39
16. Beyer H-G, Schwefel H-P (2002) Evolution strategies-a comprehensive introduction. Nat Comput 1:3–52
17. Simon D (2008) Biogeography-based optimization. IEEE Trans Evol Comput 12(6):702–713
18. Neri F, Cotta C (2012) Memetic algorithms and memetic computing optimization: a literature review. Swarm Evol Comput 2:1–14
19. Kennedy J, Eberhart R (1995) Particle swarm optimization. In: Proceedings of ICNN'95-international conference on neural networks, volume 4, pp.1942–1948. IEEE
20. Lin S, Liu A, Wang J, Kong X (2024) An improved fault-tolerant cultural-pso with probability for multi-agv path planning. Expert Syst Appl 237:121510
21. Dorigo M, Di Caro G (1999) Ant colony optimization: a new meta-heuristic. In: Proceedings of the 1999 congress on evolutionary computation-CEC99 (Cat. No. 99TH8406), volume 2, pp. 1470–1477. IEEE
22. Yang X-S (2009) Firefly algorithms for multimodal optimization. In: International symposium on stochastic algorithms, pp. 169–178. Springer
23. Yang X-S, Deb S (2009) Cuckoo search via lévy flights. In: 2009 World congress on nature & biologically inspired computing (NaBIC), p. 210–214. IEEE
24. Karaboga D (2010) Artificial bee colony algorithm. Scholarpedia 5(3):6915
25. Yang X-S, Gandomi AH (2012) Bat algorithm: a novel approach for global engineering optimization. Eng Comput 29(5):464–483

26. Amir HG, Amir HA (2012) Krill herd: a new bio-inspired optimization algorithm. Commun Nonlinear Sci Numer Simul 17(12):4831–4845
27. Abualigah L, Al-Zyod M, Ikotun AM, Shehab M, Otair M, Ezugwu AE, Hanandeh ES, Raza A, El-kenawy E-SM (2024) A review of krill herd algorithm: optimization and its applications. Metaheuristic Optim Algorithms. Elsevier, Amsterdam, pp 231–239
28. Mirjalili S, Mirjalili SM, Lewis A (2014) Grey wolf optimizer. Adv Eng Softw 69:46–61
29. Yang Z (2024) Competing leaders grey wolf optimizer and its application for training multi-layer perceptron classifier. Expert Syst Appl 239:122349
30. Mirjalili S (2015) Moth-flame optimization algorithm: a novel nature-inspired heuristic paradigm. Knowl-Based Syst 89:228–249
31. Wang G-G, Deb S, Coelho Leandro dos S (2015) Elephant herding optimization. In: 2015 3rd international symposium on computational and business intelligence (ISCBI), pp. 1–5. IEEE
32. James JQ, Li VOK (2015) A social spider algorithm for global optimization. Appl Soft Comput 30:614–627
33. Mirjalili S (2015) The ant lion optimizer. Adv Eng Softw 83:80–98
34. Mirjalili S, Lewis A (2016) The whale optimization algorithm. Adv Eng Softw 95:51–67
35. Askarzadeh A (2016) A novel metaheuristic method for solving constrained engineering optimization problems: crow search algorithm. Comput Struct 169:1–12
36. Meraihi Y, Gabis AB, Ramdane-Cherif A, Acheli D (2021) A comprehensive survey of crow search algorithm and its applications. Artif Intell Rev 54(4):2669–2716
37. Mirjalili S (2016) Dragonfly algorithm: a new meta-heuristic optimization technique for solving single-objective, discrete, and multi-objective problems. Neural Comput Appl 27(4):1053–1073
38. Mirjalili S, Gandomi AH, Mirjalili SZ, Saremi S, Faris H, Mirjalili SM (2017) Salp swarm algorithm: a bio-inspired optimizer for engineering design problems. Adv Eng Softw 114:163–191
39. Pierezan J, Coelho Leandro Dos S (2018) Coyote optimization algorithm: a new metaheuristic for global optimization problems. In: 2018 IEEE congress on evolutionary computation (CEC), pp. 1–8. IEEE
40. Mirjalili SZ, Mirjalili S, Saremi S, Faris H, Aljarah I (2018) Grasshopper optimization algorithm for multi-objective optimization problems. Appl Intell 48:805–820
41. Meraihi Y, Gabis AB, Mirjalili S, Ramdane-Cherif A (2021) Grasshopper optimization algorithm: theory, variants, and applications. IEEE Access 9:50001–50024
42. Ali AH, Seyedali M, Hossam F, Ibrahim A, Majdi M, Huiling C (2019) Harris hawks optimization: algorithm and applications. Future Gener Comput Syst 97:849–872
43. Abualigah L, Yousri D, Elaziz MA, Ewees AA, Al-Qaness MAA, Gandomi AH (2021) Aquila optimizer: a novel meta-heuristic optimization algorithm. Comput Ind Eng 157:107250
44. Taleb SM, Yasin ET, Saadi AA, Dogan M, Yahia S, Meraihi Y, Koklu M, Mirjalili S, Ramdane-Cherif A (2025) A comprehensive survey of aquila optimizer: theory, variants, hybridization, and applications. Arch Comput Methods Eng. https://doi.org/10.1007/s11831-025-10281-0
45. Hayyolalam V, Kazem AAP (2020) Black widow optimization algorithm: a novel meta-heuristic approach for solving engineering optimization problems. Eng Appl Artif Intell 87:103249
46. Shehab M, Shambour MKY, Abu HMA, Al Hamad HA, Shannaq F, Mizher M, Jaradat G, Daoud Mohammad S, Abualigah L (2024) A survey and recent advances in black widow optimization: variants and applications. Neural Comput Appl. https://doi.org/10.1007/s00521-024-09535-y
47. Abdollahzadeh B, Gharehchopogh FS, Mirjalili S (2021) African vultures optimization algorithm: a new nature-inspired metaheuristic algorithm for global optimization problems. Comput Ind Eng 158:107408
48. Hashim FA, Houssein EH, Hussain K, Mabrouk MS, Al-Atabany W (2022) Honey Badger Algorithm: new metaheuristic algorithm for solving optimization problems. Math Comput Simul 192:84–110
49. Abualigah L, Elaziz MA, Sumari P, Geem ZW, Gandomi AH (2022) Reptile search algorithm (rsa): a nature-inspired meta-heuristic optimizer. Expert Syst Appl 191:116158
50. Abu-Hashem MA, Shehab M, Shambour MK, Abualigah L (2025) Integrated local search technique with reptile search algorithm for solving large-scale bound constrained global optimization problems. Optimal Control Appl Methods 46(2):775–788
51. Braik M, Hammouri A, Atwan J, Al-Betar MA, Awadallah MA (2022) White shark optimizer: a novel bio-inspired meta-heuristic algorithm for global optimization problems. Knowl-Based Syst 243:108457
52. Abdollahzadeh B, Gharehchopogh FS, Mirjalili S (2021) Artificial gorilla troops optimizer: a new nature-inspired metaheuristic algorithm for global optimization problems. Int J Intell Syst 36(10):5887–5958
53. Hashim FA, Hussien AG (2022) Snake optimizer: a novel meta-heuristic optimization algorithm. Knowl-Based Syst 242:108320
54. Zamani H, Nadimi-Shahraki MH, Gandomi AH (2022) Starling murmuration optimizer: a novel bio-inspired algorithm for global and engineering optimization. Comput Methods Appl Mech Eng 392:114616
55. Sang-To T, Le-Minh H, Wahab MA, Thanh C-L (2023) A new metaheuristic algorithm: Shrimp and goby association search algorithm and its application for damage identification in large-scale and complex structures. Adv Eng Softw 176:103363
56. Minh H-L, Sang-To T, Theraulaz G, Wahab MA, Cuong-Le T (2023) Termite life cycle optimizer. Expert Syst Appl 213:119211
57. Ahmadi B, Giraldo JS, Hoogsteen G (2023) Dynamic hunting leadership optimization: algorithm and applications. J Comput Sci 69:102010
58. Wang X (2024) Artificial meerkat algorithm: a new metaheuristic algorithm for solving optimization problems. Phys Scr 99(12):125280
59. Zhou G, Wang D, Zhou G, Jiaxuan D, Guo J (2024) A rhinopithecus swarm optimization algorithm for complex optimization problem. Sci Reports 14(1):15628
60. Wang X (2024) Eurasian lynx optimizer: a novel metaheuristic optimization algorithm for global optimization and engineering applications. Phys Scr 99(11):115275
61. Wang X (2025) Draco lizard optimizer: a novel metaheuristic algorithm for global optimization problems. Evol Intell 18(1):1–20
62. Atashpaz-Gargari E, Lucas C (2007) Imperialist competitive algorithm: an algorithm for optimization inspired by imperialistic competition. In: 2007 IEEE congress on evolutionary computation, pp. 4661–4667. IEEE
63. Xin-She Y (2009) Harmony search as a metaheuristic algorithm. In: Geem ZW (ed) Music-inspired harmony search algorithm. Springer, Berlin, pp 1–14
64. Dai C, Zhu Y, Chen W (2007) Seeker optimization algorithm. In: Computational Intelligence and Security: International Conference, CIS 2006. Guangzhou, China, November 3–6, 2006. Revised Selected Papers, pp. 167–176. Springer
65. Tan Y, Zhu Y (2010) Fireworks algorithm for optimization. In: International conference in swarm intelligence, pp. 355–364. Springer

66. Shi Y (2011) Brain storm optimization algorithm. In: Advances in Swarm Intelligence: Second International Conference, ICSI 2011, Chongqing, China, June 12–15, 2011, Proceedings, Part I 2, pp. 303–309. Springer
67. Venkata Rao R, Savsani VJ, Vakharia DP (2011) Teaching-learning-based optimization: a novel method for constrained mechanical design optimization problems. Comput-Aided Des 43(3):303–315
68. Sadollah A, Bahreininejad A, Eskandar H, Hamdi M (2013) Mine blast algorithm: a new population based algorithm for solving constrained engineering optimization problems. Appl Soft Comput 13(5):2592–2612
69. Ghorbani N, Babaei E (2014) Exchange market algorithm. Appl Soft Comput 19:177–187
70. Ali Husseinzadeh Kashan (2014) League championship algorithm (lca): an algorithm for global optimization inspired by sport championships. Appl Soft Comput 16:171–200
71. Naser M, Babak KR (2014) Soccer league competition algorithm: a novel meta-heuristic algorithm for optimal design of water distribution networks. Swarm Evol Comput 17:14–24
72. Fadakar E, Ebrahimi M (2016) A new metaheuristic football game inspired algorithm. In: 2016 1st conference on swarm intelligence and evolutionary computation (CSIEC), pp. 6–11. IEEE
73. Seyyed HSM, Vahid KB (2019) Poor and rich optimization algorithm: a new human-based and multi populations algorithm. Eng Appl Artif Intell 86:165–181
74. Askari Q, Younas I, Saeed M (2020) Political optimizer: a novel socio-inspired meta-heuristic for global optimization. Knowl-Based Syst 195:105709
75. Al-Betar MA, Alyasseri ZAA, Awadallah MA, Doush IA (2021) Coronavirus herd immunity optimizer (chio). Neural Comput Appl 33(10):5011–5042
76. Braik M, Ryalat MH, Al-Zoubi H (2022) A novel meta-heuristic algorithm for solving numerical optimization problems: Ali baba and the forty thieves. Neural Comput Appl 34(1):409–455
77. Rahmani R, Yusof R (2014) A new simple, fast and efficient algorithm for global optimization over continuous search-space problems: radial movement optimization. Appl Math Comput 248:287–300
78. Karami H, Sanjari MJ, Gharehpetian GB (2014) Hyper-spherical search (hss) algorithm: a novel meta-heuristic algorithm to optimize nonlinear functions. Neural Comput Appl 25(6):1455–1465
79. Salimi H (2015) Stochastic fractal search: a powerful metaheuristic algorithm. Knowl-Based Syst 75:1–18
80. Mirjalili S (2016) SCA: a sine cosine algorithm for solving optimization problems. Knowl-Based Syst 96:120–133
81. Gabis AB, Meraihi Y, Mirjalili S, Ramdane-Cherif A (2021) A comprehensive survey of sine cosine algorithm: variants and applications. Artif Intell Rev 54(7):5469–5540
82. Zhao J, Tang D, Liu Z, Cai Y, Dong S (2020) Spherical search optimizer: a simple yet efficient meta-heuristic approach. Neural Comput Appl 32:9777–9808
83. Nematollahi AF, Rahiminejad A, Vahidi B (2020) A novel meta-heuristic optimization method based on golden ratio in nature. Soft Comput 24(2):1117–1151
84. Abualigah L, Diabat A, Mirjalili S, Elaziz MA, Gandomi AH (2021) The arithmetic optimization algorithm. Comput Methods Appl Mech Eng 376:113609
85. Ahmadianfar I, Heidari AA, Gandomi AH, Chu X, Chen H (2021) Run beyond the metaphor: an efficient optimization algorithm based on Runge Kutta method. Expert Syst Appl 181:115079
86. Formato RA (2007) Central force optimization. Prog Electromagn Res 77(1):425–491
87. Erol OK, Eksin I (2006) A new optimization method: big bang-big crunch. Adv Eng Softw 37(2):106–111
88. Rashedi E, Nezamabadi-Pour H, Saryazdi S (2009) Gsa: a gravitational search algorithm. Inf Sci 179(13):2232–2248
89. Kaveh A, Khayatazad M (2012) A new meta-heuristic method: ray optimization. Comput Struct 112:283–294
90. Kaveh A, Motie Share MA, Moslehi M (2013) Magnetic charged system search: a new meta-heuristic algorithm for optimization. Acta Mech 224(1):85–107
91. Ali K, Vahid RM (2014) Colliding bodies optimization: a novel meta-heuristic method. Comput Struct 139:18–27
92. Ali HK (2015) A new metaheuristic for optimization: optics inspired optimization (oio). Comput Oper Res 55:99–125
93. Abedinpourshotorban H, Shamsuddin SM, Beheshti Z, Jawawi DNA (2016) Electromagnetic field optimization: a physics-inspired metaheuristic optimization algorithm. Swarm Evol Comput 26:8–22
94. Kaveh A, Bakhshpoori T (2016) Water evaporation optimization: a novel physically inspired optimization algorithm. Comput Struct 167:69–85
95. Mirjalili S, Mirjalili SM, Hatamlou A (2016) Multi-verse optimizer: a nature-inspired algorithm for global optimization. Neural Comput Appl 27(2):495–513
96. Kaveh A, Ilchi Ghazaan M (2017) A new meta-heuristic algorithm: vibrating particles system. Sci Iran Transa A Civil Eng 24(2):551
97. Kaveh A, Dadras A (2017) A novel meta-heuristic optimization algorithm: thermal exchange optimization. Adv Eng Softw 110:69–84
98. Tzanetos A, Dounias G (2017) A new metaheuristic method for optimization: sonar inspired optimization. In: International Conference on Engineering Applications of Neural Networks, pp. 417–428. Springer
99. Zhenglei W, Changqiang H, Xiaofei W, Tong H, Yintong L (2019) Nuclear reaction optimization: a novel and powerful physics-based algorithm for global optimization. IEEE Access 7:66084–66109
100. Ahmadianfar I, Bozorg-Haddad O, Chu X (2020) Gradient-based optimizer: a new metaheuristic optimization algorithm. Inf Sci 540:131–159
101. Abualigah L, Elkhalaifa L, Ikotun AM, Al-Saqqar F, El-Bashir M, Sumari P, Shehab M, Abd EDS, Ezugwu AE (2024) Gradient-based optimizer: analysis and application of the berry software product. Metaheuristic optimization algorithms. Elsevier, Amsterdam, pp 221–229
102. Zamani H, Nadimi-Shahraki MH, Gandomi AH (2021) Qana: Quantum-based avian navigation optimizer algorithm. Eng Appl Artif Intell 104:104314
103. Braik M, Al-Hiary H, Alzoubi H, Hammouri A, Al-Betar MA, Awadallah MA (2025) Tornado optimizer with coriolis force: a novel bio-inspired meta-heuristic algorithm for solving engineering problems. Artif Intell Rev 58(4):1–99
104. Hashim FA, Houssein EH, Mabrouk MS, Al-Atabany W, Mirjalili S (2019) Henry gas solubility optimization: a novel physics-based algorithm. Future Gener Comput Syst 101:646–667
105. Neggaz N, Houssein EH, Hussain K (2020) An efficient henry gas solubility optimization for feature selection. Expert Syst Appl 152:113364
106. Nandhini S, Ashokkumar K (2022) An automatic plant leaf disease identification using densenet-121 architecture with a mutation-based henry gas solubility optimization algorithm. Neural Comput Appl 34(7):5513–5534
107. Yıldız BS, Pholdee N, Panagant N, Bureerat S, Yildiz AR, Sait SM (2021) A novel chaotic henry gas solubility optimization algorithm for solving real-world engineering problems. Eng Comput 38:871–883

108. Mohamed AE, Ibrahim A (2021) An improved henry gas solubility optimization algorithm for task scheduling in cloud computing. Artif Intell Rev 54(5):3599–3637
109. Ekinci S, Hekimoğlu B, Izci D (2021) Opposition based henry gas solubility optimization as a novel algorithm for pid control of dc motor. Eng Sci Technol 24(2):331–342
110. Ghadimi N, Sedaghat M, Azar KK, Arandian B, Fathi G, Ghadamyari M (2023) An innovative technique for optimization and sensitivity analysis of a pv/dg/bess based on converged henry gas solubility optimizer: A case study. IET Gener Transm Distri 17(21):4735–4749
111. Hashim FA, Houssein EH, Hussain K, Mabrouk MS, Al-Atabany W (2020) A modified henry gas solubility optimization for solving motif discovery problem. Neural Comput Appl 32(14):10759–10771
112. Yıldız BS, Yıldız AR, Pholdee N, Bureerat S, Sait SM, Patel V (2020) The henry gas solubility optimization algorithm for optimum structural design of automobile brake components. Mater Test 62(3):261–264
113. Mirza AF, Mansoor M, Ling Q (2020) A novel mppt technique based on henry gas solubility optimization. Energy Convers Manag 225:113409
114. El-Shorbagy MA, Bouaouda A, Nabwey HA, Abualigah L, Hashim FA (2024) Advances in henry gas solubility optimization: a physics-inspired metaheuristic algorithm with its variants and applications. IEEE Access 12:26062–26095
115. Abualigah L, Al-Hilo G, Raza A, Ezugwu AE, Al Nasar MR, Mughaid A, AlZubi S, Aldiabat K, Al-diabat M (2024) A review of henry gas solubility optimization algorithm: a robust optimizer and applications. Metaheuristic Optim Algorithms. Elsevier, Amsterdam, pp 177–192
116. Jaffino G, Sundaram M, Prabin JJ (2022) Weighted 1d-local binary pattern features and taylor-henry gas solubility optimization based deep maxout network for discovering epileptic seizure using eeg. Digital Signal Process 122:103349
117. Susheela Vishnoi E, Jain AK (2021) An improved henry gas solubility optimisation-based feature selection approach for histological image taxonomy. Int Jo Intell Syst Technol Appl 20(1):58–78
118. Utama DM, Farida BNI, Ulfa Fitriani M, Ibrahim F, Widodo DS (2021) Hybrid henry gas solubility optimization: an effective algorithm for fuel consumption vehicle routing problem. J Ilmiah Teknik Ind 20(2):141–152
119. Saranya S, Saravanan B (2020) Effect of emission in smes based unit commitment using modified henry gas solubility optimization. J Energy Storage 29:101380
120. Ye J, He X (2023) A novel hybrid of anfis-based models using optimisation approaches to predict mine blast-induced flyrock. Int J Environ Sci Technol 20(4):3673–3686
121. Nand KY, Mukesh S (2022) A novel fuzzy clustering based method for image segmentation in rgb-d images. Eng Appl Artif Intell 111:104709
122. Abbaszadeh M, Ehteram M, Ahmed AN, Singh VP, Elshafie A (2021) The copper grade estimation of porphyry deposits using machine learning algorithms and henry gas solubility optimization. Earth Sci Inform 14:2049–2075
123. Ding W, Nguyen MD, Mohammed AS, Armaghani DJ, Hasanipanah M, Van Bui L, Pham BT (2021) A new development of anfis-based henry gas solubility optimization technique for prediction of soil shear strength. Transp Geotech 29:100579
124. Mohammadi D, Abd EM, Moghdani R, Demir E, Mirjalili S (2021) Quantum henry gas solubility optimization algorithm for global optimization. Eng Comput 38:2329–2348
125. Bi J, Zhang Y (2022) An improved henry gas solubility optimization for optimization tasks. Appl Intell 52(6):5966–6006
126. Wang J, Zhou R, Wang Y, Li Z (2024) Efficient improved henry gas solubility optimization and its application in feature selection problems. Eng Lett 32(10):2023–2040
127. Ji-Sheng Y, Zhang S-K, Wang J-S, Li S, Sun J, Wang R (2023) Support vector machine optimized by henry gas solubility optimization algorithm and archimedes optimization algorithm to solve data classification problems. Eng Lett 31(2):531
128. Zhang M, Jie-Sheng Wang Y, Liu MW, Li X-D, Guo F-J (2023) Feature selection method based on stochastic fractal search henry gas solubility optimization algorithm. J Intell Fuzzy Syst 44(3):5377–5406
129. Li S, Wang J-S, Xie W, Li X-L (2022) An improved henry gas solubility optimization algorithm based on lévy flight and brown motion. Appl Intell 52(11):12584–12608
130. Hongxia X, Razmjooy N (2024) Self-adaptive henry gas solubility optimizer for identification of solid oxide fuel cell. Evol Syst 15(1):133–151
131. Zamli KZ, Kader MA, Azad S, Ahmed BS (2021) Hybrid henry gas solubility optimization algorithm with dynamic cluster-to-algorithm mapping. Neural Comput Appl 33:8389–8416
132. Sarıkaya MS, Naser YHE, Kaçar S, Yazıcı İ, Derdiyok A (2024) Chaotic-based improved henry gas solubility optimization algorithm: Application to electric motor control. Symmetry 16(11):1435
133. Hussien RM, Abohany AA, Moustafa N, Sallam KM (2023) An improved henry gas optimization algorithm for joint mining decision and resource allocation in a mec-enabled blockchain networks. Neural Comput Appl 35(25):18665–18680
134. Sathyapriya LC, Geetha AR, Nazaren M, Harin FF (2023) Autism spectrum disorder detection and classification using chaotic optimization based bi-gru network: An weighted average ensemble model. Expert Syst Appl 230:120613
135. Karasu S, Altan A (2022) Crude oil time series prediction model based on lstm network with chaotic henry gas solubility optimization. Energy 242:122964
136. Yadav NK, Saraswat M (2021) Chaotic henry gas solubility optimization algorithm. In: Intelligent Learning for Computer Vision: Proceedings of Congress on Intelligent Systems 2020, pp. 247–257. Springer
137. Agarwal R, Shekhawat NS, Luhach AK (2021) Automated classification of soil images using chaotic henrys gas solubility optimization: smart agricultural system. Microprocess Microsyst 2021:103854
138. Kahloul S, Zouache D (2025) An enhanced henry gas solubility optimization algorithm using transfer functions for feature selection problem. Multimed Tools Appl. https://doi.org/10.1007/s11042-025-20643-2
139. Yadav NK, Saraswat M (2024) A new feature selection approach with binary exponential henry gas solubility optimization and hybrid data transformation methods. MethodsX 12:102770
140. Sukpancharoen S, Prasartkaew B (2021) Combined heat and power plant using a multi-objective henry gas solubility optimization algorithm: A thermodynamic investigation of energy, exergy, and economic (3e) analysis. Heliyon 7(9):e08003
141. Kahloul S, Zouache D, Brahmi B, Got A (2022) A multi-external archive-guided henry gas solubility optimization algorithm for solving multi-objective optimization problems. Eng Appl Artif Intell 109:104588
142. Jaganathan T, Panneerselvam A, Kumaraswamy SK (2022) Object detection and multi-object tracking based on optimized deep convolutional neural network and unscented kalman filtering. Concurr Comput Pract Exp 34(25):e7245
143. Zamli KZ, Kader MA, Azad S, Ahmed BS (2021) Hybrid henry gas solubility optimization algorithm with dynamic cluster-to-algorithm mapping. Neural Comput Appl 33:8389–8416

144. Ahmed AN, Van Lam T, Hung ND, Van Thieu N, Kisi O, El-Shafie A (2021) A comprehensive comparison of recent developed meta-heuristic algorithms for streamflow time series forecasting problem. Appl Soft Comput 105:107282
145. Shehabeldeen TA, Elaziz MA, Elsheikh AH, Hassan OF, Yin Y, Xiaoyuan JX, Shen JZ (2020) A novel method for predicting tensile strength of friction stir welded aa6061 aluminium alloy joints based on hybrid random vector functional link and henry gas solubility optimization. IEEE Access 8:79896–79907
146. Rohan AB, Sunil S (2022) Compound facial expression recognition and pain intensity measurement using optimized deep neuro fuzzy network. Int J Swarm Intell Res 13(1):1–27
147. Patra R, Khuntia B, Panda DC (2022) Fractional rider gradient descent applied u-net based segmentation with optimal deep maxout network for lung cancer classification using histopathological images. Res Biomed Eng 38(2):599–615
148. Saini A, Gill NS, Gulia P, Tiwari AK, Maratha P, Shah MA (2025) Smart crop disease monitoring system in iot using optimization enabled deep residual network. Sci Reports 15(1):1456
149. Reddy GN, Ravi Kumar CV (2023) Hybrid optimization-based deep neuro-fuzzy network for designing m-user multiple-input multiple-output interference channel. Int J Commun Syst 36(17):e5606
150. Elgazzar S, Mohamed H, Haroun A (2025) Hybrid beta-henry optimization a novel feature selection approach. Int J Comput Inf. https://doi.org/10.21608/ijci.2025.331259.1182
151. Legoui KZ, Maza S, Attia A, Houssein EH (2024) Hybrid henry gas solubility optimization and the equilibrium optimizer for feature selection: real cases with twitter spam detection. Knowl Inf Syst 66(5):3055–3084
152. Nalluri S, Sasikala R (2024) Pneumonia screening on chest x-rays with optimized ensemble model. Expert Syst Appl 242:122705
153. Boopathi M (2022) Henry maxnet: tversky index based feature selection and competitive swarm henry gas solubility optimization integrated deep maxout network for intrusion detection in iot. Int J Intell Robot Appl 6(2):365–383
154. Ramkumar MP, Paul PDM, Maram B, Ananth JP (2022) Deep maxout network for lung cancer detection using optimization algorithm in smart internet of things. Concurr Comput Pract Exp 34(25):e7264
155. Daniya T, Vigneshwari S (2022) Exponential rider-henry gas solubility optimization-based deep learning for rice plant disease detection. Int J Inf Technol 14(7):3825–3835
156. Kulkarni YR, Jagdale B, Sugave SR (2023) Optimized key generation-based privacy preserving data mining model for secure data publishing. Adv Eng Softw 175:103332
157. Puppala R, Ramya V (2023) E-waste management using hybrid optimization-enabled deep learning in iot-cloud platform. Adv Eng Softw 176:103353
158. Deepa SN, Rasi D (2023) Fhgso: Flower henry gas solubility optimization integrated deep convolutional neural network for image classification. Appl Intell 53(6):7278–7297
159. Supreetha Patel Tiptur Parashivamurthy and Sannangi Viswaradhya Rajashekararadhya (2024) Recognition of Kannada character scripts using hybrid feature extraction and ensemble learning approaches. Cybernet Syst 55(8):1977–2012
160. Zhou Z, Yang X, Ji J, Wang Y, Zhu Z (2023) Classifying fabric defects with evolving inception v3 by improved l2, 1-norm regularized extreme learning machine. Textile Res J 93(3–4):936–956
161. Qiu H, Ting H, Zhang S, Xiao Y (2023) Deriving operating rules of hydropower reservoirs using multi-strategy ensemble henry gas solubility optimization-driven support vector machine. Water 15(3):437
162. Mohamed Abd Elaziz and Dalia Yousri (2021) Automatic selection of heavy-tailed distributions-based synergy henry gas solubility and harris hawk optimizer for feature selection: Case study drug design and discovery. Artif Intell Rev 54(6):4685–4730
163. Xie W, Xing C, Wang J, Guo S, Guo M-W, Zhu L-F (2020) Hybrid henry gas solubility optimization algorithm based on the harris hawk optimization. IEEE Access 8:144665–144692
164. Mohamed AE, Ibrahim A (2021) An improved henry gas solubility optimization algorithm for task scheduling in cloud computing. Artif Intell Rev 54(5):3599–3637
165. Siva KR, Kalaivani K (2024) Prostate cancer detection using henry firefly gas solubility optimization-based deep residual network. Multimed Tools Appl 83(10):29331–29352
166. Janairo AG, Baun JJ, Concepcion R, Relano R-J, Francisco K, Enriquez M L, Bandala A, Vicerra R R, Alipio M, Dadios EP (2022) Optimization of subsurface imaging antenna capacitance through geometry modeling using archimedes, lichtenberg and henry gas solubility metaheuristics. In: 2022 IEEE International IOT, Electronics and Mechatronics Conference (IEMTRONICS), pp. 1–8. IEEE
167. Chen Y, Gou L, Li H (2022) A differential evolution based henry gas solubility optimizer for dynamic performance optimization problems of pro system. Appl Soft Comput 125:109097
168. Abdel-Mawgoud H, Kamel S, Khasanov M, Khurshaid T (2021) A strategy for pv and bess allocation considering uncertainty based on a modified henry gas solubility optimizer. Electric Power Syst Res 191:106886
169. Puppala R, Ramya V, Babu RM (2024) Optimized deep learning-based e-waste management in iot application via energy-aware routing. Cybernet Syst 55(8):2041–2070
170. Nirmala Priya G, Suresh Kumar K, Suganthi N, Muppidi S (2024) Squirrel henry gas solubility optimization driven deep maxout network with multi-texture feature descriptors for digital image forgery detection. Concurr Comput Pract Exp 36(8):e7965
171. Omana SP, Dar JA, Kumar TR, Sampath AK, Sharma S (2023) Henry gas bird swarm optimization algorithm-based deep learning for brain tumor classification using magnetic resonance imaging. Concurr Comput Pract Exp 35(4):e7541
172. Li W, Wang R, Ai Q, Liu Q, Shu Xian L (2023) Estimation of compressive strength and slump of hpc concrete using neural network coupling with metaheuristic algorithms. J Intell Fuzzy Syst 45(1):577–591
173. Lakshmanan S, Gnaniyan PUM, Andi S (2023) An efficient ddos attack detection using chaos henry gas solubility optimization weight initialization based rectified linear unit. Cybernet Syst 56:544–571
174. Mathan Kumar B, Ainapure BS, Singh SP, Vyas S (2023) Feature extraction based deep indexing by deep fuzzy clustering for image retrieval using Jaro Winkler distance. Comput J 66(9):2191–2207
175. Obayya M, Alhebri A, Maashi M, Salama AS, Hilal AM, Alsaid MI, Osman AE, Alneil AA (2023) Henry gas solubility optimization algorithm based feature extraction in dermoscopic images analysis of skin cancer. Cancers 15(7):2146
176. Ninu SB (2023) An intrusion detection system using exponential henry gas solubility optimization based deep neuro fuzzy network in manet. Eng Appl Artif Intell 123:105969
177. Li H (2023) Prediction of high-performance concrete compressive strength through novel structured neural network. J Intell Fuzzy Syst 45(1):1791–1803
178. Meenalochini P, Karthick R, Sakthivel E (2023) An efficient control strategy for an extended switched coupled inductor quasi-z-source inverter for 3 ϕ grid connected system. J Circuits Syst Comput 32(11):2450011
179. Escorcia-Gutierrez J, Torres-Torres M, Madera N, Soto C (2023) Henry gas solubility optimization with deep learning enabled

traffic flow forecasting in 6g enabled vehicular networks. In: AI-Enabled 6G Networks and Applications, pp. 35–53
180. Kuldeep NT, Subhash CS (2023) An optimal trust and secure model using deep metric learning for fog-based vanet. Trans Emerg Telecommun Technol 34(8):e4805
181. Karthika J, Rajkumar M, Vishnupriyan J (2023) A hybrid control technique for small signal stability analysis for microgrids under uncertainty. J Intell Fuzzy Syst 44(1):625–645
182. Arumugasamy M, Arokiasamy A (2023) Tunicate henry gas solubility optimization-based deep residual network for fruit ripeness classification. Concurr Comput Pract Exp 35(2):e7490
183. Roy D, Dutta M (2023) An intelligent group recommender system using henry gas solubility optimization algorithm-based adaptive deep belief network. In: 2023 4th International Conference on Computing and Communication Systems (I3CS), pp. 1–6. IEEE
184. AlEisa HN, Alrowais F, Negm N, Almalki N, Khalid M, Marzouk R, Alnfiai MM, Mohammed GP, Alneil AA (2023) Henry gas solubility optimization with deep learning based facial emotion recognition for human computer interface. IEEE Access 11:62233–62241
185. Arivalahan R, Tamilarasan P, Kamalakannan M (2023) Liquid level control in two tanks spherical interacting system with fractional order proportional integral derivative controller using hybrid technique: A hybrid technique. Adv Eng Softw 175:103316
186. Fayaz Ahamed A, Sukhi Y (2023) Modeling of hybrid henry gas solubility optimization algorithm with deep learning-based led driver system. J Circuits Syst Comput 32(17):2350301
187. Ragab M, Alshammari SM, Asseri AH, Almutiry WK (2022) Optimal fusion-based handcrafted with deep features for brain cancer classification. Comput Mater Contin 73(1):801–815
188. Patra R, Khuntia B, Panda DC (2022) Hybrid optimization-based structural design of deep q network with feature selection algorithm for medical data classification. Int J Swarm Intell Res 13(1):1–20
189. Gotlur KA, Durga K, Karuna G (2022) Cnn features and optimized generative adversarial network for covid-19 detection from chest x-ray images. Crit Rev Biomed Eng 50(3):1–17
190. Li H, Gou L, Chen Y, Li H (2022) Fault diagnosis of aeroengine control system sensor based on optimized and fused multidomain feature. IEEE Access 10:96967–96983
191. Granty REJ, Mandala J, Maram B, Ramesh Kumar R (2022) Ar-hgso: Autoregressive-henry gas sailfish optimization enabled deep learning model for diabetic retinopathy detection and severity level classification. Biomed Signal Process Control 77:103712
192. Sadiq MT, Akbari H, Siuly S, Li Y, Wen P (2022) Alcoholic eeg signals recognition based on phase space dynamic and geometrical features. Chaos Solitons Fractals 158:112036
193. Mishra RK, Anurag CAR, Mohanty FS (2022) An intelligent bearing fault diagnosis based on hybrid signal processing and henry gas solubility optimization. Proc Inst Mech Eng Part C J Mech Eng Sci 236(19):10378–10391
194. Ravikumar S, Kavitha D (2021) Cnn-ohgs: Cnn-oppositional-based henry gas solubility optimization model for autonomous vehicle control system. J Field Robot 38(7):967–979
195. Jeyalakshmi S, Sekar S, Ravikumar S, Kavitha D (2022) Random forest-based oppositional henry gas solubility optimization model for service attack improvement in wsn. J Inst Eng (India) Series B 103(3):939–950
196. Islam MS, Awal MA, Laboni JN, Pinki FT, Karmokar S, Mumenin KM, Saad Al-Ahmadi Md, Ashfikur Rahman Md, Hossain S, Mirjalili S (2022) Hgsorf: Henry gas solubility optimization-based random forest for c-section prediction and xai-based cause analysis. Comput Biol Med 147:105671
197. Kathavate PN, Amudhavel J (2022) Lipoprotein detection: hybrid deep classification model with improved feature set. Multiagent Grid Syst 18(3–4):345–363
198. Chun W, Yang L (2023) Estimation of the improved high-performance concretes mechanical characteristics using unique regression methods. J Intell Fuzzy Syst 44(4):5759–5772
199. Kumar S, Robinson S (2022) Estimating the pile settlement using a machine learning technique optimized by henry's gas solubility optimization and particle swarm optimization. Adv Eng Intell Syst 1(04):50–61
200. Javadi F, Qaderi K, Ahmadi MM, Rahimpour M, Madadi MR, Mahdavi-Meymand A (2022) Application of classical and novel integrated machine learning models to predict sediment discharge during free-flow flushing. Sci Reports 12(1):19390
201. Chen L, Liu F, Fufei W (2022) Novel hybrid hgso optimized supervised machine learning approaches to predict the compressive strength of admixed concrete containing fly ash and micro-silica. Eng Res Express 4(2):025022
202. Agarwal R, Shekhawat NS (2022) Enhanced bag of features using alexnet and henry gas solubility optimization for soil image classification. In: Proceedings of International Conference on Data Science and Applications: ICDSA 2021, Volume 2, pp. 493–503. Springer
203. Alkaam NO, Sultan AM, Hussin MB, Sharif KY (2025) Hybrid henry gas-harris hawks comprehensive-opposition algorithm for task scheduling in cloud computing. IEEE Access. https://doi.org/10.1109/ACCESS.2025.3530860
204. Azlan Saleh and Mohd Asyraf Zulkifley (2025) Prediction of suspended sediment load in sungai semenyih using extreme learning machines and metaheuristic optimization approach. J Environ Manag 380:124987
205. Goswami C, Senthil Ragavan VK, Ramesh JV, Balajee J, Ronald Doni A, Saravanan TR, Siva Shankar S (2023) Deep convolutional neural network-based henry gas solubility optimization for disease prediction in data from wireless sensor network. Soft Comput 45:2273–2284
206. Vignesh RS, Mohan MS (2024) Multilevel-thermoplastic waste segregation using archimedes henry gas solubility trained deep quantum network. Proc Inst Mech Eng C J Mech Eng Sci 238(16):8339–8356
207. Prakash T, Gnanakumar G, Abhinav, Muniyandy E (2025) Dacnn based predicting tensile strength of friction stir welded aluminium alloy joints. Int J Mach Learn Cybern 16:3997–4016
208. Ekinci S, Izci D, Hekimoğlu B (2020) Henry gas solubility optimization algorithm based fopid controller design for automatic voltage regulator. In: 2020 International conference on electrical, communication, and computer engineering (ICECCE), pp. 1–6. IEEE
209. Ekinci S, İzci D, Hekimoglu B (2021) Implementing the henry gas solubility optimization algorithm for optimal power system stabilizer design. Electrica 21(2):250–258
210. Nguyen Q-H, Chou T-Y, Yeh M-L, Hoang T-V, Nguyen H-D, Bui Q-T (2021) Henrys gas solubility optimization algorithm in formulating deep neural network for landslide susceptibility assessment in mountainous areas. Environ Earth Sci 80(11):414
211. Ebrahim MA, Abdel RM, Fattah EM, Saied SM, Maksoud A, Khashab HE (2021) An islanded microgrid droop control using henry gas solubility optimization. Int J Innov Technol Explor Eng 10:43–48
212. Idir A, Khettab K, Bensafia Y (2022) Design of an optimally tuned fractionalized pid controller for dc motor speed control via a henry gas solubility optimization algorithm. Int J Intell Eng Syst 15(2):59

213. Mousakazemi SMH (2022) Henry gas solubility optimization for control of a nuclear reactor: a case study. Nucl Eng Technol 54(3):940–947
214. Qi X, Li H, Song Y (2022) Research on intelligent lpv control method of aeroengine. In: 2022 41st Chinese Control Conference (CCC), pp. 2144–2149. IEEE
215. Liu M, Liu T, Zhu M, Chen L (2022) A pi control method with hgso parameter regulator for trajectory planning of 9-dof redundant manipulator. Sensors 22(18):6860
216. Pravin KD, Ganesh Kumar P (2025) Implementation of optimal routing in heterogeneous wireless sensor network with multichannel media access control protocol using enhanced henry gas solubility optimizer. Int J Commun Syst 38(1):e5980
217. Singh P, Sandhu A (2022) Optimal parameter extraction of proton exchange membrane fuel cell using henry gas solubility optimization. Int J Energy Res 46(13):18212–18224
218. Selim A, Kamel S, Abdelkader M, Jurado F (2022) Optimal placement of pmus using henry gas solubility optimization for state estimation of power system. In: 2022 IEEE International Conference on Automation/XXV Congress of the Chilean Association of Automatic Control (ICA-ACCA)
219. Haider HT, Muhsen DH, Al-Nidawi YM, Khatib T, See OH (2022) A novel approach for multi-objective cost-peak optimization for demand response of a residential area in smart grids. Energy 254:124360
220. Hemeida AM, Rashwan A, Hasanien HM, Senjyu T (2023) Voltage and angle stability assessment of power systems based optimizated facts devices. In: 2023 IEEE Conference on Power Electronics and Renewable Energy (CPERE), pp. 1–6. IEEE
221. Mousakazemi SMH (2023) A meta-heuristic algorithm based on henry's law for the load-following of a two-point pwr model. Progr Nucl Energy 155:104520
222. Das S (2023) Application of henry gas solubility optimization algorithm for short-term hydrothermal scheduling considering variable water transportation delay and penstock head loss. E-Prime 6:100287
223. Zayermohammadi Rishehri H, Ansarifar GR (2025) Optimizing the small modular reactor core loading with dual-cooled fuel via henry gas solubility optimization algorithm. Nucl Eng Des 433:113899
224. Cao W, Liu X, Ni J (2020) Parameter optimization of support vector regression using henry gas solubility optimization algorithm. IEEE Access 8:88633–88642
225. Legoui KZ, Maza S, Attia A (2022) Equilibrium optimizer and henry gas solubility optimization algorithms for feature selection: comparison study. In: 2022 5th International Symposium on Informatics and its Applications (ISIA), pp. 1–6. IEEE
226. Elden RH, Ghonim VF, Hadhoud MMA, Al-Atabany W (2023) Transcriptomic marker screening for evaluating the mortality rate of pediatric sepsis based on henry gas solubility optimization. Alexandria Eng J 68:693–707
227. Chinta VS, Reddi SK, Yarramsetty N (2023) Optimal feature selection on serial cascaded deep learning for predictive maintenance system in automotive industry with fused optimization algorithm. Advanced Eng Inform 57:102105
228. Yamini Devi P, Sriramya P (2025) Blockchain with drug traceability in medical supply chain with henry gas solubility optimisation algorithm. Int J Wirel Mobile Comput 28(2):135–148
229. Kurban R, Durmus A, Karakose E (2021) A comparison of novel metaheuristic algorithms on color aerial image multilevel thresholding. Eng Appl Artif Intell 105:104410
230. Mishra SK, Pal R (2022) An optimal image segmentation method based on hgso for ct images. In: 2022 8th International Conference on Signal Processing and Communication (ICSC), pp. 289–293. IEEE
231. Hamdellou A, Addad D, Kadi K, Belattar H, Torche Y, Mekersi N, Ikhlef M–A, Abderazek H (2024) Modeling and optimization of ultrasound-assisted extraction of phenolic compounds from haloxylon scoparium aerial parts. Chem Afr 7(2):689–703
232. Rajendra Purohit KR, Chowdhary SDP, Pal R, Sharma H (2025) A novel parallel hybrid k-means and hgso based approach for detecting fake reviews in social media. SN Comput Sci 6(5):1–16
233. Anoosha C, Tirumala KB (2025) Enhanced meta-heuristic approach for echo suppression in synthetic aperture radar using non-periodic interrupted sampling. Traitement Signal 42(2):1097–1110
234. Aykut FG, Onur ÖM (2025) Comparative analysis and statistical performance evaluation of fractional pid controllers in fuel cell choppers optimized with metaheuristic algorithms. Neural Comput Appl 37(6):4585–4615
235. Ahmad LZ, Satish U, Trpaty A et al (2024) Developing a novel deep learning optimization method for forecasting soil friction gradient. Multidiscipl Sci J. https://doi.org/10.31893/multiscience.2024ss0316
236. Sangeetha V, Theertha K, Vishnupriya C, Varsha SD, Tanupriya R, Narendra AP (2024) Anomaly detection in rotary equipment using hybrid model with hgso optimization. In: 2024 IEEE International Conference on Electronics, Computing and Communication Technologies (CONECCT), pp. 1–6. IEEE
237. Ezzulddin YT, Ahmed AO (2025) Design of an optimally tuned fractional order pi-pd controller for dc motor speed via a henry gas solubility algorithm. Procedia Comput Sci 259:1693–1702
238. Mehta P, Abderazek H, Kumar S, Sait SM, Yıldız BS, Yildiz AR (2025) Comparative study of state-of-the-art metaheuristics for solving constrained mechanical design optimization problems: experimental analyses and performance evaluations. Mater Test 67(2):249–281
239. Bodalal R (2025) A performance comparison of eight metaheuristic algorithms for the optimal design of large-scale truss structures. J Braz Soc Mech Sci Eng 47(3):1–37
240. Zawawi MNM, Isa ZM, Ismail B, Arshad MH, Mid EC, Talib MHN, Zambak MF (2025) Harmonics elimination of reduced switch multilevel inverter using henry gas solubility optimization algorithm. Iran J Electr Electron Eng 21(2):3631
241. Idriss AI, Ramadan HS, Ahmed RA, Atteye HA (2025) Optimizing wind and green hydrogen production through balanced prioritization in site-specific scenarios. Int J Hydrogen Energy. https://doi.org/10.1016/j.ijhydene.2025.02.314
242. ELgazzar S, Mohamed H, Haroun A (2024) A hybrid feature selection approach: β-hill climbing and henry gas optimization. In: International Conference on Machine Intelligence and Smart Innovation (ICMISI) IEEE 96262–96265
243. Mahzad EF, Reza SB (2024) Application of optimization-based regression analysis for evaluation of frost durability of recycled aggregate concrete. Struct Concrete 25(1):716–737
244. Gokiladevi M, Santhoshkumar S (2024) Henry gas optimization algorithm with deep learning based chronic kidney disease detection and classification model. Int J Intell Eng Syst 17(2):645–655
245. Vignesh RS, Monica M (2025) Multilevel thermoplastic waste segregation and classification with ahgso using federated learning framework. Kybernetes 54(5):2706–2734
246. Jegan R, Kaushal B, Birajdar GK, Patil MD (2025) An optimized deep neural network with explainable artificial intelligence framework for brain tumour classification. Netw Comput Neural Syst. https://doi.org/10.1080/0954898X.2025.2500046
247. Siva KR, Kalaivani K (2024) Hybrid optimization enabled deep-learning for prostate cancer detection. Sens Imaging 25(1):52
248. Ali MU, Zafar A, Tanveer J, Khan MA, Kim SH, Alsulami MM, Lee SW (2024) Deep learning network selection and optimized information fusion for enhanced covid-19 detection. Int J Imaging Syst Technol 34(2):e23001

249. Nayana BR, Subha R, Radhakrishnan R, Geethanjali P (2025) Scalable bearing fault diagnosis using metaheuristic feature selection and machine learning for diverse operating conditions. Syst Sci Control Eng 13(1):2469606
250. AlShorman A, Shannaq F, Shehab M (2024) Machine learning approaches for enhancing smart contracts security: a systematic literature review. Int J Data Netw Sci 8(3):1349–1368